Taxonomic and Functional Interpretation of Associated Cercopithecoid Carpal Bones (KB 5378) from Kromdraai B, South Africa

MADISON ROSE
School of Anthropology and Conservation, University of Kent, Canterbury, CT2 7NR, UNITED KINGDOM; and, Department of Anthropology, University of Toronto, Scarborough M1C 1A4, CANADA; mads.rose@mail.utoronto.ca

MIRRIAM TAWANE
Ditsong National Museum of Natual History, Pretoria; and, Centre for the Exploration of the Deep Human Journey, University of the Witwatersrand, Johannesburg, SOUTH AFRICA; tawane@ditsong.org.za

TRACY L. KIVELL*
Department of Human Origins, Max Planck Institute for Evolutionary Anthropology, Leipzig 04103, GERMANY; School of Anthropology and Conservation, University of Kent, Canterbury, CT2 7NR, UNITED KINGDOM; and, Centre for the Exploration of the Deep Human Journey, University of the Witwatersrand, Johannesburg, SOUTH AFRICA; tracy_kivell@eva.mpg.de

*corresponding author: Tracy L. Kivell; *tracy_kivell@eva.mpg.de*

submitted: 14 November 2022; revised: 7 May 2023 month 202x; revised: 24 August 2023; accepted: 25 August 2023

Handling Editor in Chief: Katerina Harvati

ABSTRACT

A partial carpus belonging to a large, South African Pliocene cercopithecoid was excavated from Kromdraai B (Gauteng, South Africa) between 1977 and 1981 alongside an associated late juvenile metacarpus and several manual phalanges (KB 5378). Included in the KB 5378 carpus is a partial scaphoid, lunate, os centrale, trapezium, trapezoid, capitate, and hamate. Here we describe each carpal bone quantitatively and qualitatively in comparison to a sample of extant anthropoid primates to gain an understanding of both functional morphology and taxonomy of the KB 5378 fossils. Overall, the carpal morphology reflects that of a generalized quadruped with potential specializations for terrestrial, digitigrade locomotion. The absolute and relative size of the carpus and metacarpus indicate that they are likely from the same individual and are more likely to be attributed to a member of the *Theropithecus oswaldi* lineage, likely *T. o. oswaldi* rather than the previously suggested *Gorgopithecus major*.

INTRODUCTION

Understanding primate evolution requires drawing inferences about behavior, and particularly locomotion, from fossilized remains of the skeleton. The bones of the forearm, wrist, and hand have been used to reconstruct locomotor behavior in numerous fossil primates (e.g., Etter 1973; Hamrick 1996; Lovejoy et al. 2009; Marzke 1983; McCrossin et al. 1998; O'Connor 1975; Patel 2010a, b; Schmitt 2003; Vanhoof et al. 2021) based on morphological variation in extant primates (e.g., Daver 2012; Patel 2010a, b; Richmond 2006; Vanhoof et al. 2021). Studies of carpal morphology have played an important role in reconstructing primate behavior in the past (e.g., Ciochon 1993; Frost et al. 2015; Kivell 2016; Lovejoy et al. 2009; Marzke 1983; O'Connor 1975; Orr 2018; Tocheri et al. 2005). Here we describe for the first time the functional morphology of associated cercopithecoid carpal bones (KB 5378) from Kromdraai B, South Africa, that were originally discovered during Elisabeth Vrba's excavations in 1977–1980. These carpal fossils include a partial scaphoid and complete os centrale, lunate, hamate, capitate, trapezoid, and trapezium, all from the left side (Figure 1). They articulate well together and are considered to derive from a single individual. In this study, we qualitatively and quantitatively describe the morphology of each carpal within a comparative context of extant anthropoids from a diverse array of arboreal and terrestrial locomotor modes. Our aim is to use the morphology of the KB 5378 carpus to determine the likely taxonomic attribution and locomotor behavior of the KB 5378.

KROMDRAAI B

The KB 5378 carpal bones were uncovered in Kromdraai B (KB), a subsection of the larger Kromdraai site, which today is a rectangular, unroofed cave spanning approxi-

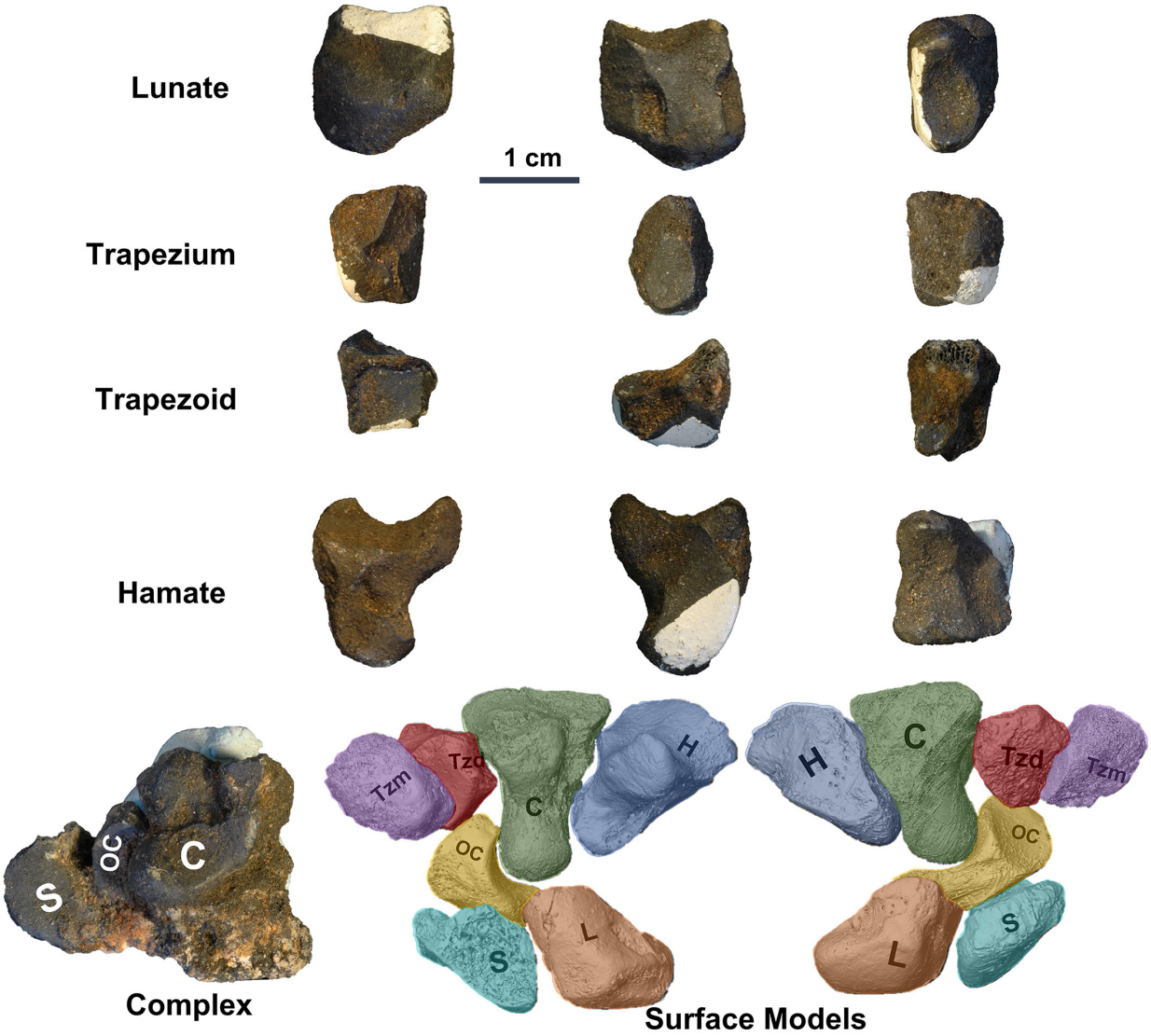

Figure 1. The KB 5378 carpal bones. Each bone is displayed in order to show the most informative morphology. From left to right, the lunate, trapezoid, and hamate are shown in radial, ulnar, and distal views and the trapezium is shown in palmar, ulnar, and dorsal views. The complex containing the capitate, os centrale, and partial scaphoid articulated in breccia is included on the bottom left. Surface models of all carpals in articulation are included and shown in palmar (left) and dorsal (right) views (H, hamate; C, capitate; Tzd, trapezoid; Tzm, trapezium; OC, os centrale; L, lunate; S, scaphoid) (Scale bar represents 1cm.)

mately 3m wide at its extreme ends and 40m long at its surface (Bruxelles et al. 2016). This site is described using a grid system established by Vrba (1981), who led excavations from 1977 through 1980. Using this grid, the KB 5378 fossils derive from breccia block 74, originally excavated at approximately 27.29m east, 3m north and 1.75m below Vrba's datum point.

Using a combination of biochronology and paleomagnetic data, deposits within KB have been tentatively dated between 1.5 to 2.0 million years (Ma) (Braga 2016; Delson, 1988; Fouvrel 2016; Thackeray 2002; Vrba 1981). More specific studies of the individual stratigraphic layers (members) within KB are limited and have focused on using paleomagnetic reversals with reference to the Olduvai Event, an interval of time from 1.95 to 1.77 Ma during which normal magnetic polarity is recorded in the sediments of Africa (Tamrat 1994). Using the Olduvai event as a reference point, in combination with faunal dating, the age of the earliest members (1 and 2) of KB is estimated to be ca. 1.9 Ma, just before the Olduvai Event took place (Thackeray 2002).

The reconstruction of the paleoecology of the entirety of Kromdraai suggests a mixture of woodland and grassland (see review in Thackeray 2017). However, there are several morphological indicators in the available fossil record that suggest a largely terrestrial lifestyle for the cercopithecoid primates that have been uncovered from the site (see below, Benefit 1987, 1999; Ciochon 1993; Delson et al. 2000; Leakey 1982; McCrossin et al. 1998). Furthermore, analyses of dental morphology indicate a diet containing a large proportion of ground level foliage in some of these

TABLE 1. THIS TABLE PROVIDES A LIST OF FOSSIL TAXA KNOWN AT EACH LOCALITY WITHIN THE CRADLE OF HUMANITY FOR PLIO-PLEISTOCENE FOSSIL BEARING SITES FROM THE LITERATURE (Freedman 1957; Folinsbee and Reisz 2013; Gilbert 2018; Jablonski 2002; Vrba 1981).*

TAXON	LOCATION	BODY MASS (KG)
CERCOPITHECOIDES WILLIAMSI	Kromdraai A, Kromdraai B, Bolt's Farm, Cooper's Cave, Sterkfontein, Makapansgat, Swartkran	♂ 20–27 ♀ 15–27
GORGOPITHECUS MAJOR	Kromdraai A, Kromdraai B	♂ 34–39 ♀ 28–32
PAPIO HAMADRYAS ANGUSTICEPS	Kromdraai A, Cooper's Cave, Bolt's Farm, Haasgat, Gladysvale, Malapa	♂ 21–22 ♀ 14–20
PAPIO ROBINSONI	Kromdraai B, Swartkrans, Cooper's Cave, Bolt's Farm	♂ 30–31 ♀ 15–17
PAPIO IZODI	Gladysvale, Sterkfontein	♂ 20–24 ♀ 20–21
PARAPAPIO BROOMI	Sterkfontein, Makapansgat, Bolt's farm	♂ 18–26 ♀ 14–16
PARAPAPIO JONESI	Kromdraai A, Sterkfontein, Makapansgat, Swartkrans	♂ 14–19 ♀ 11–12
PARAPAPIO WHITEI	Sterkfontein, Makapansgat	♂ 22–30 ♀ 16–21
THEROPITHECUS OSWALDI DARTI	Hadar, Makapansgat	♂ 24–27 ♀ 21–24
THEROPITHECUS OSWALDI OSWALDI	Swartkrans, Cooper's Cave, Bolt's Farm, Hopefield	♂ 35–54 ♀ 25–27

*Though not all are found in Kromdraai B, cercopithecoid specimens from contemporaneous fossil sites located nearby are included as well. Body mass estimates in this table were calculated by Delson et al. (2000) using dental characters. If large variation exists within taxa based on location (e.g., *C. williamsi* and *Theropithecus sp.*) estimates from South African sites are included.

cercopithecoids, further suggesting that the paleoenvironment of KB consisted at least partially of the grasslands needed to support these terrestrial cercopithecoids (Benefit 1987, 1999; Delson et al. 2000; Leakey 1982).

FOSSIL CERCOPITHECOIDES FROM KROMDRAAI

In addition to being a well-known, hominin-rich fossil site, KB has produced an array of fossil cercopithecoids from at least three genera, proposed to comprise multiple species (Benefit 1999; Broom 1940; Broom and Robinson 1949; Freedman 1957; Gilbert et al. 2018; Vrba 1981). Currently, the record of cercopithecoid taxa from KB includes *Papio robinsoni* (Gilbert et al. 2018), *Gorgopithecus major* (Broom and Robinson 1949; Vrba 1981), and *Cercopithecoides williamsi* (Freedman 1957; Jablonski 2002; Vrba 1981). The adjacent Kromdraai A site has yielded additional cercopithecoid taxa, including *Papio angusticeps* (Gilbert et al. 2018), *Parapapio jonesi* (Gilbert et al. 2018), as well as *G. major* (Broom and Robinson 1949; Jablonski 2002; Vrba 1981), and *C. willimasi* (Freedman 1957; Jablonski 2002; Vrba 1981). Cercopithecoid taxa, including *Theropithecus*, present at Kromdraai and contemporaneous sites within the Guateng region of South Africa are summarized in Table 1.

The ecologies of South African fossil cercopithecoids vary greatly. Most researchers agree that fossil *Papio* engaged primarily in terrestrial locomotion much like extant *Papio* (Delson et al. 2000; Gilbert 2018; Jablonski 2002). *Parapapio* species are reconstructed as medium sized mixed terrestrial/arborealists (Delson et al. 2000; Frost and Delson 2002; Gilbert 2018). *C. williamsi* is the only colobine monkey found in and around Kromdraai. It is reconstructed to be large (15–27kg in females and 20–27kg in males) and similar to extant *Papio* in being almost exclusively terrestrial (Anderson 2019; Frost and Delson 2002; Jablonski 2002; Leakey 1982; Williams and Geissler 2014) (see Table 1). This species also exhibits the earliest known evidence of thumb reduction in colobine fossils, showing reduction of its first metacarpal to an equal degree of modern African colobine primates (Frost et al. 2015; Jablonski et al. 2008).

The two subpecies of *Theropithecus* found in surrounding sites, *T. oswaldi oswaldi* and *T. oswaldi darti*, vary greatly in body mass (Delson et al. 2000; Guthrie 2011; see Table 1). Both *T. o. oswaldi* and *T. o. darti* are reconstructed as generally similar to the extant *T. gelada*, though *T. o. darti* may have been more arboreal (Anderson 2019; Krentz 1993). One of the most notable traits of both extant and extinct *Theropithecus* species is the marked elongation of the first metacarpal and reduction of the second digit that facilitates a distinct pincher-like grasping used during foraging among fine grasses (Anderson 2019; Frost and Delson 2002; Guthrie 2011; Krentz 1993; Napier 1967).

Finally, *G. major* (Broom 1940) was a large cercopithecoid (28–32kg in females and 34–39kg in males) with dental

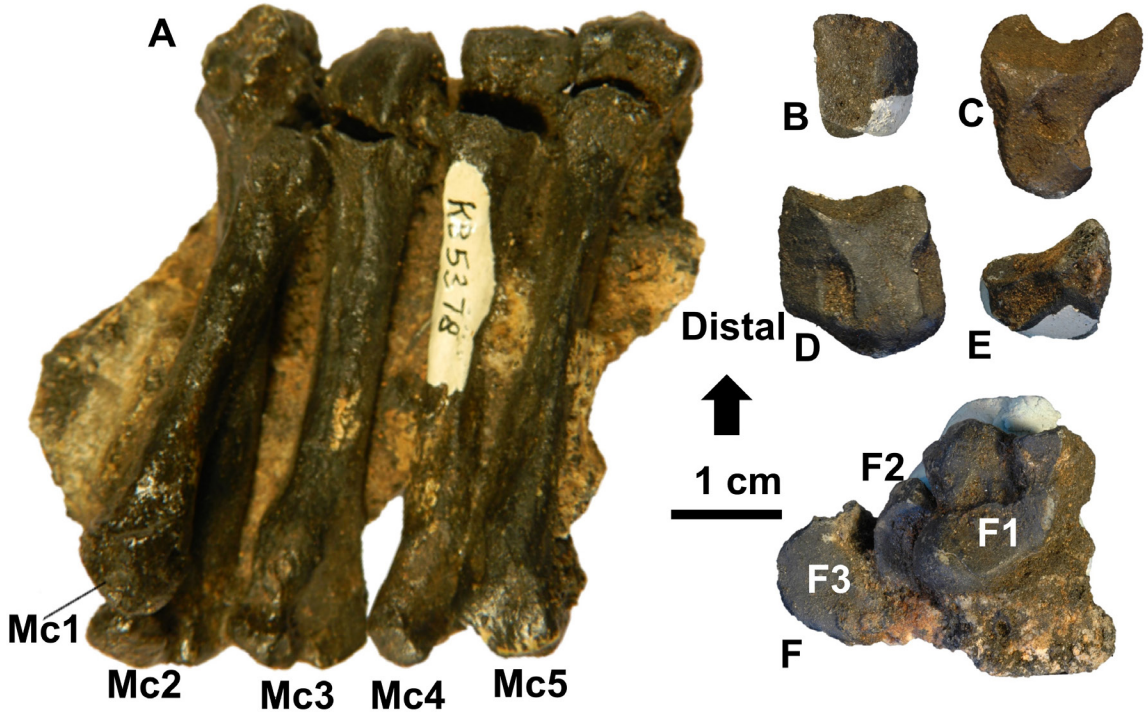

Figure 2. All bones identified as KB 5378 considered in this study. Each specimen is marked as follows: A) metacarpals 1 through 5; B) trapezium in dorsal view; C) hamate in radial view; D) lunate in ulnar view; E) trapezoid in ulnar view; F) complex including the capitate (F1), os centrale (F2), and scaphoid fragment (F3) embedded in breccia (Photo credit: TLK and Mirriam Tawane.)

morphology and microwear indicative of a diet primarily comprising leaves, grasses, and some fruits (Benefit 1999; El-Zaatari et al. 2005). Though no postcranial remains from *G. major* have been reported, terrestriality is often assumed to be the primary mode of locomotion for this species due to its body size (Delson 2000; Fleagle 1998).

KB 5378 CARPAL FOSSILS

The KB 5378 carpal fossils consist of several bones that compose a nearly complete left carpus. The capitate, os centrale, and a large fragment of scaphoid form a complex held together by matrix, while the hamate, lunate, trapezoid, and trapezium are isolated (see Figure 1; Figure 2, Table 2). Each carpal is well preserved, with the exception of the scaphoid, which is missing its distal half. All articulate well with each other.

The KB 5378 carpals were excavated directly adjacent to several other fossils in the surrounding breccia, including associated juvenile metacarpals, proximal phalanges, and an additional hamate that are also assigned KB 5378 (see

TABLE 2. TABLE LISTING ALL MATERIALS CURRENTLY IDENTIFIED AS KB 5378 (elements not evaluated in this study are denoted with an asterisk (*).[+]

Element	*Side*
Scaphoid	Left
Os centrale	Left
Lunate	Left
Trapezoid	Left
Trapezium	Left
Capitate	Left
Hamate	Left
*Hamate**	?
Metacarpals 1-5	Left
*Phalanges**	Left

[+]All elements listed are curated at the Ditsong National Museum of Natural History, Pretoria, South Africa.

Figure 2; see Table 2), as well as a juvenile mandible with dentition of a large baboon (KB 5227), and a partial hominin dentition (KB 5223) (Vrba 1981). The KB 5378 metacarpus and phalangeal sample includes all five metacarpals and four proximal phalanges of the left hand and were initially reported as being from a large, juvenile baboon (Vrba 1981). However, a full description of these hand bones has yet to be published. KB 5227 is a partial juvenile mandible preserving fully erupted second molars and premolars as well as unerupted third molars and a canine (Vrba 1981). Due to size, preservation and, in the case of KB 5227, similarities in third premolar size with *G. major* premolars from Kromdraai A (KA 150), both the KB 5227 mandible and KB 5378 carpus and hand bones have been suggested to belong to a juvenile *G. major* (Vrba 1981).

Here we provide the first morphological description and functional interpretation of the fossil cercopithecoid carpus KB 5378 within a comparative context of a diverse sample of extant primates. We aim to understand its potential taxonomic affiliation and its locomotor behavior. We test the following predictions based on the reported suggestion that the KB 5378 carpal (and hand) fossils are attributed to *G. major* (Vrba 1981):

1. We expect the carpals of KB 5378 to be larger than any other fossil papionin (*Papio* and *Parapapio*) from Kromdraai and contemporaneous sites.
2. We expect the external carpal morphology to be more similar to that of extant large-bodied terrestrial quadrupedal monkeys than that of arboreal quadrupedal monkeys in our study sample.
3. We expect the KB 5378 carpals and associated metacarpals to lack morphological specializations of other known contemporaneous fossil taxa (e.g., a reduced first metacarpal seen in *C. williamsi* or an elongated first metacarpal seen in *Theropithecus* species).

MATERIALS AND METHODS

SAMPLE

The KB 5378 carpals are curated at the Ditsong National Museum of Natural History, Pretoria, South Africa. These carpals were compared to a diverse sample of extant hominoid, cercopithecoid, and platyrrhine taxa (Table 3). The comparative sample was chosen to encompass all major locomotor groups among extant monkeys, with comparative outgroups. Comparative extant samples are curated at the following institutions: University of Toronto Biological Anthropology collections (BAA), University of Toronto at Scarborough (UTSC), and Royal Ontario Museum (ROM) in Canada; the Museum of Comparative Zoology, Harvard (MCZ), State University New York (SUNY), Cleveland Museum of Natural History (CMNH), American Museum of Natural History (AMNH), and Smithsonian National Museum of Natural History (NMNH) in the USA; Royal Museum for Central Africa (MRAC), Belgium; Museum für Naturkunde—Leibniz Institute for Evolution and Biodiversity Science, Berlin (ZMB), Max Planck Institute for Evolutionary Anthropology Taï Chimpanzee collection (MPI-EVA), and Senckenberg Museum Frankfurt (SMF) in Germany; and Powell Cotton Museum (PCM), UK.

Extant taxa were categorized by locomotor behavior based on their degree of terrestriality vs. arboreality, recognizing that species within each category engage in a variety of different locomotor behaviors and at different frequencies. Our locomotor groups include knuckle-walkers (*Pan, Gorilla*), terrestrial quadrupeds (*Papio, Theropithecus, Mandrillus, Macaca mulatta, Erythrocebus*), arboreal quadrupeds (*Alouatta, Cercocebus, Cercopithecus, Chlorocebus, Colobus, Lagothrix, Lophocebus, Macaca fascicularis, Presybtis*), and suspensory primates (*Hylobates, Ateles)*. Our sample was divided at the genus level, apart from *M. mulatta* and *M. fascicularis* that were distinguished at the species level due to the high degree of terrestriality in *M. mulatta* compared to the more arboreal *M. fascicularis* (Fleagle 1998; Patel 2010a, b; Rodman 1979; Tuttle 1969). A full list of taxa and associated literature used to define the locomotor group of each taxon are listed in supplementary materials (Supplementary Table 1).

EXTERNAL MORPHOLOGICAL ANALYSIS

The external morphology of each carpal was assessed through qualitative comparisons and quantitative linear measurements. The morphometric variables used to quantify each carpal are listed and defined in Table 4 (for images of measurements, see Kivell and Begun 2009; Kivell et al. 2018). All linear measurements of the extant samples were taken manually using digital calipers (Wiha digimax or Mitutoyo digital calipers) on original specimens by MR or TLK. These data are provided for KB 5378 in Table 4, and for the comparative sample in Supplementary Table 2.

Linear measurements of the KB 5378 carpals were taken directly from the fossils, apart from specific measurements that were inaccessible due to their preservation within the breccia. In these cases, measurements were taken digitally from surface models rendered from high-resolution microCT scans in Avizo 9.0 lite (Thermo Fisher Scientific 2019) (Table 5). All of the KB 5378 carpals were scanned using a Diondo 1 microCT scanner housed at the Imaging Centre for Life Sciences, University of Kent (Canterbury, UK) at 140kV, 140Ma, and a resolution of 24.035 microns. The three carpals articulated within the breccia were segmented manually in Avizo 9.0 lite (Thermo Fisher Scientific 2019). A 3D surface model of each carpal was generated and measured using the 3D measure tool in Avizo 9.0 lite (Thermo Fisher Scientific 2019). Measurements of the associated KB 5378 metacarpals were taken from photographs using ImageJ (version 1.53r).

To test the influence of intraobserver error, each carpal variable was measured twice on separate days on a sample of select taxa from the Powell Cotton Museum including *Cercocebus* (n=7), *Cercopithecus* (n=11), *Colobus* (n=8), *Lophocebus* (n=6), *Mandrillus* (n=3), and *Papio* (n=7). KB 5378 carpals were also measured by hand (or digitally for specific variables) three times over the course of several weeks. Linear measurements of the KB 5378 metacarpals from photographs were also repeated three times. To mitigate the in-

TABLE 3. MAXIMUM COMPARATIVE SAMPLE OF EXTANT TAXA.[+]

Genus	*Species*	*Body Mass (kg)*	*Element*	*n*	♀	♂	*?*
Alouatta	*palliata*	♂ 4.5–9.8[1] ♀3.1–7.6[1]	Lunate, Capitate, Hamate	9	6	3	-
	caraya	♂ 5–8.2[1] ♀3.8–5.4[1]	Lunate, Capitate, Hamate	2	1	1	-
	fusca	♂5.3–7.1[1] ♀4.1–5.0[1]	Lunate, Capitate, Hamate	1	1	-	-
	sp.		Lunate, Capitate, Hamate	4	3	-	1
			TOTAL	**16**	**11**	**4**	**1**
Ateles	*paniscus*	♂5.5–9.2[1] ♀6.5–11[1]	Lunate, Hamate	1	-	1	-
	geoffroyi	♂7.4–9.0[1] ♀6–8.9[1]	Lunate, Capitate, Hamate	2	1	-	1
	fusciceps	♂8.9[1] ♀8.8[1]	Lunate, Hamate Capitate	2	-	2	-
	sp.		Lunate, Capitate, Hamate	1	1	-	-
			TOTAL	**6**	**2**	**3**	**1**
Cercocebus	*torquatus*	♂10.7[1] ♀5.5[3]	Lunate, Trapezium, Trapezoid, Capitate, Hamate, OC	7	2	5	-
			TOTAL	**7**	**2**	**5**	**0**
Cercopithecus	*neglectus*	♂7.0–8.0[1] ♀4.5[1]	Lunate,	1	-	1	-
	nictitans	♂6.3[1] ♀4.1[1]	Lunate, Trapezium, Trapezoid, Capitate, Hamate, OC	6	3	4	-
	ascanius	♂4.2[1] ♀3.3[1]	Lunate, Hamate, OC	1	-	1	-
	mitis	♂7.4[1] ♀4.2[1]	Lunate, Capitate, Hamate	11	5	6	-
			TOTAL	**19**	**8**	**11**	**0**
Chlorocebus	*aethiops*	♂5–5.5[2] ♀3–3.5[2]	Lunate, Capitate, Hamate, OC	12	2	8	2
			TOTAL	**12**	**2**	**8**	**2**
Colobus	*guereza*	♂11–13[2] ♀7.5–9[2]	Lunate, Trapezium, Trapezoid, Capitate, Hamate, OC	7	2	5	-
	badius	♂8.3[1] ♀8.2[1]	Lunate, Trapezium, Trapezoid, Capitate, Hamate, OC	1	-	1	-
			TOTAL	**8**	**2**	**6**	**0**
Erythrocebus	*patas*	♂7.0–13.0[1] ♀4.0–7.0[1]	Capitate, Hamate, OC	6	2	3	1
			TOTAL	**6**	**2**	**3**	**1**
Gorilla	*gorilla*	♂169.5[1] ♀71.5[1]	Lunate, Trapezium, Trapezoid, Capitate, Hamate	23	12	10	1
	beringei	♂159.2[1] ♀97.7[1]	Lunate, Trapezium, Trapezoid, Capitate, Hamate	12	6	6	-
			TOTAL	**35**	**18**	**16**	**1**

TABLE 3. MAXIMUM COMPARATIVE SAMPLE OF EXTANT TAXA (continued).+

Genus	*Species*	*Body Mass (kg)*	*Element*	*n*	*♀*	*♂*	*?*
Hylobates	*lar*	♂4.9–7.6[1] ♀4.4–6.8[1]	Lunate, Capitate, Hamate, OC	29	13	14	2
	moloch	♂/♀ 5.7[1]	OC	2	-	2	-
	muelleri	♂/♀ 5.0–6.4[1]	OC	2	2	-	-
	pileatus	♂7.9–10.4[1] ♀6.3–8.6[1]	OC	1	-	1	-
	concolor	♂/♀ 4.5–9.0[1]	OC	1	-	1	-
	agilis	♂5.88[3] ♀5.5–6.4[1]	OC	1	-	1	-
	klossi	♂/♀ 5.8[1]	OC	1	1	-	-
	sp.		OC	2	1	1	-
			TOTAL	**39**	**17**	**20**	**2**
Lagothrix	*lagrothricha*	♂3.6–10.0[1] ♀3.5–6.5[1]	Lunate, Capitate, Hamate	6	3	3	-
	sp.		Lunate, Capitate, Hamate	1	-	1	-
			TOTAL	**7**	**3**	**4**	**0**
Lophocebus	*albigena*	♂10.5–16[2] ♀5.5–7.5[2]	Lunate, Trapezium, Trapezoid, Capitate, Hamate, OC, MC1-5	6	2	4	-
			TOTAL	**6**	**2**	**4**	**0**
Macaca	*fascicularis*	♂4.7–8.3[1] ♀2.5–5.7[1]	Lunate, Capitate, Hamate, OC	35	18	17	-
	mulatta	♂5.6–10.9[1] ♀4.4–10.9[1]	Lunate, Capitate, Hamate, OC	33	15	13	5
			TOTAL	**68**	**33**	**30**	**5**
Mandrillus	*leucophaeus*	♂17.0[1] ♀10.0[1]	Lunate, Trapezium, Trapezoid, Capitate, Hamate, OC, MC1-5	2	1	1	-
	sphinx	♂29–47[2] ♀6.9–12[2]	Lunate, Trapezium, Trapezoid, Capitate, Hamate, OC, MC1-5	1	-	1	-
			TOTAL	**3**	**1**	**2**	**0**
Pan	*paniscus*	♂39.0[1] ♀31.0[1]	Lunate, Trapezium, Trapezoid, Capitate, Hamate, MC1-5	12	5	7	-
	troglodytes	♂40–60[1] ♀32–47[1]	Lunate, Trapezium, Trapezoid, Capitate, Hamate, MC1-5	26	13	10	3
			TOTAL	**38**	**18**	**17**	**3**
Papio	*anubis*	♂22–37.2[1] ♀14.5–14.9[1]	Lunate, Trapezium, Trapezoid, Capitate, Hamate, OC, MC1-5	13	5	8	-
	hamadryas	♂21.3[1] ♀12[1]	Lunate, Trapezium, Trapezoid, Capitate, Hamate, OC	3	1	2	-
	cynocephalus	♂24–27[2] ♀11–13[2]	OC	1	1	-	-
	papio	♂/♀ 17.6[1]	Lunate, Hamate OC, MC1-5	1	1	-	-
	doguera	♂22–37.2[1] ♀14.5–14.9[1]	Lunate, Hamate OC	2	-	2	-
	sp.		Lunate, Hamate OC,	2	-	1	1
			TOTAL	**22**	**8**	**13**	**1**

TABLE 3. MAXIMUM COMPARATIVE SAMPLE OF EXTANT TAXA (continued).[+]

Genus	*Species*	*Body Mass (kg)*	*Element*	*n*	♀	♂	*?*
	frontatus	♂5.6[1] ♀5.7[1]	Capitate, Hamate	1	1	-	-
	sp.		Lunate, Capitate, Hamate	1	-	1	-
			TOTAL	**3**	**1**	**2**	**0**
Theropithecus	*gelada*	♂14–19[2] ♀9–12[2]	Capitate, Hamate, Metacarpal 1*	10	4	6	-
			TOTAL	**10**	**4**	**6**	**0**
			FULL SAMPLE	**305**	**134**	**154**	**17**

[+]Sample varies per carpal so the elements present per species are listed. '?' denotes individuals of an unknown sex. An asterisk (*) indicates elements of a species taken from literature (Frost et al. 2015). Body masses taken from literature including Rowe et. Al 1996 ([1]) Delson et al. 2000 ([2]), and Smith and Jungers 1997 ([3]).

TABLE 4. DESCRIPTION OF EACH LINEAR VARIABLE USED TO QUANTIFY THE EXTERNAL MORPHOLOGY OF EACH CARPAL.

Variable	Description
Scaphoid	
SBH	Maximum dorsopalmar measure of the the scaphoid body
SBL	Maximum proximodistal measure of the scaphoid body
SBB	Maximum radioulnar measure of the scaphoid body
SPRFH	Maximum dorsopalmar measure of the scaphoid partial radial facet
SPRFL	Maximum proximodistal measure of the scaphoid partial radial facet
SPLFL	Maximum proximodistal measure of the scaphoid partial lunate facet
SPLFH	Maximum dorsopalmar measure of the scaphoid partial lunate facet
SPCFL	Maximum proximodistal measure of the partial capitate facet
SPCFH	Maximum dorsopalmar measure of the partial capitate facet
Os Centrale	
OCH	Maximum dorsopalmar measure of os centrale body
OCB	Maximum radioulnar measure of os centrale body
OCL	Maximum proximodistal measure of os centrale body
OCDFH	Maximum dorsopalmar measure of distal facet of os centrale
OCDFL	Maximum proximodistal measure of distal facet of os centrale

TABLE 4. DESCRIPTION OF EACH LINEAR VARIABLE USED TO QUANTIFY THE EXTERNAL MORPHOLOGY OF EACH CARPAL (continued).

Variable	Description
Lunate	
HLB	Maximum dorsopalmar measure of lunate body
LLB	Maximum proximodistal measure of lunate body
LLSF	Maximum proximodistal measure of lunate scaphoid facet
HLSF	Maximum dorsopalmar measure of lunate scaphoid facet
LLTF	Maximum proximodistal measure of lunate triquetrum facet
HLTF	Maximum dorsopalmar measure of lunate triquetrum facet
HLDF	Maximum dorsopalmar measure of lunate distal facet
BLDF	Maximum radioulnar measure of lunate distal facet
BLB	Maximum radioulnar measure of lunate base in palmar view
BLRF	Maximum radioulnar measure of lunate radial facet
HLRF	Maximum dorsopalmar measure of lunate radial facet
Trapezium	
LTMB	Maximum proximodistal measure of trapezium body
HTMB	Maximum dorsopalmar measure of trapezium
LMC1F*	In hominoids: Maximum proximodistal measure of the trapezium Mc1 facet In non-hominoids: Maximum measure across proximal most edge of trapezium Mc1 facet
BMC1F*	In hominoids: Maximum radioulnar measure of the trapezium Mc1 facet In non-hominoids: Maximum measure perpendicular to LMC1F of the trapezium Mc1 facet.
LTDF	Maximum proximodistal measure of the trapezium trapezoid facet
HTDF	Maximum dorsopalmar measure of the trapezium trapezoid facet
BTPF	Maximum radioulnar measure of trapezium proximal facet, encompassing scaphoid facet (hominoids) and os centrale facet (non-hominoids) if present.
LTPF	Maximum proximodistal measure of trapezium proximal facet, encompassing both scaphoid facet (hominoid) and os centrale facet (non-hominoid) if present.
LTDSF	Total maximum measure from extreme distal edge of trapezoid facet to extreme proximal, or opposite edge of proximal facet encompassing the entire trapezoid, scaphoid and os centrale facets.
Trapezoid	
HTDB	Maximum dorsopalmar measure of trapezoid body
LTDPS	Maximum proximodistal measure of trapezoid palmar surface
BTDDS	Maximum radioulnar measure of trapezoid distal surface
LDDS	Maximum proximodistal measure of trapezoid distal surface
HTDMC2	Maximum dorsopalmar measure of trapezoid Mc2 facet
BTDMC2	Maximum radioulnar measure of trapezoid Mc2 facet
HTDTMF	Maximum measure from border of trapezoid Mc2 facet to opposite, typically palmar, extreme of trapezoid trapezium facet.
LTDTMF	Maximum proximodistal measure of trapezoid trapezium facet

TABLE 4. DESCRIPTION OF EACH LINEAR VARIABLE USED TO QUANTIFY THE EXTERNAL MORPHOLOGY OF EACH CARPAL (continued).

Variable	Description
Capitate	
LCB	Maximum proximodistal measure of capitate body
HCB	Maximum dorsopalmar measure of capitate body
BCB	Maximum radioulnar measure of capitate body
LCHF	Maximum proximodistal measure of capitate hamate facet
HCHF	Maximum dorsopalmar measure of capitate hamate facet
HCTF	Maximum dorsopalmar measure of capitate trapezoid facet
LCTF	Maximum proximodistal measure of capitate trapezoid facet
HMC2	Maximum dorsopalmar measure of the total capitate Mc2 facet (if facet presented discontinuously, individual heights were summed and totaled to equal this variable).
LMC2	Maximum proximodistal measure of the total capitate Mc2 facet
DBMC3	Maximum radioulnar measure of the dorsal extreme of capitate Mc3 facet
PBMC3	Maximum radioulnar measure of the proximal extreme of capitate Mc3 facet
HMC3	Maximum dorsopalmar measure of capitate Mc3 facet
BCN	Minimum radioulnar measure of thinnest portion of capitate neck
HCPF	Maximum dorsopalmar measure of capitate proximal facet
BCPF	Maximum radioulnar measure of capitate proximal facet
Hamate	
HHB	Maximum dorsopalmar measure of hamate, including hamulus
HHB-H	Maximum dorsopalmar measure of hamate, excluding hamulus
HHH	Maximum dorsopalmar measure of hamate hamulus, typically obtained from subtraction of HHB-H from HHB
LHB	Maximum proximodistal measure of hamate, including hamulus
LHB-H	Maximum proximodistal measure of hamate, excluding hamulus
LHH	Maximum proximodistal measure of hamulus, typically obtained from subtraction of LHB-H from LHB.
HHCF	Maximum dorsopalmar measure of hamate capitate facet
LCHF	Maximum proximodistal measure of hamate capitate facet
HHTF	Maximum dorsopalmar measure of hamate triquetrum facet
LHTF	Maximum proximodistal measure of hamate triquetrum facet
BHB	Maximum radioulnar measure of hamate from dorsal view
BHDF	Maximum radioulnar measure of hamate distal facet, encompassing all metacarpal facets
HHDF	Maximum dorsopalmar measure of hamate distal facet, encompassing all metacarpal facets
BMC4	Maximum radioulnar measure of hamate Mc4 facet
HMC4	Maximum dorsopalmar measure of hamate Mc4 facet
BMC5	Maximum radioulnar measure of hamate Mc5 facet
HMC5	Maximum dorsopalmar measure of hamate Mc5 facet

TABLE 4. DESCRIPTION OF EACH LINEAR VARIABLE USED TO QUANTIFY THE EXTERNAL MORPHOLOGY OF EACH CARPAL (continued).

Variable	Description
Metacarpals	
LMC1	Maximum proximodistal length of the first metacarpal
LMC2	Maximum proximodistal length of the second metacarpal
LMC3	Maximum proximodistal length of the third metacarpal
LMC4	Maximum proximodistal length of the fourth metacarpal
LMC5	Maximum proximodistal length of the fifth metacarpal

TABLE 5. UNADJUSTED MEASUREMENTS OF ALL CARPAL ELEMENTS OF KB 5378.*

Scaphoid Fragment

SBH	*SBL*	*SBB*	*SPRFH*	*SPRFL*	*SPLFL*	*SPLFH*	*SPCFL*	*SPCFH*
13.1	10.8	5.4	11.1	12.9	10.8	6.2	9.1	8.9

Os Centrale

OCH	*OCL*	*OCB*	*ODCFH*	*OCDFL*
9.2	11.7	5.9	9.3	8.8

Lunate

LLB	*HLB*	*BLB*	*HLSF*	*LLSF*	*HLDF*	*BLDF*	*HLRF*	*BLRF*	*HLTF*	*LLTF*
14.7	13.7	8.7	11.0	5.9	10.4	6.2	13.2	9.7	9.6	10.9

Trapezium

LTMB	*HTMB*	*LTDF*	*HTDF*	*BTPF*	*LTPF*	*LMC1F*	*BMC1F*	*LTDSF*	*LTMB*	*HTMB*
12.7	8.4	7.4	5.7	5.5	6.0	7.3	8.5	9.6	12.7	8.41

Trapezoid

HTDB	*LTDPS*	*LTDDS*	*BTDDS*	*HTDTMF*	*LTDTMF*	*HTDMC2*	*BTDMC2*
12.5	5.1	12.6	9.3	7.3	5.9	11.9	8.9

Capitate

LCB	*HCB*	*BCB*	*HCHF*	*LCHF*	*BCPF*	*HCPF*	*BCN*
17.2	14.6	13.3	10.8	12.2	6.1	7.0	5.9

Hamate

LHB	*LHB-H*	*HHB*	*HHB-H*	*BHB*	*HHCF*	*LHCF*	*HHTF*	*LHTF*
17.1	17.1	13.2	8.4	11.1	8.1	11.5	7.2	13.6

Metacarpals

LMC1	*LMC2*	*LMC3*	*LMC4*	*LMC5*
48.7	63.4	61.3	60.7	62.5

*All measurements were taken by MR using digital calipers, or, in the case of bones inaccessible for measurement due to preservation in breccia, using Avizo 9.0 lite (Thermo Fisher Scientific 2019). Refer to Table 3 for definitions of all carpal shape variable abbreviations. All

fluence of interobserver error, TLK and MR collected data simultaneously and confirmed accuracy to 0.1mm between measurements.

To account for variation in body (and consequently gross carpal) size across the comparative sample, a geometric mean of a custom set of measurements for each bone was calculated (Supplementary Table 3) and used in all comparative analyses, excluding those of absolute size. Each morphometric variable was divided by a geometric mean of the respective carpal to create 'size adjusted' variables (Jungers et al. 1995), in addition to the raw variables. For analyses of absolute size, raw data were used.

STATISTICAL ANALYSES

All data were analyzed in R Studio (v4.1.2 packages dplry, Ggally and ggplot2; R Core Team 2021; Schloerke et al. 2021; Wickham 2016; Wickham et al. 2021) and PAST (version 4.03; Hammer et al. 2001). Normality of the data was assessed using a Shapiro-Wilk test for all variables and each taxon. Covariance between variables was assessed using Pearson's correlation coefficients to exclude any variables that were significantly correlated ($r>0.9$). Variation in individual measured variables between taxa was investigated using box-and-whiskers plots. Further, to assess variation in shape ratios, within-group, covariance-variance principal component analyses (PCA) were performed in PAST. Covariance-variance matrix based, within-group PCA was favored for this study because all variables within this study are measured in the same units, and because differences in the variance between variables are the main factor being identified (Queen et al. 2002). Due to the irregular and often small ($n=<10$) number of individuals per taxon in this study, between group PCA tests were deemed inappropriate (Bookstein 2019). Variables included in the PCA plots and their loadings for each carpal are listed in Supplementary Table 4. Finally, bivariate plots comparing the length of the capitate body to the lengths of each metacarpal were performed to assess whether the KB 5378 carpus and metacarpus could be attributed to the same individual. In this study, the length of the capitate body was used as a proxy to general carpus size.

RESULTS

ANATOMICAL DESCRIPTION OF KB 5378 CARPALS

All of the KB 5378 carpals described below are from the left side and appear to be adult in morphology—the preserved anatomy appears fully developed, including the tip of the hamulus which is one of the last regions to fully ossify, and the facets are well-defined (Kivell 2007). However, the tip of the scaphoid tubercle and the pisiform epiphysis are also regions that ossify late in the primate carpus and are not preserved, complicating definitive age assignment.

Scaphoid Fragment

Preservation: The scaphoid of KB 5378 preserves only the proximal half, including partial facets for the radius, os centrale, and lunate (Figure 3). It remains embedded within matrix together with the capitate and os centrale. A digital surface model reveals that the cortex is well preserved outside of the area of breakage.

Morphology: The scaphoid fragment measures 13.1mm in dorsopalmar height, 10.8mm in proximodistal length, and 5.4mm in radioulnar breadth. No complete facets are preserved. The partial radial facet is radioulnarly and dorsopalmarly flat and measures 11.1mm in dorsopalmar height and 12.9mm in proximodistal length. The fragment contains a nearly complete lunate facet, missing only its palmar-most edge, measuring 10.8mm in proximodistal length and 6.2mm in dorsopalmar height. The lunate facet is slightly convex and is oriented ulnarly. The partial capitate facet is missing its palmar edge, is concave, and measures 9.1mm proximodistally and 8.9mm dorsopalmarly.

Os Centrale

Preservation: The KB 5378 os centrale is complete and all facets are well preserved. However, it remains embedded within matrix roughly in anatomical position with the capitate and the partial scaphoid (Figure 4). Thus, the morphology described below is based on the digital reconstruction from high-resolution microCT scans.

Morphology: The os centrale measures 9.2mm in dorsopalmar height, 11.7mm in proximodistal length, and 5.9mm in radioulnar breadth. The distal facet for the capitate is concave and circular in shape, measuring 9.3mm dorsopalmarly and 8.8mm proximodistally. Additionally, there is a small facet present on the proximoulnar corner measuring 5.6mm proximodistally and 2.7mm radioulnarly that contacts the distal most edge of the radial facet of the lunate. The scaphoid facet of the os centrale is convex, measuring 7.1mm in dorsopalmar height and 7.2mm in proximodistal length. Finally, the trapezoid-trapezium facet is round, concave, and expands across the entire radial side of the os centrale. It measures 9.7mm in radioulnar breadth and 7.9mm in dorsopalmar height. The angle between the scaphoid and trapezium facet, taken at the approximate midpoint of each facet, is 88.1°.

Lunate

Preservation: The lunate is complete and well preserved. All facets are clearly distinguishable and well defined (Figure 5). There is a crack in the cortex that obliquely crosses the triquetrum facet from the radial facet to the distal facet and continues dorsopalmarly across the distal facet to its dorsal extreme. This crack does not significantly alter the facet morphology.

Morphology: The KB 5378 lunate body is 14.7mm in proximodistal length, 13.7mm in dorsopalmar height and 8.7mm in radioulnar breadth. The scaphoid facet is flat and extends dorsopalmarly along the entire edge of the distal facet. The scaphoid facet measures a maximum of 5.9mm in proximodistal length and 11.0mm in dorsopalmar height, and its palmar half is proximodistally longer than the dorsal half. The distal articulation is concave and shows only an articulation for the capitate (i.e., a hamate facet is not

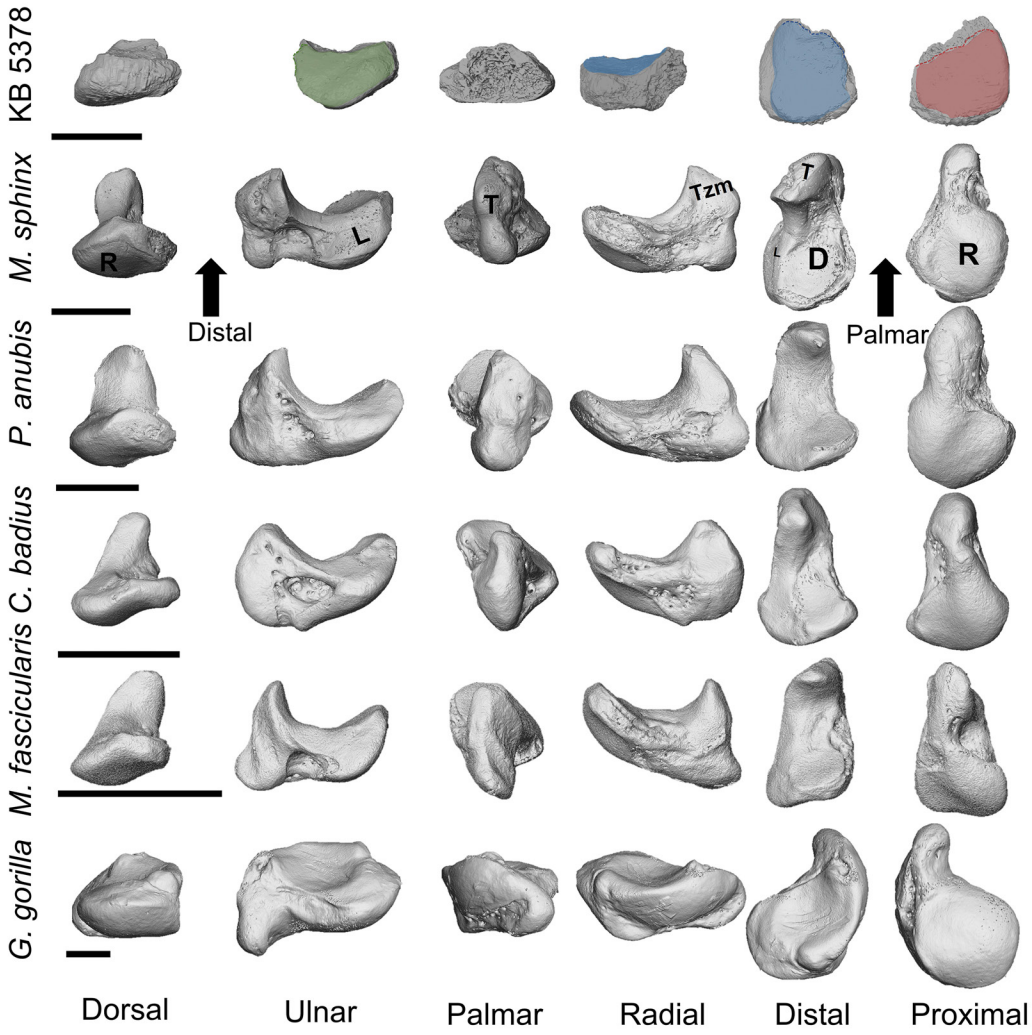

Figure 3. Anatomical views of the KB 5378 scaphoid in comparison to, from top to bottom, M. sphinx, P. Anubis, C. badius, M. fascicularis, *and* G. gorilla. *All bones are oriented to represent the left side and are scaled to the same size, with the bar beneath each taxon representing 1cm. The articular facets are labelled in* M. sphinx *as follows: R, radial facet; L, lunate; T, tubercle; Tzm, trapezium and/or trapezoid shared facet; D, distal facet. Note that the broken areas of the KB 5378 fragment are clearest in the palmar and radial view.*

present), measuring 10.4mm in dorsopalmar height and 6.2mm in radioulnar breadth. The triquetrum facet is flat and rectangular, expanding across nearly the full proximodistal length of the ulnar side of the lunate, and measures 9.6mm in dorsopalmar height and 10.9mm in proximodistal length. The radial facet is large, proximodistally convex, and dominates the proximal view of the lunate measuring 13.2mm in dorsopalmar height and 9.7mm in radioulnar breadth.

Trapezium

Preservation: The trapezium shows small areas of cortical wear on the first metacarpal (Mc1) facet, rendering that facet rough in texture (Figure 6). Otherwise, the bone is complete, and all facets are clearly distinguishable.

Morphology: The trapezium of KB 5378 is rectangular in dorsal view and does not have a pronounced tubercle. Its overall size is 12.7mm in proximodistal length, 8.4mm in dorsopalmar height, and 8.0mm in radioulnar breadth. The Mc1 facet is oval-shaped, slightly convex, and spans the entire distal length of the bone, measuring 8.5mm in radioulnar breadth and 7.3mm in proximodistal length. The trapezoid facet is also oval in shape, slightly convex radioulnarly, and covers approximately half of the ulnar side of the bone. It is 7.4mm in proximodistal length and 5.7mm in dorsopalmar height. The proximal facet, which articulates with the scaphoid and, in monkeys, the os centrale, is small, oblong, and measures 5.5mm in radioulnar breadth and 6.0mm in proximodistal length. It is positioned parallel to the Mc1 facet's distal-most edge.

Trapezoid

Preservation: The trapezoid is complete and well preserved apart from a small area of cortical wear at the dorsal-most

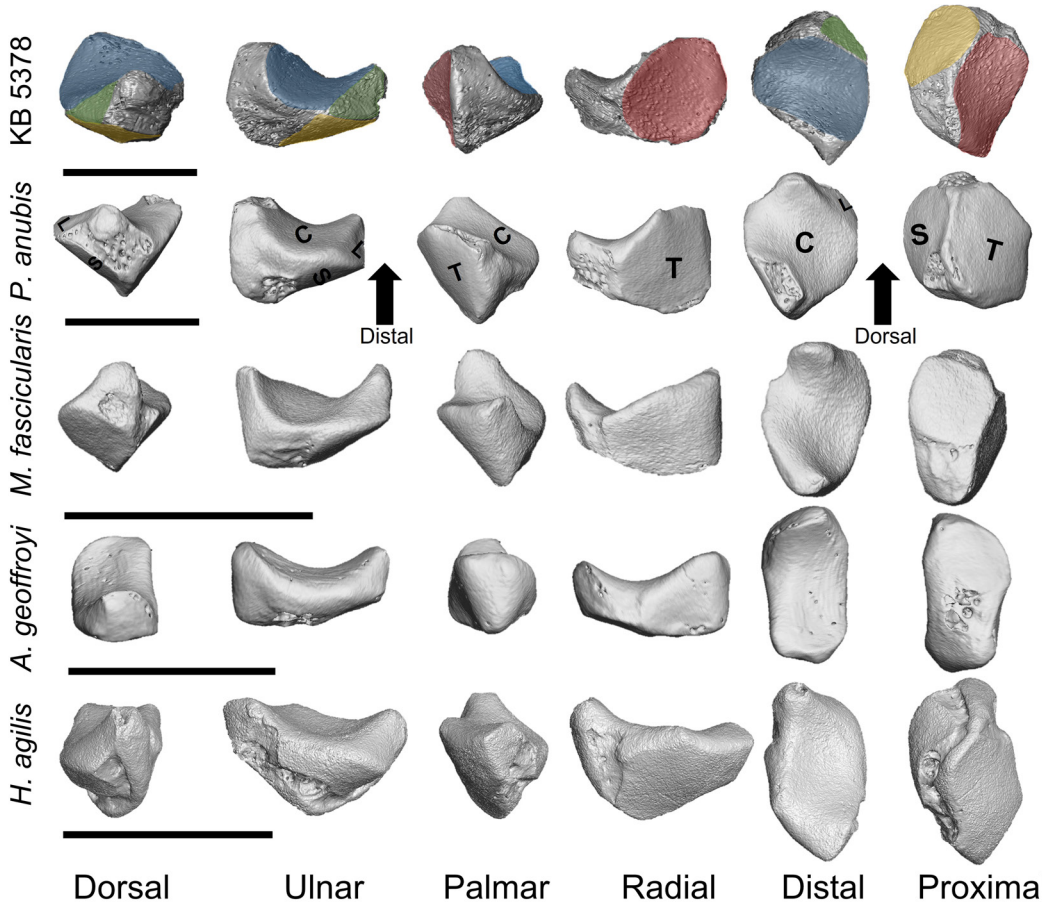

Figure 4. Anatomical views of the KB 5378 os centrale in comparison to, from top to bottom, P. anubis, M. fascicularis, A. geoffroyi, *and* H. agilis. *All bones are oriented to represent the left side and are scaled to the same size, with a bar placed beneath each taxa representing 1cm. The articular facets are labelled in* P. anubis *as follows: D, non-articular dorsal surface; S, scaphoid; C, capitate; L, lunate; T, trapezoid/trapezium shared facet.*

edge of the Mc2 articular surface that exposes trabecular bone (Figure 7).

Morphology: The trapezoid is triangular in shape in radial and ulnar view. Overall, its body measures 12.5mm in proximodistal length, 12.3mm in dorsopalmar height and 9.1mm in radioulnar breadth. The Mc2 articulation of the trapezoid is slightly concave and measures 11.9mm dorsopalmarly and 8.9mm radioulnarly. The trapezoid is keeled distally, but the ridge on the dorsal-most edge that creates a keeled appearance does not extend palmarly onto the Mc2 facet. The capitate facet is smooth and convex, measuring 9.3mm dorsopalmarly and 5.8mm proximodistally and covers most of the ulnar side of the bone. A sulcus measuring 3.2mm in proximodistal length and 8.8mm in dorsopalmar height for the capito-trapezoid interosseous ligament separates the capitate and Mc2 facets. The trapezium facet is rectangular in shape, flat, and measures 5.9mm in proximodistal length and 7.3mm in dorsopalmar height.

Capitate

Preservation: The capitate of KB 5378 is complete, and still partially embedded in the matrix also containing the os centrale and partial scaphoid fragment (Figure 8). The cortex is eroded in some areas of the distal metacarpal facets to expose trabecular bone. The descriptions below were based on both the physical bone and 3D surface models.

Morphology: The capitate body measures 17.2mm in proximodistal length, 14.7mm in dorsopalmar height and 13.3mm in radioulnar breadth. It exhibits clear constriction at the neck of the capitate, which measures 5.9mm in radioulnar breadth. The proximal facet is round and measures 6.1mm in radioulnar breadth, 7.0mm in dorsopalmar height, and does not show a clear distinction between the scaphoid and lunate articulations. The trapezoid facet is triangular and bordered palmarly by the sulcus for the capitate-trapezoid interosseous ligament. It measures 3.3mm in dorsopalmar height and 6.6mm in proximodistal length. The Mc3 facet dominates the entire distal surface of the capitate, measuring 14.0mm in dorsopalmar height. It is radioulnarly broader dorsally (13.3mm) than it is palmarly (4.4mm), such that it tapers to a point towards its palmar end. The Mc3 facet surface is dorsally concave but flattens palmarly. The Mc2 facet is split into two proximodistally narrow, radially facing facets by a non-articular sulcus. Its dorsal portion is rectangular, measuring 2.8mm in proximodistal length and 4.5mm in dorsopalmar height, while

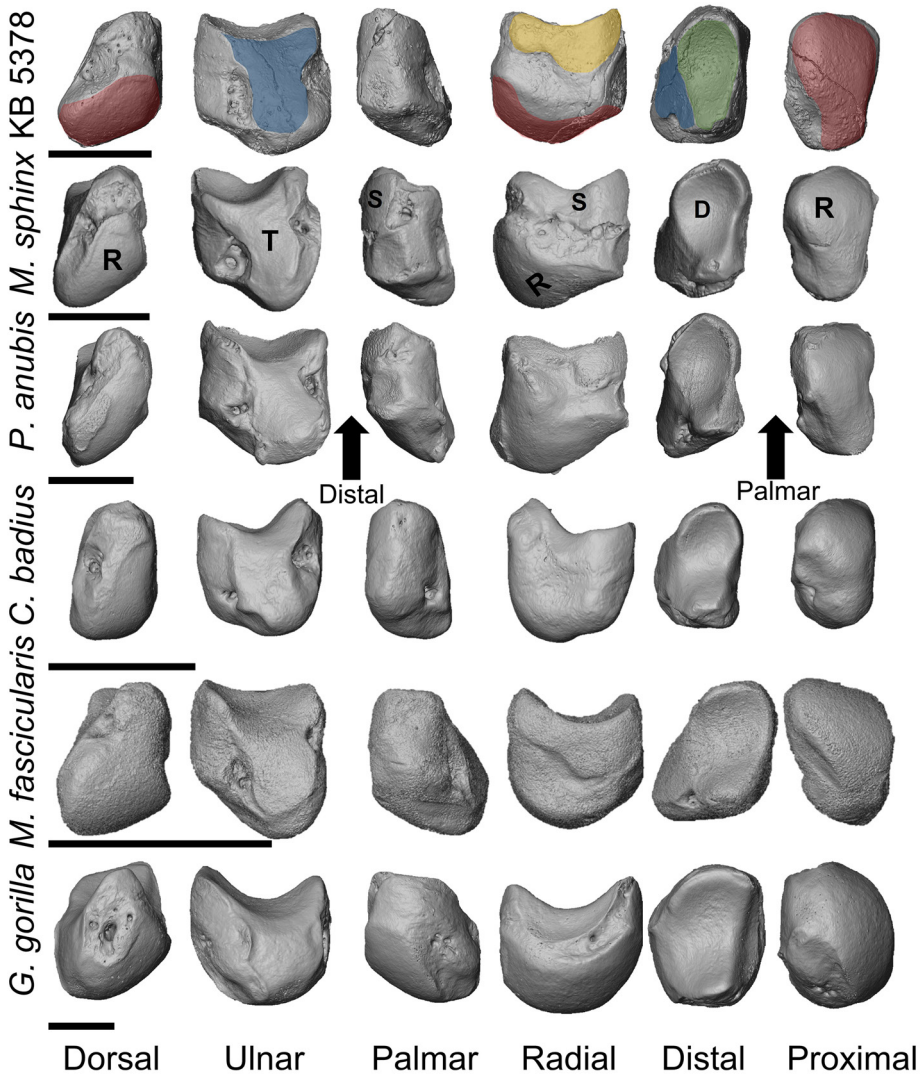

Figure 5. Anatomical views of the KB 5378 lunate in comparison to, from top to bottom, M. sphinx, P. anubis, C. badius, M. fascicularis, *and* G. gorilla. *All bones are oriented to represent the left side and are scaled to the same size, with a bar beneath each taxon representing 1cm. The articular facets are labelled in* M. sphinx *as follows: R, radial; T, triquetrum; S, scaphoid; D, distal facet.*

its palmar portion is 0.5mm in proximodistal length and 3.1mm in dorsopalmar height. Together, including the distance across the sulcus, the Mc2 facets measure 13.8mm in dorsopalmar height and 2.8mm in proximodistal length. Finally, the hamate facet measures 10.8mm in dorsopalmar height and 12.2mm in proximodistal length and follows the entire dorsal edge of the ulnar side of the capitate. It is slightly concave at its proximodistal midpoint as it follows the taper of the capitate neck. The hamate facet's proximal end is round and radioulnarly concave while the distal end is dorsopalmarly narrow and flat and ends at the edge of the Mc3 facet.

Hamate

Preservation: The hamate is complete and well preserved; all facets are clearly distinguishable (Figure 9).

Morphology: The hamate body is 17.1mm in proximodistal length, 11.1mm in radioulnar breadth, and 13.2mm in dorsopalmar height, giving it an overall narrow appearance. Its hamulus is small, radioulnarly broad, and rounded, extending palmarly only slightly beyond the distal metacarpal articular surfaces. The hamulus extends distally and does not curve ulnarly or radially. The capitate facet takes up most of the radial side of the hamate, measuring 8.1mm in dorsopalmar height and 11.5mm in proximodistal length. This facet is constricted at its approximate proximodistal midline giving it a curved "hourglass" shape. It is flat distally but follows the overall curve of the proximal end of the hamate to become convex at its proximal extreme. The triquetrum facet measures 7.2mm in dorsopalmar height and 13.6mm in proximodistal length, covering the entire ulnar side of the hamate. It is flat proximally but becomes radioulnarly concave distally, and the entire facet is proximoulnarly oriented when in articulation (see Figure 1). The Mc4 facet measures 10.8mm in dorsopalmar height and 6.4mm in radioulnar breadth, with its

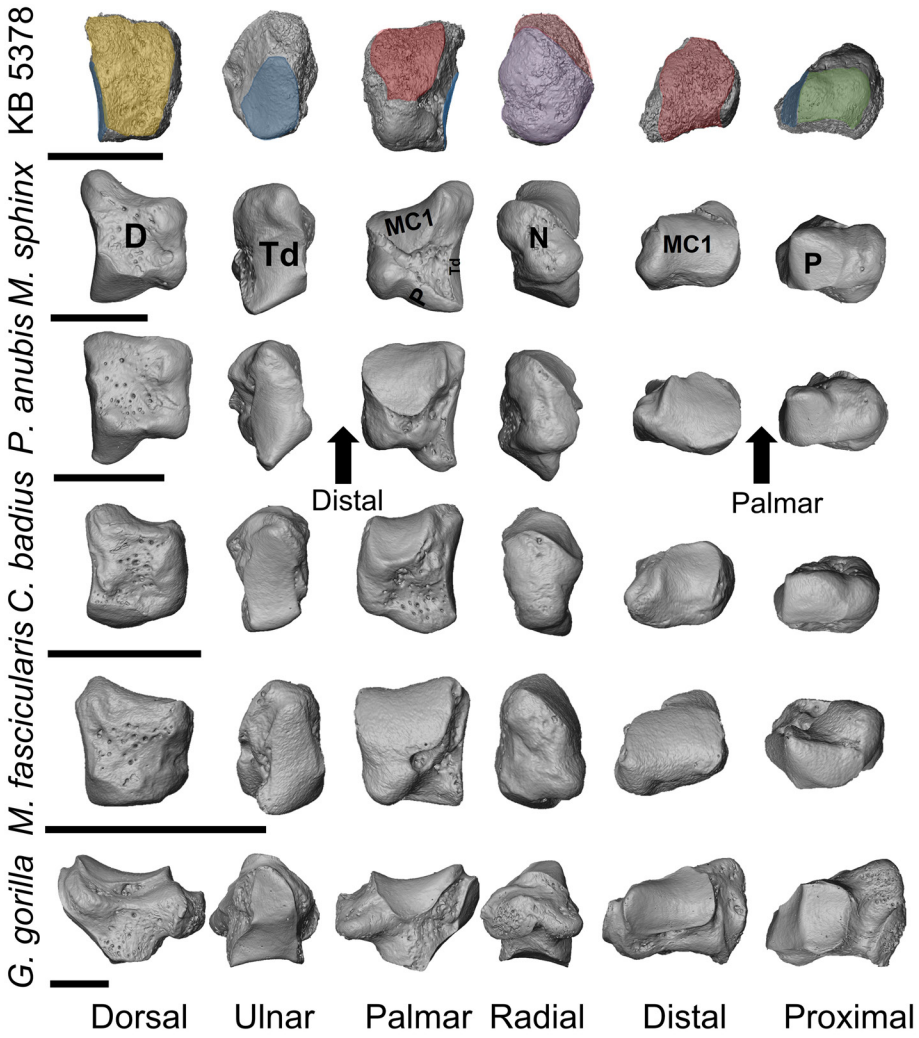

Figure 6. Anatomical views of the KB 5378 trapezium in comparison to, from top to bottom, M. sphinx, P. Anubis, C. badius, M. fascicularis, *and* G. gorilla. *All bones are oriented to represent the left side bone and scaled to the same size, with a bar placed beneath each taxa representing 1cm for scale. The articular facets are labelled in* M. sphinx *as follows: D, non-articular dorsal surface; Td, trapezoid; Mc1, metacarpal 1; N, radial non articular surface; P, proximal facet encompassing the scaphoid facet (hominoids) and os centrale facet (non-hominoids) if present.*

palmar border at the start of the hamulus. It is angled radially at approximately 45° relative to the distally facing Mc5 facet. The Mc5 facet is rectangular and concave, measuring 11.0mm in dorsopalmar height and 7.7mm in radioulnar breadth. The angled morphology of the Mc4 and Mc5 facets produce a sharply angled distal edge of the dorsal surface of the hamate.

COMPARATIVE MORPHOLOGY

Below we describe the morphology of each KB 5378 carpal within the context of the comparative sample. All measurements discussed below have been divided by a geometric mean to facilitate comparisons among specimens of different overall sizes. For each carpal bone (excluding the scaphoid), univariate comparisons via box-and-whisker plots of the most informative variables are described first, followed by the PCA results. Results described but not figured in text can be found figured in supplementary materials. Latter sections on absolute size comparisons are based on raw data.

Scaphoid

The scaphoid of KB 5378 preserves only limited informative morphology. The most functionally (and taxonomically) diagnostic features of the scaphoid, such as the size and orientation of the tubercle, are not preserved, and none of the facets are complete (see Figure 3). The lunate facet is the best preserved and is similar in morphology to *Mandrillus* and, to a lesser degree, *M. fascicularis* in being dorsopalmarly broad, flat, and oriented distoulnarly. The partial radial facet is flat and most similar to other cercopithecoids in our sample. The partial os centrale facet is shallowly concave like *Mandrillus* and other cercopithecoids in our sample and unlike the more deeply concave os centrale facet of the arboreal *Colobus*.

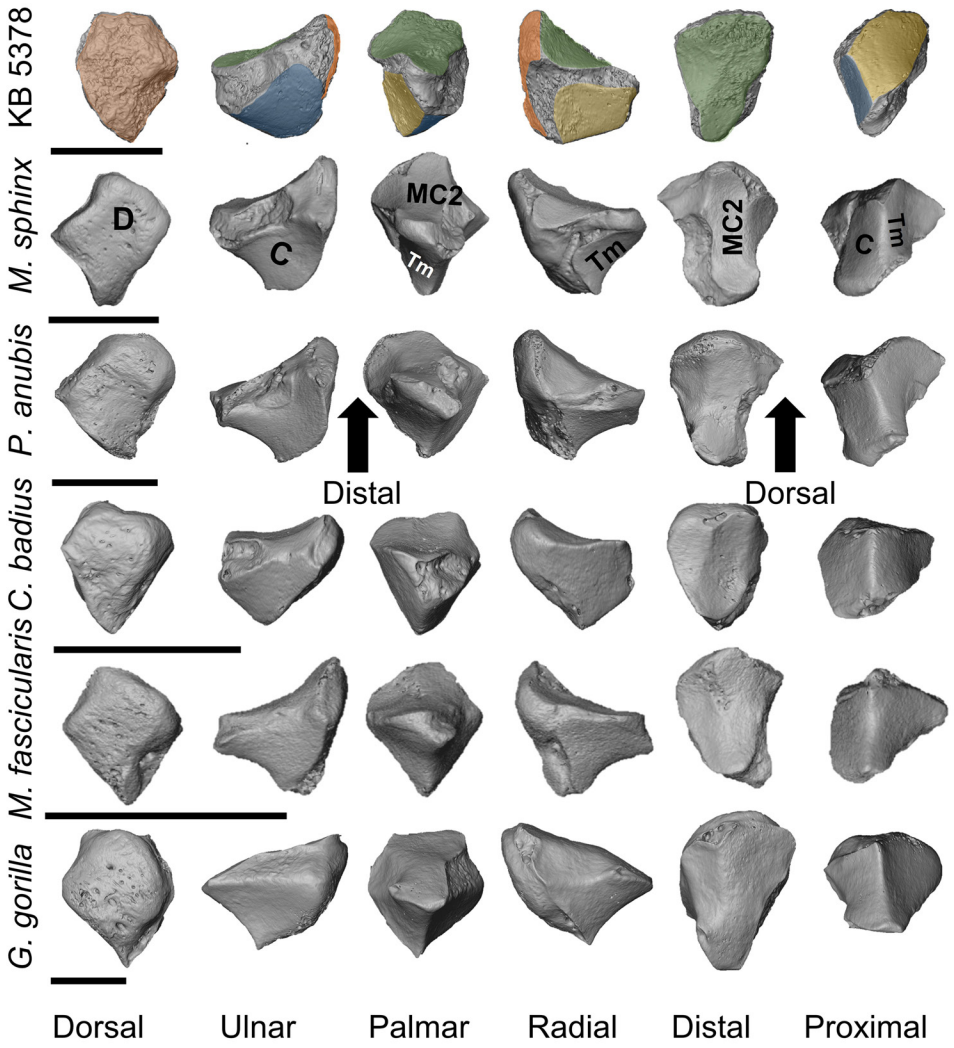

Figure 7. Anatomical views of the KB 5378 trapezoid bone in comparison to, from top to bottom, M. sphinx, P. anubis, C. badius, M. fascicularis, *and* G. gorilla. *All bones are oriented to represent the left side and scaled to the same size, with a bar placed beneath each taxa representing 1cm for scale. The articular facets are labelled in* M. sphinx *as follows: D, non-articular dorsal surface; C, capitate; Tm, trapezium facet; Mc2, metacarpal 2.*

Os Centrale

KB 5378 has an os centrale characterized by a radioulnarly narrow and dorsopalmarly tall body when compared to all extant taxa, although box-and-whisker plots reveal substantial overlap with both arboreal and terrestrial quadrupedal monkeys. Its distal facet for the capitate is distinct among the comparative sample in being particularly dorsopalmarly tall but proximodistally short (Figure 10). In dorsopalmar height, it falls outside the range of variation of all taxa and is only similar to the outliers of *M. fascicularis*. However, its proximodistal length is most similar to *Colobus* and terrestrial monkeys. In general, the os centrale morphology of KB 5378 does not align with any particular locomotor group.

The PCA supports the findings of the box-and-whiskers plots of the os centrale in showing that KB 5378 is only truly distinct in morphology from suspensory taxa along both PC1 and PC2 (which describe 60.0% and 25.4% of the total variance, respectively, of the os centrale) (Supplementary Figure 1; see Supplementary Table 4).

Lunate

The radioulnar breadth of the KB 5378 lunate body is most similar to the arboreal quadrupedal *M. fascicularis* and *Colobus*, but in dorsopalmar height and proximodistal length of the body KB 5378 falls within the ranges of most comparative taxa, excluding *Pan, Presbytis*, and *Colobus* (Figure 11). It has a small distal facet for the capitate in both radioulnar breadth and dorsopalmar height (see Figure 11). The reduced size of the distal facet combined with the average-sized radial facet (in both radioulnar breadth and dorsopalmar height) creates a lunate body which becomes gradually radioulnarly broader from distal to proximal end, similar to the morphology seen in *Mandrillus* and *M. mulatta.* Additionally, KB 5378 shows a proximodistally and dorsopalmarly expanded triquetrum facet similar in height

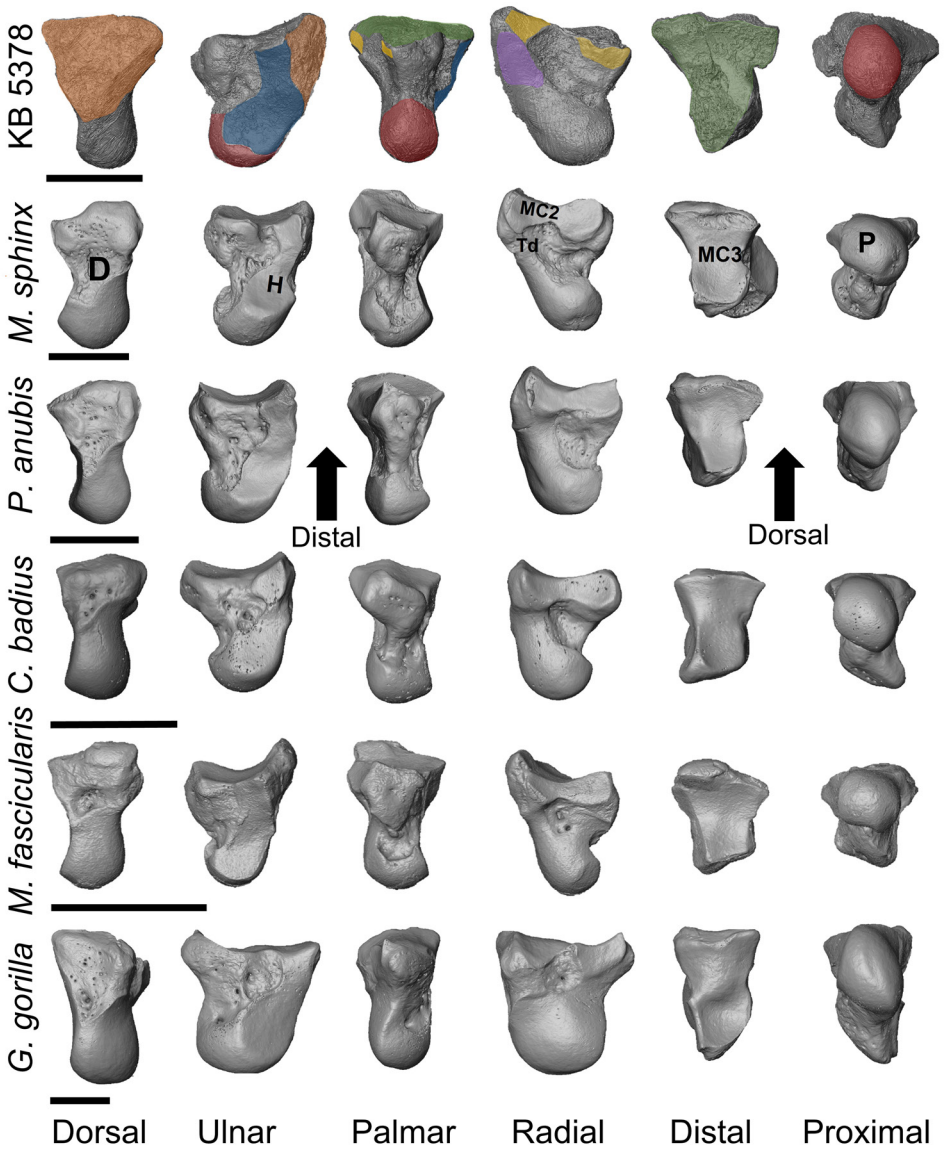

Figure 8. Anatomical views of the KB 5378 capitate bone in comparison to, from top to bottom, M. sphinx, *P. anubis,* C. badius, M. fascicularis, *and* G. gorilla. *All bones are oriented to represent the left sided bone and scaled to the same size, with a bar placed beneath each taxa representing 1cm for scale. Articular facets are labelled in* M. sphinx *as follows: D, dorsal non articular surface; H, hamate; MC2, metacarpal 2; Td, trapezoid; Mc3, metacarpal 3; P, proximal facet/ "head" of the capitate.*

only to *Colobus* and *Lophocebus*, and in length to *Mandrillus* (Supplementary Figure 2). Overall, box-and-whisker plots show that the KB 5378 lunate morphology is distinct from knuckle-walking taxa, but generally falls within the range of variation of all other locomotor groups (see Figure 11).

Principal component analysis reveals similar trends in morphology to those of the box-and-whisker plots. KB 5378 occupies shared space with both terrestrial and arboreal quadrupedal monkeys. Along PC1 (which accounts for 27.5% of total variance), KB 5378 is only separate from suspensory taxa, while along PC2 (18.1% of the remaining variance) it is distinct from suspensory taxa and, less so, from knuckle-walkers (Supplementary Figure 3; see Supplementary Table 4).

Trapezium

The dorsopalmar height and proximodistal length of the KB 5378 trapezium body is intermediate between—yet outside of the ranges of—both arboreal and terrestrial quadrupeds and knuckle-walking taxa (Figure 12). Note that due to variation in the orientation of the Mc1 facet between taxa, the terminology used to describe the "proximodistal length" of the Mc1 facet of monkeys actually represents the maximum measure across the proximal most edge of trapezium Mc1 facet, and the "radioulnar breadth" represents the maximum measure of the facet perpendicular to this (see Table 4). This reorientation ensures variables being compared are anatomically homologous across monkeys and hominoids in our sample. The KB 5378 Mc1 facet is

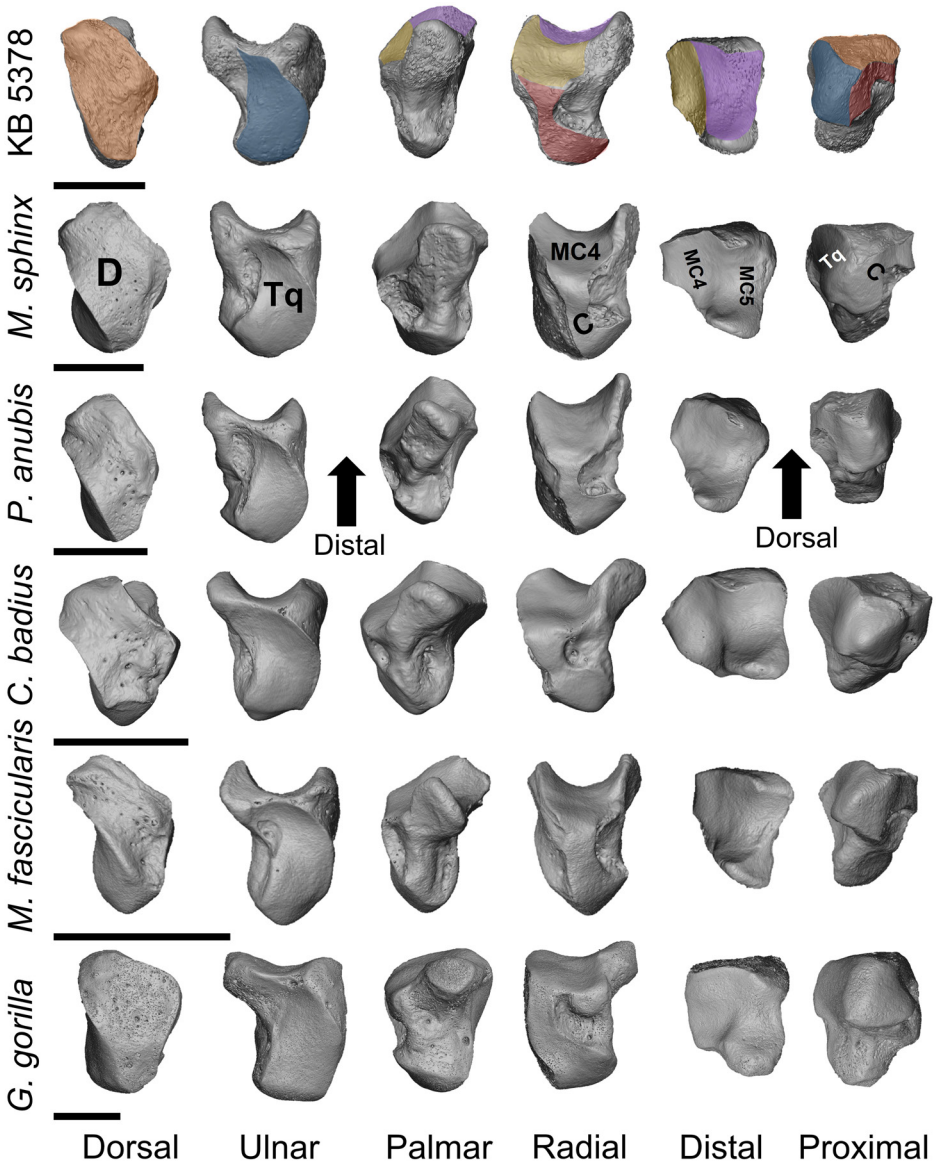

Figure 9. Anatomical views of the KB 5378 hamate in comparison to, from top to bottom, M. sphinx, P. anubis, C. badius, M. fascicularis, *and* G. gorilla. *All bones are oriented to represent the left side and scaled to the same size, with a bar placed beneath each taxa representing 1cm for scale. Articular facets are labelled in* M. sphinx *as follows: D, non-articular dorsal surface; Tq, triquetrum; Mc4, metacarpal 4; C, capitate; Mc5, metacarpal 5.*

intermediate in proximodistal length but falls outside the range of variation of all taxa in our comparative sample in radioulnar breath and is closest to *Pan* (see Figure 12). The latter measurement reflects the KB 5378 facet morphology that extends farther along the palmar surface of the body of the trapezium than is typical of other taxa. Overall, univariate analyses indicate that the KB 5378 trapezium quantitatively shares some features with both knuckle-walkers and arboreal and terrestrial quadrupeds but is distinct in other measurements.

The PCA further supports similarities in morphology between KB 5378 and knuckle-walking taxa (Figure 13). PC1 describes 35.5% of the variance within the trapezium. Along PC1, KB 5378 is distinguished from both the arboreal and terrestrial quadrupeds and overlaps with knuckle-walkers in having a dorsopalmarly tall body, a proximodistally shortened trapezoid facet, and similarly shortened total distal facet surfaces. PC2 describes 17.8% of the total variance. Along PC2, KB 5378 is distinct from terrestrial quadrupeds but overlaps with knuckle-walkers and some arboreal quadrupeds in having both a body and Mc1 facet of intermediate proximodistal length. Overall, the PCA results highlight KB 5378 similarities with knuckle-walking taxa.

Trapezoid

The KB 5378 trapezoid morphology shows significant overlap between each locomotor group when dorsopalmar height of the body, size of the dorsal surface, and size of the Mc2 facet are considered. However, in the proximodistal

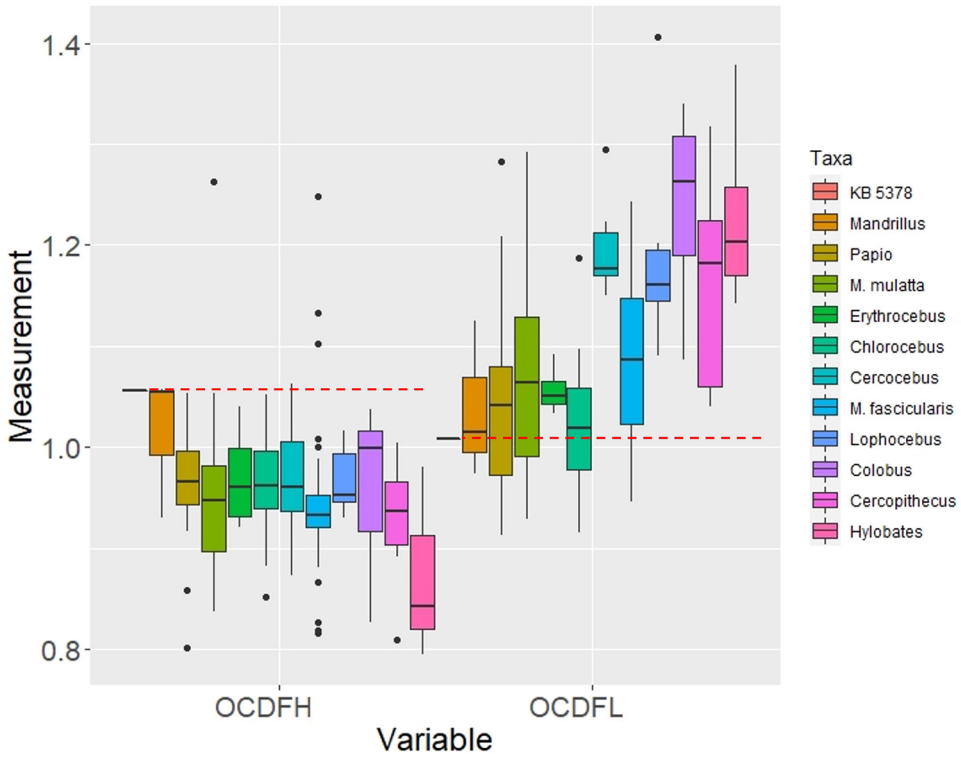

Figure 10. Box-and-whisker plots of the dorsopalmar height (OCDFH) and proximodistal length (OCDFL) of the os centrale distal facet. All values are scaled by geometric mean. The measurement value of KB 5378 is represented by a dashed red line.

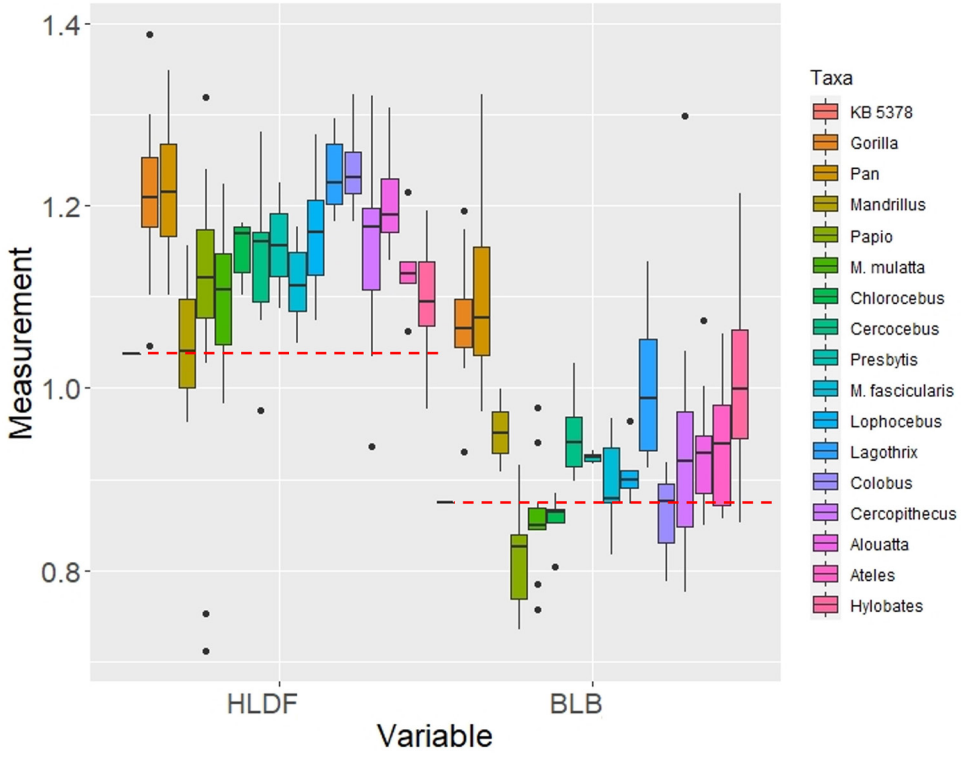

Figure 11. Box-and-whisker plots of the dorsopalmar height of the lunate distal facet (HLDF), and radioulnar breadth of the lunate body (BLB). All values are scaled by geometric mean. The measurement value of KB 5378 is represented by a dashed red line.

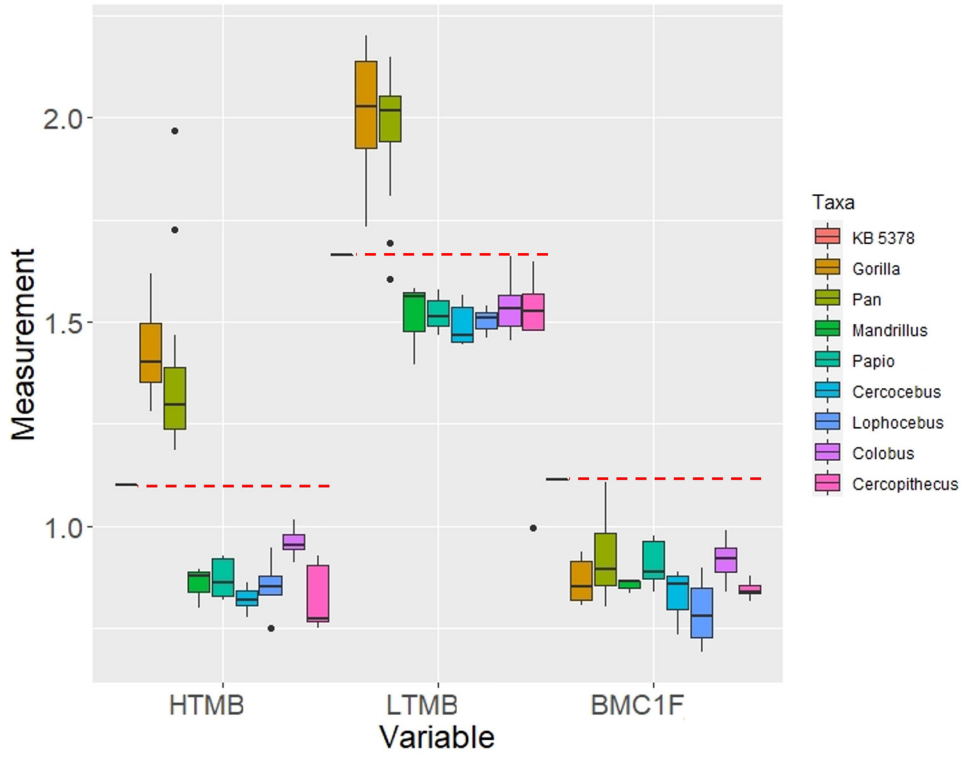

Figure 12. Box-and-whisker plots of the dorsopalmar height (HTMB) and proximodistal length (LTMB) of the trapezium body and the radioulnar breadth (BMC1F) of the trapezium Mc1 facet. All values are scaled by geometric mean. The measurement value of KB 5378 is represented by a dashed red line.

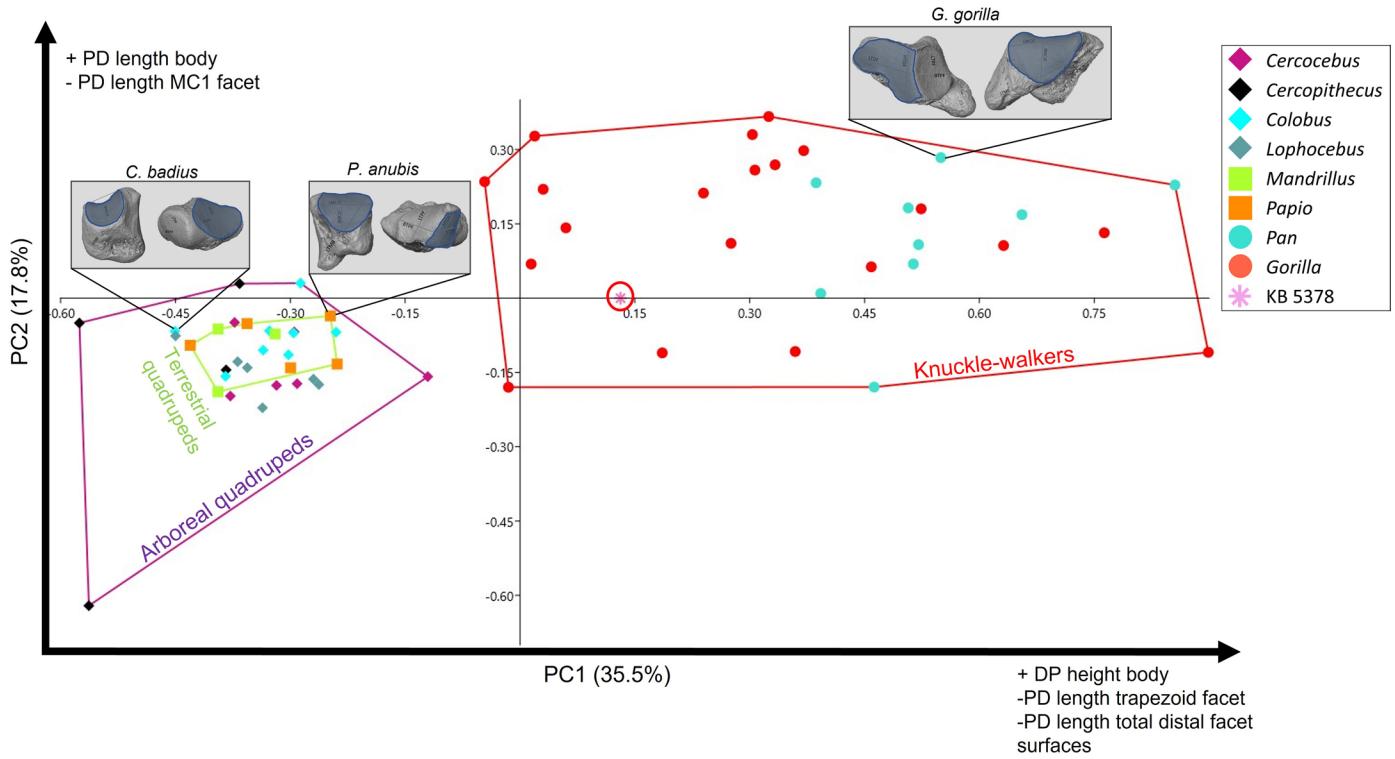

Figure 13. Within-group PCA results of the trapezium. The percentage of variation described by each PC is provided in brackets on their respective axes. Locomotor groups are each surrounded by labelled convex hulls. Surface models of representative taxa are included to demonstrate the morphology reflected at various points of the plot. Relevant facets on each surface model are shaded for clarification of the change in morphology along each axis.

length of its palmar surface overlap occurs only with *Papio, Mandrillus, Colobus*, and the knuckle-walkers. Furthermore, in both the proximodistal length and dorsopalmar height of its trapezium facet, KB 5378 falls within the ranges of *Papio*, knuckle-walkers, and *Colobus,* but outside the ranges of all other arboreal quadrupeds (Figure 14). In dorsopalmar height, the KB 5378 trapezoid trapezium facet similarly overlaps with *Papio* and the knuckle-walkers, and additionally overlaps with *Mandrillus* (see Figure 14). This indicates that while the body and Mc2 facet of KB 5378 trapezoid is not particularly distinct, it aligns more with the trapezium facet morphology of knuckle-walkers and the terrestrial quadrupeds. It is noteworthy that the trapezoid's trapezium facet is similar in size to that of the knuckle-walkers, the locomotor group with whom KB 5378 seems to share the majority of its trapezium facet morphology.

Principal component analyses support the trends in trapezoid morphology revealed by box-and-whisker plots. Along both PC1 (which describes 34.8% of the total variance) and PC2 (which describes 22.4% of the remaining variance), KB 5378 is not distinguished from any locomotor group (Supplementary Figure 4; see Supplementary Table 4).

Capitate

The capitate of KB 5378 is characterized by a mosaic of features from all locomotor groups. Though it is intermediate in proximodistal length, the body of the KB 5378 capitate is particularly dorsopalmarly tall and radioulnarly broad, reflecting the general morphology of *Hylobates*, *M. mulatta, Pan*, and *Gorilla* in dorsopalmar height, and *Alouatta* and *Lophocebus* in radioulnar breadth (Supplementary Figure 5). The morphology of the proximal capitate facet is similar to that of suspensory taxa, including *Ateles* in being dorsopalmarly short, and both *Hylobates* and *Ateles,* as well as the arboreal quadruped *Alouatta,* in being radioulnarly narrow (Figure 15). The hamate facet of KB 5378 is uniquely dorsopalmarly tall, falling above the ranges of all taxa, and is shorter in proximodistal length than most taxa excluding only *Hylobates* and knuckle-walkers (see Supplementary Figure 5). Thus, the morphology of the capitate of KB 5378 does not differentiate it from any particular locomotor group except for in dorsopalmar height of the hamate facet.

Similarly, PCA plots do not distinguish well among locomotor groups and KB 5378. Along PC1 (which explains 41.9% of the total variance), KB 5378 is only slightly distinct from arboreal quadrupeds, and otherwise overlaps within all other locomotor groups Along PC2 (which describes 17.1% of the remaining variance), KB 5378 overlaps with all locomotor groups. Overall, PCA results show that KB 5378 shares morphologies with all locomotor groups, but does so more strongly with knuckle-walking, suspensory, and terrestrial taxa (Supplementary Figure 6, see Supplementary Table 4).

Hamate

The KB 5378 hamate overlaps with most other taxa in the proximodistal length of the body (including the hamulus) and size of the capitate facet. However, the body of the hamate, excluding the hamulus, is dorsopalmarly short and proximodistally long compared to most other taxa, but overlap still occurs across multiple locomotor groups (Figure 16). This indicates that the hamulus of KB 5378 is notably distally extended and less palmarly extended compared with some other taxa in our sample. The KB 5378 triquetrum facet is dorsopalmarly short relative to most taxa, but again there is overlap between KB 5378 and the lower ranges of all taxa excluding *Cercocebus, Chlorocebus*, and *Erythrocebus* (Supplementary Figure 7). Overall, the morphology of the KB 5378 hamate does not align with any one locomotor group or taxon.

Principal component analyses agree with the findings of the box-and-whisker plots. Both PC1 (which accounts for 43.5% of the total variance) and PC2 (21.5% of the remaining variance) do not distinguish between locomotor groups. This overlap indicates that the hamate of KB 5378 does not reflect the morphology of a specific taxon or locomotor group (Supplementary Figure 8; see Supplementary Table 4).

Comparison of Absolute Carpal Size

Univariate analyses were performed using raw variables (i.e., not divided by a geometric mean) of overall proximodistal length, radioulnar breadth, and dorsopalmar height of each carpal to assess absolute size of KB 5378 relative to the comparative sample. Overall, each of the KB 5378 carpal bones consistently fall out as most similar in absolute size to *Mandrillus* (body mass (BM) range 6.5–12kg (female) to 29–47kg (male); Delson et al. 2000) and *Papio* (BM range 11–14.9kg (female) to 22–37.2kg (male); Delson et al. 2000) (Figure 17). More specifically, the KB 5378 carpals are consistently smaller than the range of variation found in knuckle-walkers for every bone, and typically larger than all arboreal quadrupeds and suspensory taxa in our sample. The only notable exceptions to this pattern are for the proximodistal length of the hamate, which also overlaps with *Hylobates*, and the dorsopalmar height of the trapezoid and radioulnar breadth of the capitate, which overlap with the lowest range of variation in *Pan.*

Comparison of Carpal and Metacarpal Size

We also assessed the maximum proximodistal length of metacarpals 1–5 for select comparative taxa and the fossil metacarpals associated with KB 5378 to aid our understanding of the association between the KB 5378 carpals and metacarpals and their taxonomic attribution. Although the metacarpals distal epiphyses are not fully fused, their morphology suggests they are of a late juvenile stage and thus the proximodistal length of each bone would not substantially differ from the adult length. To investigate the potential association between the KB 5378 carpals and metacarpals, we assessed metacarpal proximodistal length relative to the proximodistal length of the capitate, which was used as a proxy for overall carpus size due to the consistent presence of a capitate within the sample of individuals who also had metacarpals (see also Lovejoy et al. 2009).

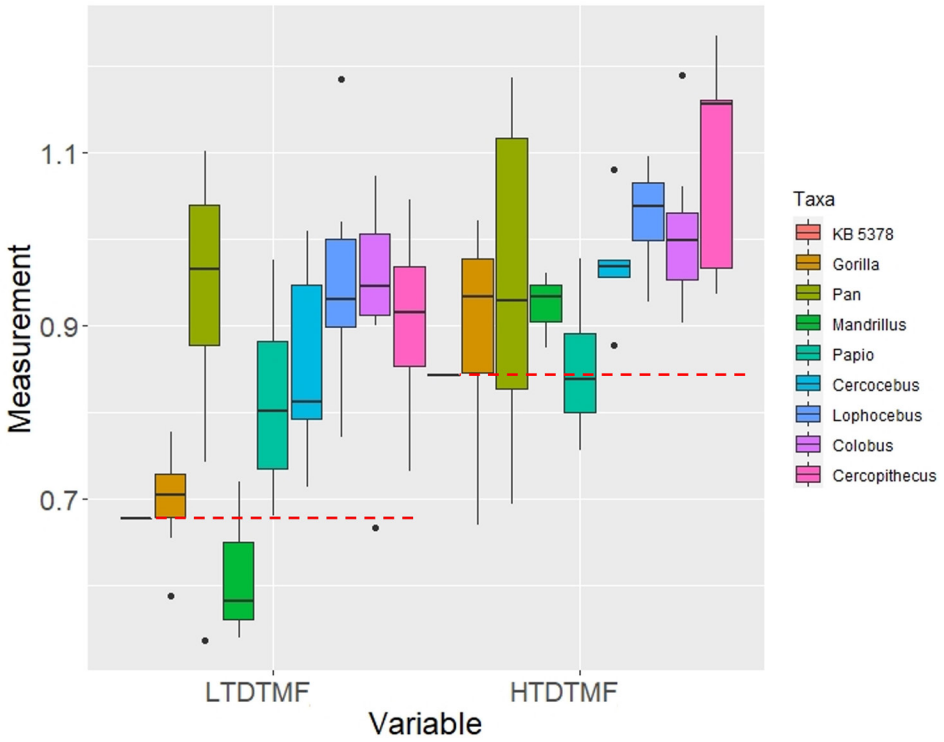

Figure 14. Box-and-whisker plots of the proximodistal length (LTDTMF) and dorsopalmar height (HTDTMF) of the trapezoid trapezium facet. All values are scaled by geometric mean. The measurement value of KB 5378 is represented by a dashed red line.

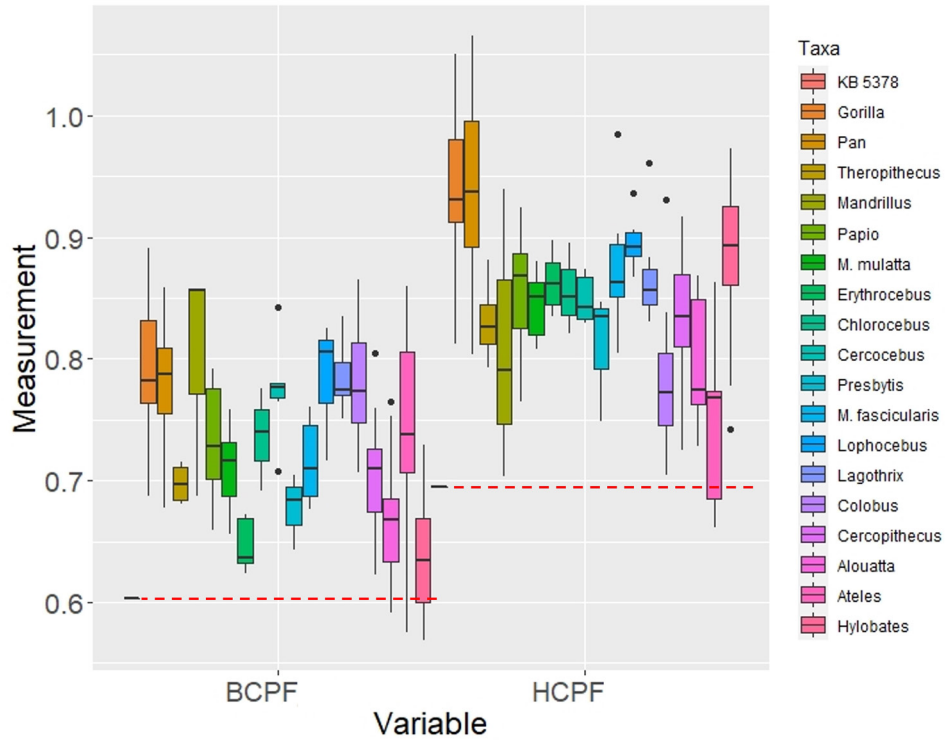

Figure 15. Box-and-whisker plots of the radioulnar breath (BCPF) and dorsopalmar height (HCPF) of the capitate proximal facet. All values are scaled by geometric mean. The measurement value of KB 5378 is represented by a dashed red line.

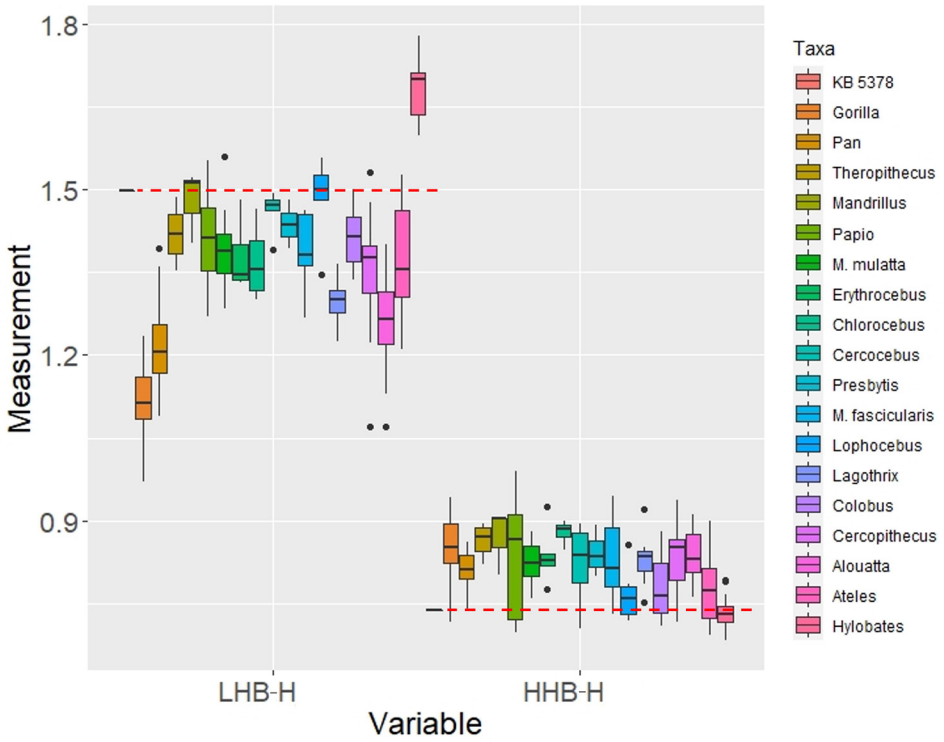

Figure 16. Box-and-whisker plots of the proximodistal length (LHB-H) and dorsopalmar height (HHB-H) of the hamate body excluding the hamulus. All values are scaled by geometric mean. The measurement value of KB 5378 is represented by a dashed red line.

Bivariate plots for each metacarpal were assessed and the patterns found in Mc2-5 were similar. As such, Figure 18 depicts only the relationship between capitate length and Mc3 length, which illustrates the overall trends for Mc2-5. These plots reveal that KB 5378 falls with *Mandrillus* and *Papio* in relative capitate to Mc2-5 proximodistal length. However, the relationship is different for the Mc1—KB 5378 falls above the ranges of all other taxa except for *Gorilla* in these plots (see Figure 18). To further investigate the marked elongation of Mc1 in KB 5378, we performed an additional box-and-whisker-plot integrating *Theropithecus* data from Frost et al. (2015) adjusted by a geometric mean (see Supplementary Table 3). When adjusted by the geometric mean size proxy, comparisons confirmed that KB 5378 has an exceptionally long Mc1, similar only to extant *Theropithecus* (Figure 19). Together, these findings indicate KB 5378 has a much longer Mc1 than expected for a primate of its size (see Figures 18, 19).

DISCUSSION

This study qualitatively and quantitatively described the functional morphology of the KB 5378 associated carpus to assess its potential locomotor behavior, taxonomic attribution, and its association with KB 5378 late juvenile metacarpals. Summarizing the quantitative results reveals that, although there is substantial overlap across locomotor groups in our comparative sample, KB 5378 is most similar to terrestrial cercopithecoids. Overall, the carpus KB 5378 shares qualitative (and quantitative) morphology and absolute size specifically with *Papio* and *Mandrillus*, which does not support our first prediction that KB 5378 would be absolutely larger than these taxa but does support our second prediction of shared morphology with large-bodied terrestrial cercopithecoids. Meanwhile, the Mc1 of KB 5378 reflects specialized elongation similar to that of extant and extinct *Theropithecus*, which does not support our third prediction that KB 5378 would not show specialized metacarpal morphology already documented in other fossil cercopithecoids (Frost and Delson 2002; Frost et al. 2015). Results are discussed below for each carpal in more detail.

COMPARATIVE MORPHOLOGY

Scaphoid

The preserved morphology of the KB 5378 partial scaphoid is best interpreted as reflecting generalized quadrupedalism. The flat, broad radial facet and a shallow os centrale facet suggest increased stability at the radiocarpal and midcarpal joints and are most similar to terrestrial quadrupedal taxa in our sample. However, limited preservation of scaphoid, including the lack of tubercle and incomplete articular facets, prohibit further functional interpretation.

Os Centrale

Results of our quantitative analyses reveal that the KB 5378 os centrale shares morphological traits with both arboreal and terrestrial quadrupeds but is distinct from suspensory taxa (see Figure 10; see Supplementary Figure 1). Qualitatively, the KB 5378 has a distinct proximoulnar lunate facet (see Figure 4). This facet is absent in arboreal species

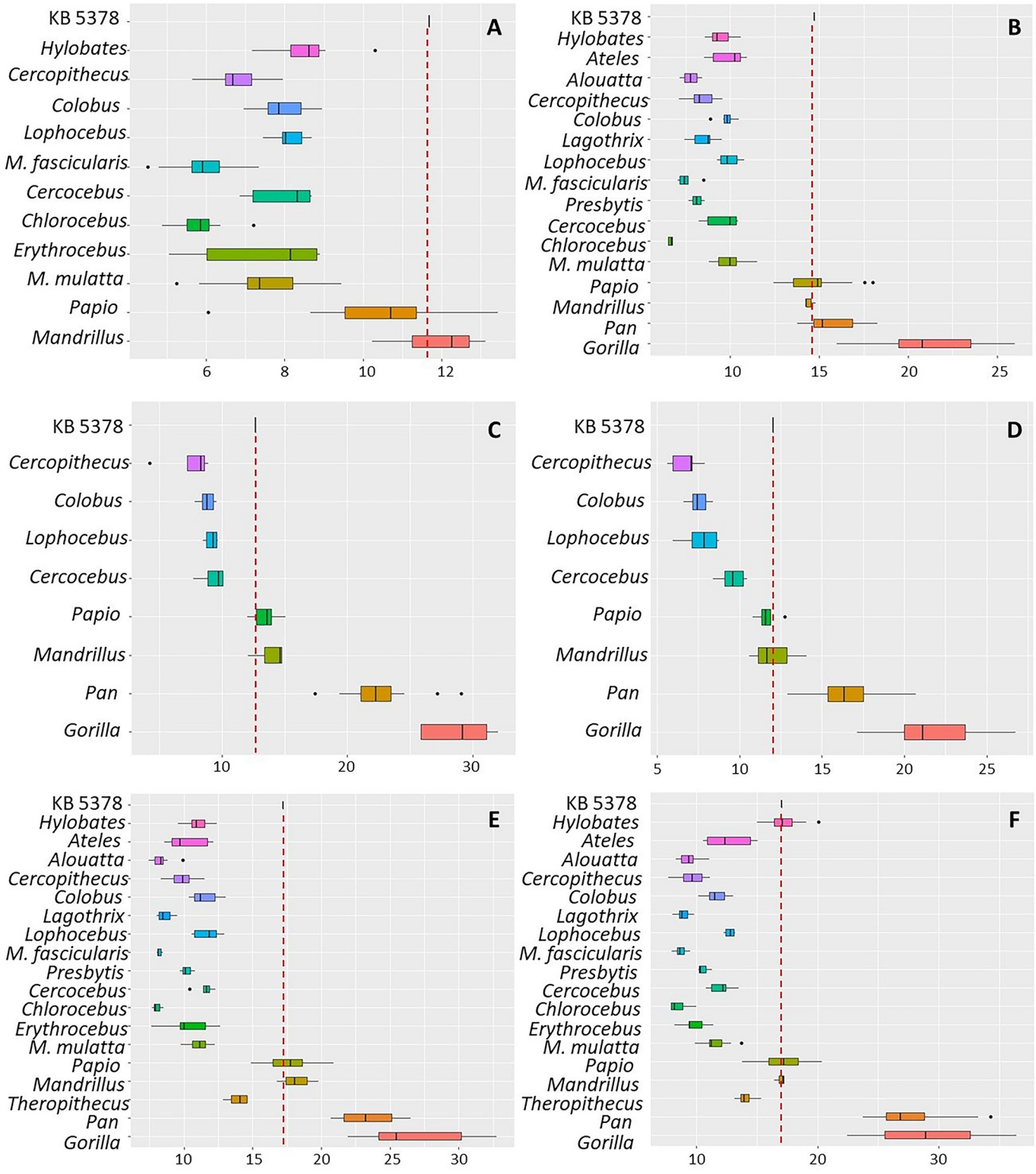

Figure 17. Box-and-whisker plots of the proximodistal length (mm) of the os centrale (A), lunate body (B), trapezium body (C), trapezoid dorsal (D) surface. Capitate body (E) and hamate body (F) not scaled by geometric mean.

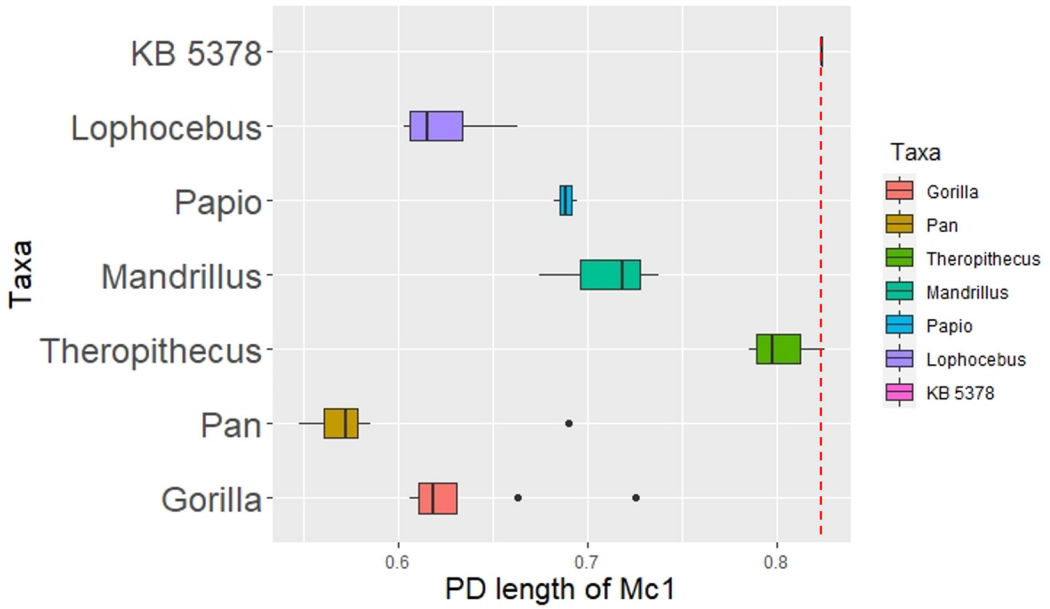

Figure 18. Bivariate plots comparing the PD length of the capitate body to the PD length of each metacarpal. A regression line is placed at a confidence interval of 95%. Trends in Mc2, 4, and 5 are similar to those seen in Mc3.

including *Ateles* and *Pongo* and is more commonly found in papionines such as *Papio* and *M. mulatta* who frequently use terrestrial, digitigrade locomotion (Orr 2018). This facet, in tandem with the radially-oriented trapezoid-trapezium facet, has been shown in studies using CT-based motion capture of cadaveric wrists to facilitate rotation of the os centrale characterized by early contact with the capitate head during extension (Orr 2018). This early contact improves joint congruence and load transfer through the joint, thus increasing stability during terrestrial quadrupedal locomotion (Orr 2018).

The angle between the trapezoid-trapezium and scaphoid facets of the os centrale has also been shown to be informative about mobility and stability of the scapho-capitate-centrale joint (Orr 2018). In KB 5378, the angle between the scaphoid and trapezoid-trapezium facet, taken at the approximate midpoint of each facet, is 88.1°. In digitigrade species like *Papio,* this angle is typically acute, while species

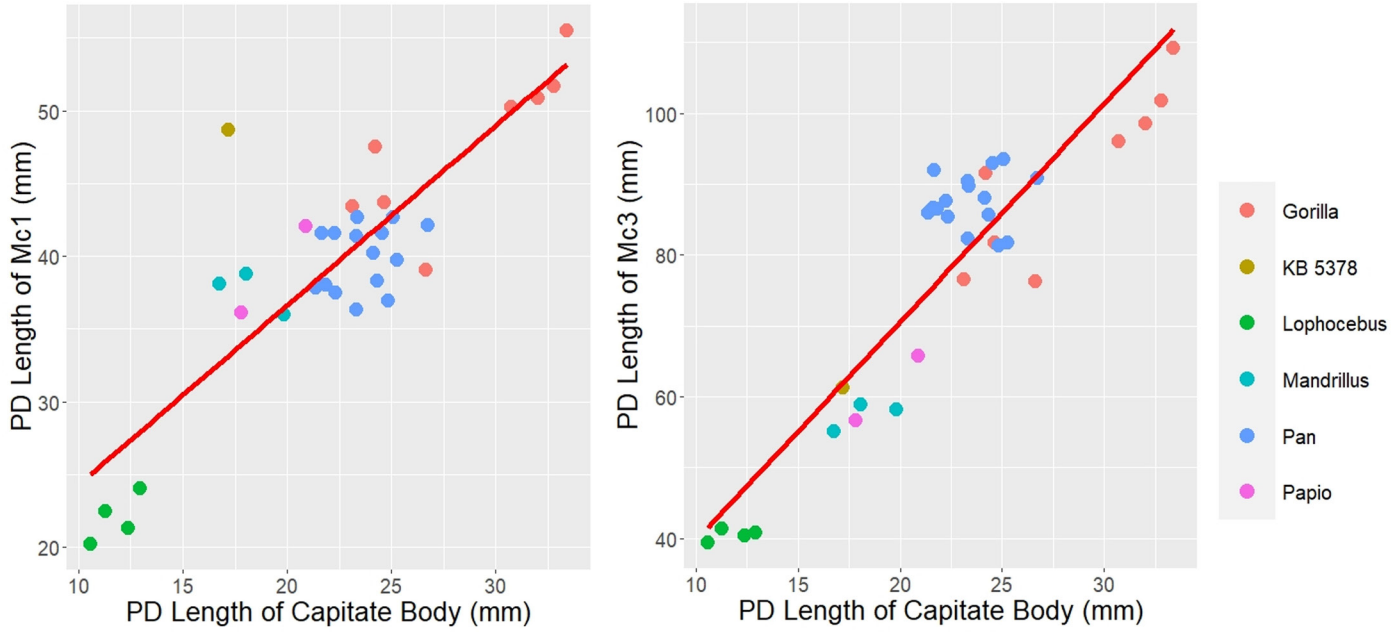

Figure 19. Box-and-whiskers plots of the proximodistal length of Mc1 scaled by geometric mean. All Theropithecus *data come from literature (Frost et al. 2015, Supplementary Information).*

that use a mix of digitigrade and palmigrade postures, such as *M. mulatta,* and those that utilize arboreal, palmigrade locomotion, such as *Colobus*, exhibit a right, or obtuse angle respectively between these facets (Orr 2018). During extension, having an acute angle at these facets creates a more tightly packed articulation between the trapezoid, os centrale, and capitate that limits extension and further facilitates more effective transmission of forces through the joint during digitigrade locomotion (Orr 2018). KB 5378 has a slightly acute, but approaching a right angle between these facets, indicating an intermediate morphology between *Papio* and both species of *Macaca,* all of whom engage in terrestrial quadrupedal locomotion, but to varying degrees. This intermediate angle, along with the facet morphology described above, suggests that KB 5378 had os centrale morphology most similar to a generalized quadruped, with specializations for terrestrial quadrupedalism.

Lunate

The KB 5378 lunate morphology overlaps with several locomotor groups and taxa, but overall is most similar qualitatively and quantitatively to quadrupedal cercopithecoids and particularly terrestrial quadrupedal taxa. Results of our quantitative analysis reveal that the KB 5378 lunate body is relatively radioulnarly narrow, which is a morphology common in cercopithecoids and unlike the radioulnarly broader lunates of great apes (see Figure 11) (Lewis 1989; Sarmiento 1988). The distal capitate facet of the KB 5378 lunate is unique in being both dorsopalmarly tall and radioulnarly narrow (see Figure 11). The reduced size of the articulation between the lunate and capitate suggests limited mobility but also limited surface area for transfer of load at the capitolunate joint.

The triquetrum facet of KB 5378 lunate is both proximodistally long and dorsopalmarly tall relative to other taxa. The functional morphology of the lunate triquetrum facet has not yet been explored. Due to the lack of a preserved triquetrum in KB 5378, no further functional information can be derived from this facet's morphology.

Finally, the radial facet is large and expands across the entire proximal aspect of the KB 5378 lunate. When articulated with the scaphoid, it creates a coplanar surface with the scaphoid's radial facet (see Figure 5). The flat and continuous articulation between the radial surfaces of the scaphoid and lunate is a feature often characterizing knuckle-walkers and terrestrial quadrupeds to increase the stability of the radiocarpal joint (Begun 2004; Kivell 2016; Richmond et al. 2001).

Trapezium

The KB 5378 trapezium has a mix of both knuckle-walking and arboreal/terrestrial quadruped morphology. Comparative quantitative results of the facet morphology reveal striking similarities between KB 5378 and the knuckle-walking taxa in our sample (see Figures 12 and 13). However, qualitatively, the overall KB 5378 trapezium morphology is unlike knuckle-walkers and most similar to that of quadrupedal monkeys (see Figure 6).

The trapezium-Mc1 joint of KB 5378 is not saddle-shaped. Instead, it is oval-shaped, with a flat edge at its distal-most extreme, and it becomes convex as it expands proximally along the palmar aspect of the bone (see Figure 6; Figure 20). In our sample, this morphology is unique to KB 5378. Even though many cercopithecoids in our sample had a flattened trapezium-Mc1 facet (see *Papio* and *Mandrillus* in Figure 6), their facets were consistently more concave, and therefore maintained some degree of a saddle shape. The trapezium-Mc1 facet of KB 5378 is additionally uniquely broad, expanding farther palmarly than in any other comparative taxa.

There is great variation in the curvature and shape of the trapezium-Mc1 joint between and within monkeys and apes (Raffery 1990; Tocheri et al. 2003; 2005). For example, knuckle-walking apes consistently have a saddle-shaped trapezium-Mc1 joint creating a stable thumb still capable of opposition (Tocheri et al. 2003; 2005). In contrast, cercopithecoids, and in particular terrestrial cercopithecoids such as *Papio* and *M. mulatta*, have a convex Mc1 facet on the trapezium and shallowly concave trapezium facet on the Mc1, which creates an incongruent and hinge-like joint (Markze et al. 2010; Rafferty 1990; Van Leeuven et al. 2022). Furthermore, the lack of congruency between the trapezium and the Mc1 permits axial rotation, which is stabilized by the highly congruent saddle-shaped configuration in other taxa (Markze et al. 2010; Rafferty 1990; Van Leeuven et al. 2022). This incongruency effectively increases the radioulnar mobility at the trapezium-Mc1 joint, but consequently creates instability in the joint (Markze et al. 2010; Rafferty 1990; Van Leeuven et al. 2022). Both *M. mulatta* and *Papio* have limited ranges of motion at this joint when compared to hominoids, likely due to the lack of smooth, concave curvature at the Mc1 facet (Markze et al. 2010; Van Leeuven et al. 2022).

The convex Mc1 facet surface of the KB 5378 trapezium suggests a cercopithecoid-like joint with somewhat limited mobility. However, the Mc1 facet is also uniquely radioulnarly broad (see Figures 12 and 20). In the fossil species *T. o. brumpti*, Guthrie (2011) reports that the Mc1 facet extends farther palmarly than other comparative taxa. *T. o. brumpti*, another subspecies of the fossil species *T. oswaldi* has been reconstructed as having a highly opposable thumb that was likely advantageous for foraging behaviors similar to those seen in the extant *T. gelada* (Guthrie 2011; Jablonski 2002). Therefore, it is possible that the broad Mc1 facet of KB 5378 may be a similar adaptation to opposability as seen in *T. o. brumpti*.

Additionally, unlike the trapezia of African apes (Tocheri et al. 2005), the trapezium of KB 5378 does not show a clear facet for Mc2. The presence of an Mc2 facet was variable within our monkey sample (only present in 46.9%), indicating that the lack of an Mc2 facet in KB 5378 may be a shared trait with extant monkeys. However, the orientation of the Mc2 facet on the trapezium has been discussed in humans and great apes as an indicator of manipulative and gripping abilities, as well as for the distribution of force during locomotion across the carpus (Tocheri et al., 2003).

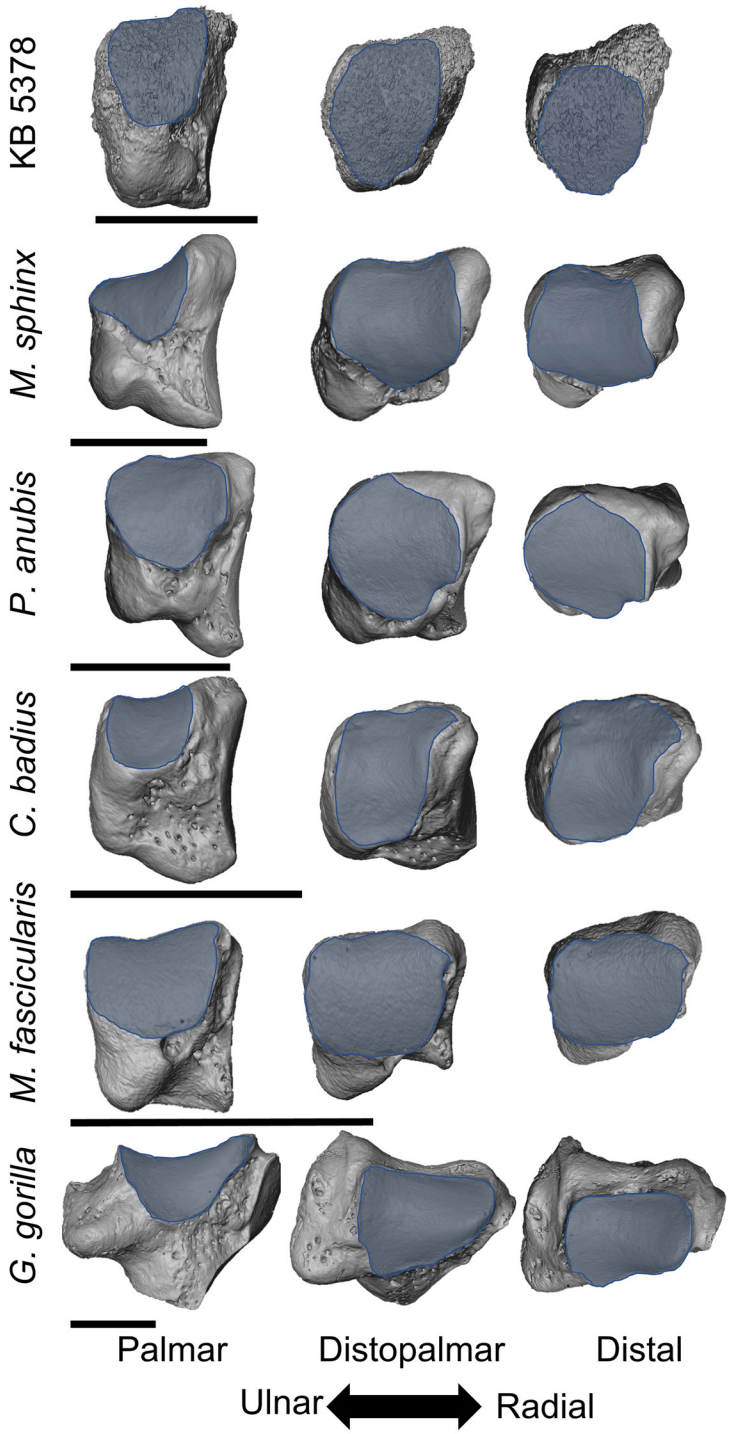

Figure 20. Surface models of the palmar, distopalmar, and distal view of trapezia of KB 5378 and representative comparative taxa are shown with a focus on the MC1 facet. Each bone is scaled to a similar size, with a 1cm scale bar placed beneath each for reference.

In humans, the Mc2 facet of the trapezium is oriented sagittally, allowing for a greater degree of Mc2 pronation compared with African apes (Tocheri et al. 2003). If the presence of an Mc2 facet in apes and humans serves to increase mobility for Mc2, the lack of an Mc2 facet of the trapezium of KB 5378 may indicate that it had limited Mc2 mobility. The lack of a facet for Mc2 paired with the morphology of the facet for Mc1 on the trapezium, indicates a hand with possibly *Theropithecus*-like mobility of the thumb and limited mobility of the index finger.

Further differentiating the trapezium of KB 5378 from knuckle-walkers is the lack of a proximo-ulnar tubercle. In apes, this tubercle serves as an attachment point for flexor retinaculum, a fibrous band that protects and supports the flexor muscles of the forearm (Deak and Bordoni 2019). The KB 5378 trapezium lacks a projecting tubercle, which

is similar to the morphology of many of the terrestrial cercopithecids in our sample, including *Papio* and *Mandrillus*, but also arboreal cercopithecids such as *Colobus* and *M. fascicularis*. This morphology likely suggests more limited development of the flexor muscles used in arboreal locomotion compared to hominoids but does not rule out some degree of arboreal locomotion, as indicated by its presence in *M. fascicularis* and *Colobus*. This, in combination with the morphologies described above, suggests that the KB 5378 trapezium is best adapted for terrestrial quadrupedalism with limited climbing and particularly limited thumb mobility compared to humans and apes, but possibly more thumb mobility than extant monkeys.

Trapezoid

Quantitative comparisons of the KB 5378 trapezoid generally reveal considerable overlap with all locomotor groups. Despite significant overlap with the morphology of arboreal quadrupeds in many measurements, the morphology of the trapezoid's trapezium facet and the proximodistal length of the palmar surface of the trapezoid indicates that, overall, the KB 5378 trapezoid shares some similarities in morphology to terrestrial cercopithecoids and to knuckle-walkers, but that there is much overlap with other functional groups (see Figure 14). Functional interpretations of this bone, however, are complicated by the limited literature on its morphology in non-hominoid primates.

In arboreal quadrupedal strepsirrhines, the proximal embrasure between the capitate and the trapezoid—which articulates with the os centrale—is wider dorsally to facilitate pronation during midcarpal rotation (Hamrick 2007; Kivell 2016). Conversely, in leaping strepsirrhines the embrasure is wider palmarly to promote supination during midcarpal rotation (Hamrick 2007; Kivell 2016). In KB 5378, the capitate-trapezoid embrasure is wider dorsally indicating a midcarpal joint more capable of palmar rotation during midcarpal rotation and greater stability at that joint during quadrupedal locomotion. Additionally, the Mc2 facet of the trapezoid of KB 5378 is keeled in dorsal view (see Figure 7). In extant cercopithecoids and African apes, this keeling creates a tight articulation with a complementarily concave Mc2 proximal facet, which creates a more stable joint (see Figure 7) (Begun 2004; Kivell 2016; Richmond et al. 2001). Overall, the morphology of the KB 5378 trapezoid suggests it is well adapted to generalized quadrupedalism, but not specifically adapted for terrestrial locomotion.

Capitate

Quantitative comparisons indicate the proximal capitate morphology of KB 5378 is similar to suspensory and arboreal taxa including *Ateles*, *Hylobates*, and *Alouatta* (see Figure 15). The capitate proximal head is often discussed in the context of midcarpal joint mobility and stability (Daver et al. 2012; Kivell 2016; Lewis 1989; Richmond 2006). More specifically, the capitate's proximal surface is broader in taxa that habitually use terrestrial quadrupedalism, as this adds stability to a joint that experiences high forces during such locomotion (Daver et al. 2012; Kivell 2016; Lewis 1989). Conversely, taxa that typically use suspensory locomotion, such as the hylobatids, tend to have a radioulnarly narrow proximal head of the capitate, which, combined with broader proximal hamate, allows for greater mobility at the midcarpal joint (Kivell 2016; Lewis 1989). Though the KB 5378 capitate head is notably narrower than other cercopithecoids in our sample and overlaps with suspensory taxa, including *Ateles* and *Hylobates* in particular, it also overlaps with the lower range of variation seen in the palmigrade arboreal quadruped, *Alouatta* (see Figure 15). The breadth of the capitate head also shows a considerable amount of variation across our comparative sample, often even within locomotor groups. This complicates functional interpretation of this feature but does not detract from the importance of KB 5378 having morphology that is distinct from all terrestrial taxa. Moreover, the proximal hamate does not reflect suspensory morphology in its radioulnar breadth (described further below), suggesting the KB 5378 midcarpal joint is not similar to suspensory taxa overall. The relatively narrow capitate head in KB 5378 therefore suggests less stability than the broader capitate heads of terrestrial cercopithecoids and, together with the hamate (see below), a midcarpal joint morphology that is most similar to arboreal quadrupedal monkeys.

The metacarpal facets of the KB 5378 capitate are generally planar and smooth with small, shallow concave regions in the dorsal region of the facet (see Figure 8). The relative flatness of the Mc3 facet of KB 5378 is shared with many cercopithecoids. A planar Mc3 articulation is less stable as it cannot resist torsion or shear forces within the carpo-metacarpal joint (Lovejoy et al. 2009; Marzke 1983). In contrast, the deeply concave metacarpal facets of African apes limit sliding and rotation of the metacarpals and consequently add stability to the joints (Begun 2004; Marzke 1983; Richmond et al. 2001). Moreover, the Mc2 facet of KB 5378 is angled sharply radially, a trait commonly observed in knuckle-walking apes that allows the capitate to act as a buttress against torsional forces and increases the stability of the carpometacarpal joints (Lovejoy et al. 2009; Marzke 1983). Overall, the metacarpal facets of KB 5378 reflect combined morphology of both a generalized joint and one specialized for stability during high force locomotion (Lovejoy et al. 2009; Marzke 1983).

Hamate

The hamate of KB 5378 is characterized by a generalized monkey morphology in its overall size and shape. Quantitatively, the KB 5378 hamate overlaps with taxa from all locomotor groups and is best described by the morphologies of a generalized quadruped in being generally wedge-shaped, and of equal size to the capitate (Lewis 1989). However, specific qualitative morphologies separate KB 5378 from both suspensory taxa and arboreal quadrupedal monkeys including the orientation of its triquetrum facet and its relatively small hamulus.

The orientation of the hamate's triquetrum facet can be used to interpret stability of the midcarpal joint. It is broad and proximally oriented in quadrupeds, which limits ra-

dioulnar deviation and supination, creating a more stable joint during extended postures often used during digitigrade locomotion (Daver et al. 2012; Kivell 2016; Lewis 1989; O'Connor 1975). In KB 5378, the triquetrum facet is proximoulnarly oriented, creating a stable midcarpal joint, which would be advantageous for terrestrial quadrupedalism (see Figure 9).

In addition to the angle of the triquetrum facet, the size of the hamate hamulus can be informative of both joint stability and associated soft tissue configuration (Corruccini et al. 1975; Kivell 2016; O'Connor 1975; Ward 2002; Ward et al. 1999). KB 5378 exhibits a proximodistally long and dorsopalmarly short hamulus when compared with extant monkey taxa. However, the hamulus is overall considerably smaller for both measures than any hominoid included in our sample. Having a smaller hamulus permits a greater degree of dorsiflexion at the carpometacarpal joints which is advantageous for palmigrade/digitigrade substrate contact (which is normally checked by the extended hamulus in hominoids at the hamate-Mc5 joint) (Corruccini et al. 1975; Kivell 2016; O'Connor 1975; Ward 2002; Ward et al. 1999). Additionally, the typically hominid trait of a large, pronounced hamulus has been associated with having a deep carpal tunnel capable of accommodating strong digital flexors of the forearm used during climbing and suspension (Corruccini et al. 1975; Kivell 2016; Ward 2002; Ward et al. 1999). Therefore, the lack of a large hamate hamulus in KB 5378 reflects a shallow carpal tunnel and less pronounced digital flexor musculature of the forearm, suggesting climbing and suspensory behaviors were not emphasized.

OVERALL CARPAL FUNCTION

The carpus of KB 5378 presents an interesting mosaic of features representative of those found in arboreal and terrestrial monkeys, but that are typically distinct from knuckle-walking and suspensory taxa. The features of the scaphoid preserved well enough for analysis, including its generally broad radial facet and shallow os centrale facet, are considered adaptations to increasing stability of the radiocarpal and midcarpal joints often seen in terrestrial quadrupeds (Kivell 2016; Richmond 2006; Richmond et al. 2001). The presence of a distoradial lunate facet, as well as the slightly acute angle between the scaphoid and trapezoid facets on the os centrale, create a joint with improved congruency early on in extension, which stabilizes the carpus. The morphology of the lunate tends to support an antebrachial joint built for stability proximally and ulnarly during terrestrial locomotion, but distally does not show traits associated with maximizing midcarpal stability. The trapezium of KB 5378 has distinct morphology relative to our comparative sample, with a flat, broad, oval-shaped Mc1 facet that extends particularly far palmarly. Additionally, it does not have a facet for the Mc2. This morphology suggests a potentially *Theropithecus*-like thumb mobility, and limited mobility at the Mc2 joint. The dorsally wide capitate-trapezoid embrasure and keeled Mc2 facet of the trapezoid each aid in creating a stable carpus by promoting pronation during midcarpal rotation and decreasing rotation and radioulnar translation of the Mc2 at the carpometacarpal joint. The KB 5378 capitate has radioulnarly narrow capitate head, consistent with a radioulnarly narrow distal facet on the lunate, and planar metacarpal joints that are best described as a generalized morphology that is not specialized for either extreme mobility at the midcarpal joint or stability at the carpometacarpal joints. Finally, the hamate of KB 5378 has a morphology suggestive of general quadrupedal locomotion based on the proximoulnar orientation of its triquetrum facet, with limited emphasis on climbing and suspensory behaviors due to the diminutive size of its hamulus. Altogether, the KB 5378 carpal functional morphology is best described as that of quadrupedal monkey with specializations for terrestrial locomotion, supporting our second prediction about KB 5378 carpal functional morphology.

METACARPALS: SIZE, ASSOCIATION, AND DEVELOPMENT

The KB 5378 carpus is considered to be associated with the KB 5378 juvenile metacarpus (Mc1-Mc5) (Vrba 1981). The metacarpal fossils were not available for study and thus we only tested the association between the carpals and metacarpals via an assessment of absolute length. Bivariate plots of KB 5378 metacarpals indicate that their size is consistent with the carpus of a primate roughly the size of *Papio* or *Mandrillus* (see Figure 18), thus aligning well with the absolute size of the KB 5378 carpals. Therefore, this study supports the previous hypothesis that the carpals and metacarpals assigned KB 5378 likely belong to the same individual. Additionally, the KB 5378 Mc2-5 are similar in length to each other, which is a pattern often seen in terrestrial digitigrade primates and distinct from the different metacarpal length proportions found in arboreal quadrupeds and especially hominoids (Etter 1973; Patel 2010a, b; Patel and Maiolino 2016). This, in addition to morphology of the carpus, supports the likelihood that KB 5378 spent a substantial amount of time engaging in terrestrial quadrupedalism.

Interestingly, though KB 5378 Mc2-5 each consistently align with *Papio* and *Mandrillus* in analyses of size, both relative to each other and to the capitate, the length of the Mc1 is considerably longer than that of all quadrupedal monkeys in our sample with the notable exception of *Theropithecus* (see Figure 19). *T. gelada* has a particularly elongated Mc1 that it uses in combination with a shortened second digital ray to finely pluck the roots and grasses that make up its diet (Almécija et al. 2015; Etter 1973; Patel and Maiolino 2016). Interestingly, *P. hamadryas* also displays an elongated MC1, though to a lesser degree than *T. gelada*, likely also related to foraging of fine grasses and roots (Etter 1973). The exceptional length of the KB 5378 Mc1 may therefore be indicative of a diet consisting partly of grasses and roots that requires precision manipulation like that of *T. gelada* and *P. hamadryas.* Enhanced manipulation in KB 5378 may have also been facilitated by increased thumb flexion, as suggested by its distinct trapezium-Mc1 facet morphology. This, in combination with the results of our

univariate analyses of the metacarpals and qualitative morphology described above, supports the inference that KB 5378 had a hand adapted for terrestrial quadrupedalism and possibly terrestrial foraging.

The KB 5378 carpals reflect markers of adult morphology including smooth, homogenous cortical surfaces, clearly delineated articular facets, and a fully developed, well-defined hamate hamulus (Kivell 2007; Kivell and Begun 2007). Conversely, the metacarpals of KB 5378 display unfused (but attached) metacarpal epiphyses indicating that they are juvenile. Studies on the timing of epiphyseal fusion in metacarpals of non-hominoid primates are rare relative to larger long bones (e.g., Bolter and Zihlman 2003; Michejda and Bacher 1981; Newell-Morris et al. 1980; Van Wagenen and Asling 1964). Ontogenetic studies of these long bones in various species of *Macaca* have shown that the rate of epiphyseal fusion is irregular, asynchronous, and varies by region of the skeleton and by sex (Bolter and Zihlman 2003; Michejda and Bacher 1981; Newell-Morris et al. 1980; Van Wagenen and Asling 1964). Limited studies on *Macaca* of known ages have found that, while the lunate and capitate are fully ossified between 5 and 6 years of age, the metacarpals do not fuse until 5 to 8 years of age (Hamada 1984; Kimura and Hamada 1990). Although the KB 5378 preserved carpals appear fully adult, we lack preservation of the scaphoid tubercle and pisiform, two regions/bones that are typically last to fully ossify in the primate carpus (Kivell 2007; Newell-Morris et al. 1980). Given the limited information available on carpal and metacarpal ossification in non-hominoid primates, it is possible that the carpals (at least the ones preserved in KB 5378) reach adult morphology prior to metacarpal epiphyseal fusion. Therefore, we propose that KB 5378 was likely a late juvenile individual whose carpus was potentially almost fully or fully developed before its metacarpals, leaving the epiphyseal regions still cartilaginous enough to become fully disjointed (as seen in Figure 2) during the process of fossilization. Moreover, a late juvenile status for the carpals and metacarpals of KB 53787 aligns well with the ontogenetic status of the associated mandible, KB 5227, which has unerupted third molars (Vrba 1981).

TAXONOMY

Although the carpus is not the ideal anatomical region from which to assess taxonomy, this study provides sufficient evidence to aid in the taxomonic attribution of KB 5378. Comparative analyses of overall size suggest that the KB 5378 carpals are most similar to extant *Mandrillus* and *Papio*. These taxa range in body mass from 11–14.9kg (female) to 22–37kg (male) in *Papio*, and 6.5–12kg (female) to 29–47kg (male) in *Mandrillus* (Rowe et al. 1996). Delson et al. (2000) estimate *G. major* males to have weighed 34–39kg and females at 28–31kg. As such, *G. major* cannot be ruled out as a taxonomic assignment for KB 5378 based on size alone, which does not support our first prediction that KB 5378 would be larger than all other contemporaneous papionins. However, known fossil cercopithecoids from Kromdraai and the surrounding contemporaneous fossil bearing sites that are estimated to have body masses within the range of extant *Papio* and *Mandrillus* also include *Papio*, *Parapapio*, *C. williamsi,* and two subspecies of *Theropithecus, T. o. oswaldi* and *T. o darti* (see Table 1; Delson et al. 2000). Thus, taxonomic attribution of KB 5378 cannot be ascertained based on size alone.

Our quantitative and qualitative comparative assessment of the KB 5378 external morphology, as well as the estimated size of KB 5378, revealed that a mixed arboreal/terrestrial locomotor repertoire is the most likely reconstruction partially supporting the second prediction of this study. This supports the likelihood that KB 5378 belongs to a species of *Papio, Parapapio,* or a member of the *T. oswaldi* lineage but may decrease the likelihood for identification as *C. williamsi* or *G. major* due to the highly terrestrial reconstructions of these taxa (Anderson 2019; Delson et al. 2000; Fleagle 1998; Frost and Delson 2002; Gilbert et al. 2018; Jablonski 2002; Krentz 1993; Leakey 1982; Williams and Geissler 2014). Moreover, the striking elongation of the Mc1 of KB 5378 excludes *C. williamsi* as a possible taxonomic attribution since this taxon is known to have a significantly reduced Mc1 similar to extant African colobines (Frost and Delson 2015; Jablonski et al. 2008).

The elongation of Mc1 seen in KB 5378 in addition to previously discussed trapezium morphology are consistent with morphology found in *T. o. brumpti*, providing strong support that KB 5378 belongs to a fossil member of the *T. oswaldi* lineage (Guthrie 2011). The two *T. oswaldi* subspecies present at sites near (see Table 1) Kromdraai are suggested to have diverged as chronospecies at around 2.5 Ma, evolving via anagenesis from *T. o. darti* to *T. o. oswaldi* (Frost et al. 2022; Getahun et al. 2023). KB 5378 is dated with relative certainty to be between 1.5 and 2 Ma old (Braga 2016; Delson 1988; Fouvrel 2016; Thackeray 2002; Vrba 1981). Therefore, KB 5378 is chronologically more likely to align with *T. o. oswaldi* than the earlier subspecies, *T. o. darti* (Frost et al. 2022; Getahun et al. 2023). Moreover, despite the male members of *T. o. oswaldi* having an exceptionally high body mass, the body mass range of female *T. o. oswaldi* frequently overlaps with the larger species of extant *Papio* and *Mandrillus,* the extant species with whom KB 5378 shares the most carpal morphology (Delson et al. 2000; see Tables 1 and 2). Thus, due to similarities in geological age and with our reconstruction of KB 5378 size, we conclude that KB 5378 as well as its associated metacarpals, are most likely attributed to *T. oswaldi*, and specifically *T. o. oswaldi*. Moreover, due to the close proximity between KB 5378 and the juvenile mandible KB 5227 (Vrba 1981), as well as similarities in preservation and approximate maturity, it is possible that KB 5227 may also belong to a member of *T. o. oswaldi.* However, further independent assessment is necessary to taxonomically assign KB 5227 with certainty. If our taxonomic assessment is correct, this would mark the first documented presence of this taxon at Kromdraai B and increases our understanding of both the size, geographic range, and locomotor repertoire of *T. o. oswaldi*.

CONCLUSIONS

Results from our quantitative and qualitative comparisons of the KB 5378 associated, partial carpus indicate morphology that is most consistent with arboreal and terrestrial quadrupedal monkeys, with some distinct features of the trapezium and capitate that overlap with knuckle-walking and suspensory taxa, respectively. Overall, we describe the functional morphology of the KB 5378 carpus as reflecting that of a generalized quadruped that likely engaged in a substantial proportion of terrestrial quadrupedalism. This conclusion is also supported by the relatively equal lengths of the associated KB 5378 Mc2-5 and the comparatively long length of the Mc1 that may suggest precision manipulation of grasses was part of its diet. Comparisons of absolute size do not discriminate between many of the contemporaneous taxa present at KB. However, the combination of these comparisons with contemporaneous fossil reconstructed locomotor types and the elongated Mc1 shared between KB 5378 and *Theropithecus* species, leads us to conclude that KB 5378 likely did not belong to *G. major*, as originally proposed (Vrba, 1981), but rather to a representative of *T. oswaldi*, possibly the subspecies *T. o. oswaldi*.

ACKNOWLEDGEMENTS

We thank the following institutions and individuals for access to comparative extant and/or fossil specimens: Mike Rose, the Ditsong National Museum of Natural History, Kenyan National Museum, University of Toronto Biological Anthropology collections, Royal Ontario Museum, Museum of Comparative Zoology, Harvard, State University New York, University of Toronto at Scarborough, Museum für Naturkunde, Berlin, Cleveland Museum of Natural History, Royal Museum for Central Africa, University of Toronto, Max Planck Institute for Evolutionary Anthropology, Tai chimp collection, Senckenberg Museum Frankfurt, Powell Cotton Museum, American Museum of Natural History, and the Smithsonian National Museum of Natural History. We are grateful to Matthew Skinner, Chris Dunmore, Samar Syeda, Emma Bird, Mykolas Imbrasas, Marine Cazenave, and Theodore Rose for their assistance in all aspects of this study. We thank Jose Braga, Stephany Potze, and Lazarus Kgasi for the opportunity to work on these fossils. Finally, we are grateful to Caley Orr and two anonymous reviewers for the constructive feedback that substantially improved this manuscript.

DATA AVAILABILITY STATEMENT

All data used to support the findings of this study are available openly in the supplementary information associated with this publication.

This work is distributed under the terms of a Creative Commons Attribution-NonCommercial 4.0 Unported License.

REFERENCES

Almécija, S., Smaers, J., Jungers, W., 2015. The evolution of human and ape hand proportions. Nat. Commun. 6, 7717.

Anderson, M., 2019. Functional morphology, variation, and niche separation in the large-bodied fossil colobines. Ph.D. dissertation. University of Oregon.

Begun, D.R., 2004. Knuckle-walking and the origin of human bipedalism. In: Meldrum, D.J., Hilton, C.E. (Eds.), From Biped to Strider: The Emergence of Modern Human Walking, Running, and Resource Transport. Springer New York, pp. 9–33.

Benefit, B., 1999. Biogeography, dietary specialization, and the diversification of African Plio-Pleistocene monkeys. In: Bromage, T.G. (Ed.) African Biogeography, Climate Change, and Human Evolution. Oxford University Press, New York, pp. 172–188.

Bettridge, C.M., Dunbar, R., 2012. Modeling the biogeography of fossil baboons. Int. J. Primatol. 33, 1278–1308.

Bolter, D.R., Zihlman, A.L., 2003. Morphometric analysis of growth and development in wild-collected vervet monkeys (*Cercopithecus aethiops*), with implications for growth patterns in Old World monkeys, apes and humans. J. Zool. 260, 99–110.

Bookstein, F.L., 2019. Pathologies of between-groups principal components analysis in geometric morphometrics. Evol. Biol. 46, 271–302.

Braga, J., Fourvel, J.-B., Lans, B., Bruxelles, L., Thackeray, J.F., Braga, J., Thackeray, J., 2016. Evolutionary, chronocultural and palaeoenvironmental backgrounds to the Kromdraai site: a regional perspective. In: Thackeray, J.F. (Ed.), Kromdraai: A Birthplace of *Paranthropus* in the Cradle of Humankind. African Sun Media, Stellenbosch, pp.1–16.

Braga, J., Thackeray, J.F., Bruxelles, L., Dumoncel, J., Fourvel, J.-B., 2017. Stretching the time span of hominin evolution at Kromdraai (Gauteng, South Africa): recent discoveries. C. R. Palevol. 16, 58–70.

Brain, C., 1975. An interpretation of the bone assemblage from the Kromdraai australopithecine site, South Africa. In: Tuttle, R.H. (Ed.), Paleoanthropology, Morphology and Paleoecology. Mouton Publishers, The Hague, pp. 225–243.

Broom, R., 1940. The South African Pleistocene cercopithecid apes. Ann. Transvaal Mus. 20, 89–100.

Broom, R., Robinson, J., 1949. A new type of fossil baboon, *Gorgopithecus major*. Proc. Zool. Soc. Lond. 119, 379–386.

Bruxelles, L., Maire, R., Couzens, R., Thackeray, J.F., Braga, J., 2016. A revised stratigraphy of Kromdraai. In: Thackeray, J.F. (Ed.) Kromdraai, a Birthplace of *Paranthropus* in the Cradle of Humankind. African Sun Media, Stellenbosch, pp. 31–47.

Cant, J.G.H., 1988. Positional behavior of long-tailed macaques (*Macaca fascicularis*) in northern Sumatra. Am. J. of Phys. Anthropol. 76, 29–37.

Cant, J.G.H., 1986. Locomotion and feeding postures of spider and howling monkeys: field study and evolutionary interpretation. Folia Primatol. 46, 1–14.

Carlson, K.J., Patel, B.A., 2006. Habitual use of the primate forelimb is reflected in the material properties of subchondral bone in the distal radius. J. Anat. 208, 659–670.

Ciochon, R., 1993. Evolution of the Cercopithecoid Forelimb: Phylogenetic and Functional Implications from Morphometric Analyses. University of California Press, Berkeley.

Corruccini, R.S., Ciochon, R.L., McHenry, H.M., 1975. Osteometric shape relationships in the wrist joint of some anthropoids. Folia Primatol., 24(4), 250–274.

Daver, G., Berillon, G., Grimaud-Hervé, D., 2012. Carpal kinematics in quadrupedal monkeys: towards a better understanding of wrist morphology and function. J. Anat. 220, 42–56.

Deak, N., Bordoni, B., 2019. Anatomy, Shoulder and Upper Limb, Wrist Flexor Retinaculum. Stat Pearls Publishing LLC, Florida.

Defler, T.R., 2000. Locomotion and posture in *Lagothrix lagotricha*. Folia Primatol. 70, 313–327.

Delson, E., 1993. *Theropithecus* fossils from Africa and India and the taxonomy of the genus. In: Jablonski, N.G. (Ed.), *Therpithecus*: The Rise and Fall of a Primate Genus. Cambridge University Press, Cambridge, pp. 157–189.

Delson, E., Terranova, C.J., Jungers, W.L., Sargis, E.J., Jablonski, N.G., 2000. Body mass in Cercopithecidae (Primates, Mammalia): estimation and scaling in extinct and extant taxa. Anthropol. Papers Am. Nat. Hist. no. 83, New York.

Dunbar, R., Dunbar, E., 1974. Ecological relations and niche separation between sympatric terrestrial primates in Ethiopia. Folia Primatol. 21, 36–60.

Eck, G.G., 1993. *Theropithecus darti* from the Hadar formation, Ethiopia. In: Jablonski, N.G. (Ed.), *Therpithecus*: The Rise and Fall of a Primate Genus. Cambridge University Press, Cambridge, pp. 15–83.

El-Zaatari, S., Grine, F.E., Teaford, M.F., Smith, H.F., 2005. Molar microwear and dietary reconstructions of fossil Cercopithecoidea from the Plio-Pleistocene deposits of South Africa. J. Hum. Evol. 49, 180–205.

Etter, H., 1973. Terrestrial adaptations in the hands of Cercopithecinae. Folia Primatol. 20, 331–350.

Fleagle, J., 1978. Locomotion, posture and habitat utilization in two sympatric Malayan leaf monkeys. In: Montgomery, G.G (Ed.), Ecology of Arboreal Folivores. Smithsonian Institution Press, Washington, pp. 243–251.

Fleagle, J.G., 1976. Locomotion and posture of the Malayan siamang and implications for hominoid evolution. Folia Primatol. 26, 245–269.

Fleagle, J.G., 1998. Primate Adaptation and Evolution. Elsevier, Amsterdam.

Folinsbee, K E., Reisz, R R., 2013. New craniodental fossils of papionin monkeys from Cooper's D, South Africa. Am. J. Phys. Anthropol. 151, 613–629.

Fourvel, J.B., Brink, J., O'regan, H., Beaudet, A., Pavia, M., 2016. Some preliminary interpretations of the oldest faunal assemblage from Kromdraai. In: Thackeray, J.F. (Ed.), Kromdraai, a Birthplace of *Paranthropus* in the Cradle of Humankind. African Sun Media, Stellenbosch, pp. 71–104.

Freedman, L., 1957. The fossil cercopithecoidea of South Africa. Ann. Transvaal Mus. 23, 121–262.

Frost, S.R., Delson, E., 2002. Fossil Cercopithecidae from the Hadar Formation and surrounding areas of the Afar Depression, Ethiopia. J. Hum. Evol. 43, 687–748.

Frost, S.R., Gilbert, C.C., Pugh, K.D., Guthrie, E.H., Delson, E., 2015. The hand of *Cercopithecoides williamsi* (Mammalia, Primates): earliest evidence for thumb reduction among colobine monkeys. PloS One 10, e0125030.

Frost, S.R., White, F.J., Reda, H.G., Gilbert, C.C., 2022. Biochronology of South African hominin-bearing sites: a reassessment using cercopithecid primates. Proc. Nat. Acad. Sci. 119, e2210627119.

Gear, J., 1926. A preliminary account of the baboon remains from Taungs. S. Afr. J. Sci. 23, 731–747.

Gebo, D.L., Chapman, C.A., 1995. Positional behavior in five sympatric Old World monkeys. Am. J. Phys. Anthropol. 97, 49–76.

Gebo, D.L., Sargis, E.J., 1994. Terrestrial adaptations in the postcranial skeletons of guenons. Am. J. Phys. Anthropol. 93, 341–371.

Getahun, D.A., Delson, E., Seyoum, C.M. 2023. A review of *Theropithecus oswaldi* with the proposal of a new subspecies. J. Hum. Evol. 180, 103373.

Gilbert, C.C., 2007. Identification and description of the first *Theropithecus* (Primates: Cercopithecidae) material from Bolt's Farm, South Africa. Ann. Transvaal Mus, 44, 1–10.

Gilbert, C.C., Frost, S.R., Pugh, K.D., Anderson, M., Delson, E., 2018. Evolution of the modern baboon (*Papio hamadryas*): a reassessment of the African Plio-Pleistocene record. J. Hum. Evol. 122, 38–69.

Guthrie, E.H., 2011. Functional morphology of the postcranium of *Theropithecus brumpti* (Primates: Cercopithecidae). Ph.D. Dissertation. University of Oregon.

Hamada, Y., 1984. Age changes of the carpal bones in macaques: application of the Fourier analysis on the radiographs. Primates 25, 485–506.

Hammer, Ø., Harper, D.A.T., Ryan, P.D., 2001. PAST: Paleontological Statistics Software Package for Education and Data Analysis. Palaeontol. Electron. 4(1), 9.

Hamrick, M.W., 1996. Locomotor adaptations reflected in the wrist joints of early Tertiary primates (Adapiformes). Am. J. Phys. Anthropol.100, 585–604.

Hamrick, M.W., 2007. Evolvability, limb morphology, and primate origins. In: Ravosa, M.J., Dagosto, M. (Eds.), Primate Origins: Adaptations and Evolution. Springer, Boston. pp. 381–401.

Hunt, K.D., 1991. Positional behavior in the Hominoidea. Int. J. Primatol. 12, 95–118.

Jablonski, N.G., 2002. Fossil Old World monkeys: the Late Neogene radiation. In: Hartwig, W.C. (Ed.), The Primate Fossil Record. Cambridge University Press, Cambridge, pp. 255–299.

Jablonski, N.G., Leakey, M.G., Ward, C.V., Antón, M. 2008. Systematic paleontology of the large colobines. In:

Jablonski, N.G., Leakey, M.G. (Eds.), Koobi Fora Research Project, vol. 6. California Academy of Sciences, San Francisco, pp. 31–102.

Jungers, W.L., Falsetti, A.B., Wall, C.E., 1995. Shape, relative size, and size-adjustments in morphometrics. Am. J. Phys. Anthropol. 38, 137–161.

Kerley, E.R., 1966. Skeletal age changes in the chimpanzee. Tulane Studies Zool. 13, 71–82.

Kimura, T., Hamada, Y., 1990. Development of epiphyseal union in Japanese macaques of known chronological age. Primates 31, 79–93.

Kivell, T.L., 2016. The primate wrist. In: Kivell, T.L., Lemelin, P., Richmond, B.G., Schmitt, D. (Eds.), The Evolution of the Primate Hand: Anatomical, Developmental, Functional and Paleontological Evidence. Springer, Berlin, pp. 17–54.

Kivell, T.L., 2007. Ontogeny of the hominoid midcarpal joint and implications for the origin of hominin bipedalism. Ph.D. Dissertation. University of Toronto.

Kivell, T.L., Begun, D.R., 2007. Frequency and timing of scaphoid-centrale fusion in hominoids. J. Hum. Evol. 52, 321–340.

Kivell, T.L., Begun, D.R., 2009. New primate carpal bones from Rudabánya (late Miocene, Hungary): taxonomic and functional implications. J. Hum. Evol. 57, 697–709.

Krentz, H.B., 1993. Postcranial anatomy of extant and extinct species of *Theropithecus*. In: Jablonski, N.G. (Ed.), *Theropithecus*: The Rise and Fall of a Primate Genus. Cambridge University Press, Cambridge, pp. 383–422.

Kivell, T.L., Davenport, R., Hublin, J.J., Thackeray, J.F., Skinner, M.M., 2018. Trabecular architecture and joint loading of the proximal humerus in extant hominoids, *Ateles*, and *Australopithecus africanus*. Am. J. Phys. Anthropol. 167, 348–365.

Leakey, M.G., 1982. Extinct large colobines from the Plio-Pleistocene of Africa. Am. J. Phys. Anthropol. 58, 153–172.

Lewis, O.J., 1989. Functional Morphology of the Evolving Hand and Foot. Oxford University Press, Oxford.

Lovejoy, C.O., Simpson, S.W., White, T.D., Asfaw, B., Suwa, G., 2009. Careful climbing in the Miocene: the forelimbs of *Ardipithecus ramidus* and humans are primitive. Science 326, 70-70e8.

Marzke, M.W., 1983. Joint functions and grips of the *Australopithecus afarensis* hand, with special reference to the region of the capitate. J. Hum. Evol. 12, 197–211.

McCrossin, M.L., Benefit, B.R., Gitau, S.N., Palmer, A.K., Blue, K.T., 1998. Fossil evidence for the origins of terrestriality among Old World higher primates. In: Strasser, E., Fleagle, J.G., Rosenberger, A.L., McHenry, H.M. (Eds.), Primate Locomotion. Springer, Boston. pp. 353–396.

Marzke, M.W., Tocheri, M.W., Steinberg, B., Femiani, J.D., Reece, S.P., Linscheid, R.L., Orr, C.M., Marzke, R.F., 2010. Comparative 3D quantitative analyses of trapeziometacarpal joint surface curvatures among living catarrhines and fossil hominins. Am. J. Phys. Anthropol. 141(1), 38–51.

McGraw, W.S., 2004. Diversity of guenon positional behavior. In: Glenn, M.E, Cords, M. (Eds.), The Guenons: Diversity and Adaptation in African Monkeys. Springer, Boston pp. 113–131.

Michejda, M., Bacher, J., 1981. Skeletal age as a determinant of gestation in *Macaca mulatta*: a radiographic study. J. Med. Primatol. 10, 293–301.

Mittermeier, R.A., 1978. Locomotion and posture in *Ateles geoffroyi* and *Ateles paniscus*. Folia Primatol. 30, 161–193.

Morbeck, M.E., 1977. Positional behavior, selective use of habitat substrate and associated non-positional behavior in free-ranging *Colobus guereza* (Rüppel, 1835). Primates 18, 35–58.

Napier, J.R., 1967. Evolutionary aspects of primate locomotion. Am. J. Phys. Anthropol. 27, 333–341.

Nakatsukasa, M., 1994. Morphology of the humerus and femur in African mangabeys and guenons: functional adaptation and implications for the evolution of positional behavior. Afr. Study Monogr. Suppl. 21, 1–61.

Newell-Morris, L., Tarrant, L.H., Fahrenbruch, C.E., Burbacher, T.M., Sackett, G.P., 1980. Ossification in the hand and foot of the pigtail macaque (*Macaca nemestrina*). II. Order of appearance of centers and variability in sequence. Am. J. Phys. Anthropol. 53, 423–439.

O'Connor, B.L., 1975. The functional morphology of the cercopithecoid wrist and inferior radioulnar joints, and their bearing on some problems in the evolution of the Hominoidea. Am. J. Phys. Anthropol. 43, 113–121.

Orr, C.M., 2018. Kinematics of the anthropoid os centrale and the functional consequences of scaphoid-centrale fusion in African apes and hominins. J. Hum. Evol. 114, 102–117.

Patel, B.A., 2010a. Functional morphology of cercopithecoid primate metacarpals. J. Hum. Evol. 58, 320–337.

Patel, B.A., 2010b. The interplay between speed, kinetics, and hand postures during primate terrestrial locomotion. Am. J. Phys. Anthropol. 141, 222–234.

Patel, B.A., Maiolino, S.A., 2016. Morphological diversity in the digital rays of primate hands. In: Kivell, T.L., Lemelin, P., Richmond, B.G., Schmitt, D. (Eds.), The Evolution of the Primate Hand: Anatomical, Developmental, Functional and Paleontological Evidence. Springer, Berlin, pp. 55–100.

Queen, J.P., Quinn, G.P., Keough, M.J., 2002. Experimental Design and Data Analysis for Biologists. Cambridge University Press, Cambridge.

R Core Team, 2021. R: A Language and Environment for Statistical Computing. R Foundation for Statistical Computing, Vienna, Austria.

Rafferty, K.F., 1990. The functional and phylogenetic significance of the carpometacarpal joint of the thumb in anthropoid primates. Ph.D. Dissertation. New York University.

Richmond, B.G., 2006. Functional morphology of the midcarpal joint in knuckle-walkers and terrestrial quadrupeds. In: Ishida, H., Tuttle, R., Pickford, M., Ogihara, N., Nakatsukasa, M. (Eds.), Human Origins and Environmental Backgrounds. Developments in Primatology:

Progress and Prospects. Springer, Boston, pp. 105–122.
Richmond B.G., Begun D.R., Strait D.S., 2001 Origin of human bipedalism: the knuckle-walking hypothesis revisited. Am. J. of Phys. Anthropol. 116(S33), 70–105.
Rodman, P.S., 1979. Skeletal differentiation of *Macaca fascicularis* and *Macaca nemestrina* in relation to arboreal and terrestrial quadrupedalism. Am. J. of Phys. Anthropol. 51, 51–62.
Rose, M., 1973. Quadrupedalism in primates. Primates 14, 337–357.
Rowe, N., Goodall, J., Mittermeier, R., 1996. The Pictorial Guide to the Living Primates. Pogonias Press, New York.
Sarmiento, E.E., 1988. Anatomy of the hominoid wrist joint: its evolutionary and functional implications. Int. J. Primatology. 9, 281–345.
Schloerke, B., Cook, D., Larmarange, J., Briatte, F., Marbach, M., Thoen, E., Elberg, A., Crowley, J., 2021. Ggally: Extension to 'ggplot2'. R package version 2.1.2. R Foundation for Statistical Computing, Vienna.
Schmitt, D., 2003. Mediolateral reaction forces and forelimb anatomy in quadrupedal primates: implications for interpreting locomotor behavior in fossil primates. J. Hum. Evol. 44, 47–58.
Smith, R.J., Jungers, W.L. 1997. Body mass in comparative primatology. J. Hum. Evol. 32(6), 523–559.
Thackeray, J.F., 2017. Kromdraai: A Birthplace of *Paranthropus* in the Cradle of Humankind. Sun Press Media, Stellenbosch.
Tocheri, M.W., Marzke, M., Liu, D., Bae, M., Jones, G., Williams, R., Razdan, A., 2003. Functional capabilities of modern and fossil hominid hands: three-dimensional analysis of trapezia. Am. J. Phys. Anthropol. 122, 101–112.
Tocheri, M.W., Razdan, A., Williams, R., Marzke, M., 2005. A 3D quantitative comparison of trapezium and trapezoid relative articular and nonarticular surface areas in modern humans and great apes. J. Hum. Evol. 49, 570–586.
Tuttle, R., 1969. Terrestrial trends in the hands of the Anthropoidea. A preliminary report. In: Carpenter, C.R. (Ed.), Recent Advances in Primatology. S. Karger, New York, pp. 187–191.
Tuttle, R.H., 1967. Knuckle-walking and the evolution of hominoid hands. Am. J. Phys. Anthropol. 26, 171–206.
Van der Spuy Mollett, O., 1947. Fossil mammals from the Makapan valley, Potgietersrust, I. Primates. S. Afr. J. Sci. 43, 295–303.
Van Wagenen, G., Asling, C., 1964. Ossification in the fetal monkey (*Macaca mulatta*). Estimation of age and progress of gestation by roentgenography. Am. J. Anat. 114, 107–132.
Vanhoof, M.J., Galletta, L., De Groote, I., Vereecke, E.E., 2021. Functional signals and covariation in triquetrum and hamate shape of extant primates using 3D geometric morphometrics. J. Morphol. 282, 1382–1401.
Van Leeuwen, T., Vanneste, M., D'Agostino, P., Vereecke, E.E., 2022. Trapeziometacarpal joint mobility in gibbons (fam. Hylobatidae) and rhesus macaques (*Macaca mulatta*). Am. J. Biol. Anthropol. 177(4), 708–718.
Vrba, E., 1981. The Kromdraai australopithecine site revisited in 1980; recent investigations and results. Ann. Transvaal Mus. 33, 17–60.
Ward, C., Leakey, M., Brown, B., Brown, F., Harris, J., Walker, A., 1999. South Turkwel: a new Pliocene hominid site in Kenya. J. Hum. Evol. 36, 69–95.
Ward, C.V., 2002. Interpreting the posture and locomotion of *Australopithecus afarensis*: where do we stand? Am. J. Phys. Anthropol. 119, 185–215.
Wickham, H., 2016. Ggplot2: Elegant Graphics for Data Analysis. Springer-Verlag, New York.
Wickham, H., François, R., Henry, L., Müller, K., 2021. Dplyr: A Grammar of Data Manipulation. R package version 1.0.7. R Foundation for Statistical Computing, Vienna.
Williams, F.L.E., Geissler, E., 2014. Reconstructing the diet and paleoecology of Plio-Pleistocene *Cercopithecoides williamsi* from Sterkfontein, South Africa. Palaios 29, 483–494.

Supplement 1: Taxonomic and Functional Interpretation of Associated Cercopithecoid Carpal Bones (KB 5378) from Kromdraai B, South Africa

MADISON ROSE
School of Anthropology and Conservation, University of Kent, Canterbury, CT2 7NR, UNITED KINGDOM; and, Department of Anthropology, University of Toronto, Scarborough M1C 1A4, CANADA; mads.rose@mail.utoronto.ca

MIRRIAM TAWANE
Ditsong National Museum of Natual History, Pretoria; and, Centre for the Exploration of the Deep Human Journey, University of the Witwatersrand, Johannesburg, SOUTH AFRICA; tawane@ditsong.org.za

TRACY L. KIVELL*
Department of Human Origins, Max Planck Institute for Evolutionary Anthropology, Leipzig 04103, GERMANY; School of Anthropology and Conservation, University of Kent, Canterbury, CT2 7NR, UNITED KINGDOM; and, Centre for the Exploration of the Deep Human Journey, University of the Witwatersrand, Johannesburg, SOUTH AFRICA; tracy_kivell@eva.mpg.de

SUPPLEMENT 1
This file includes: Supplementary Figures 1–8 and Tables 1–4.

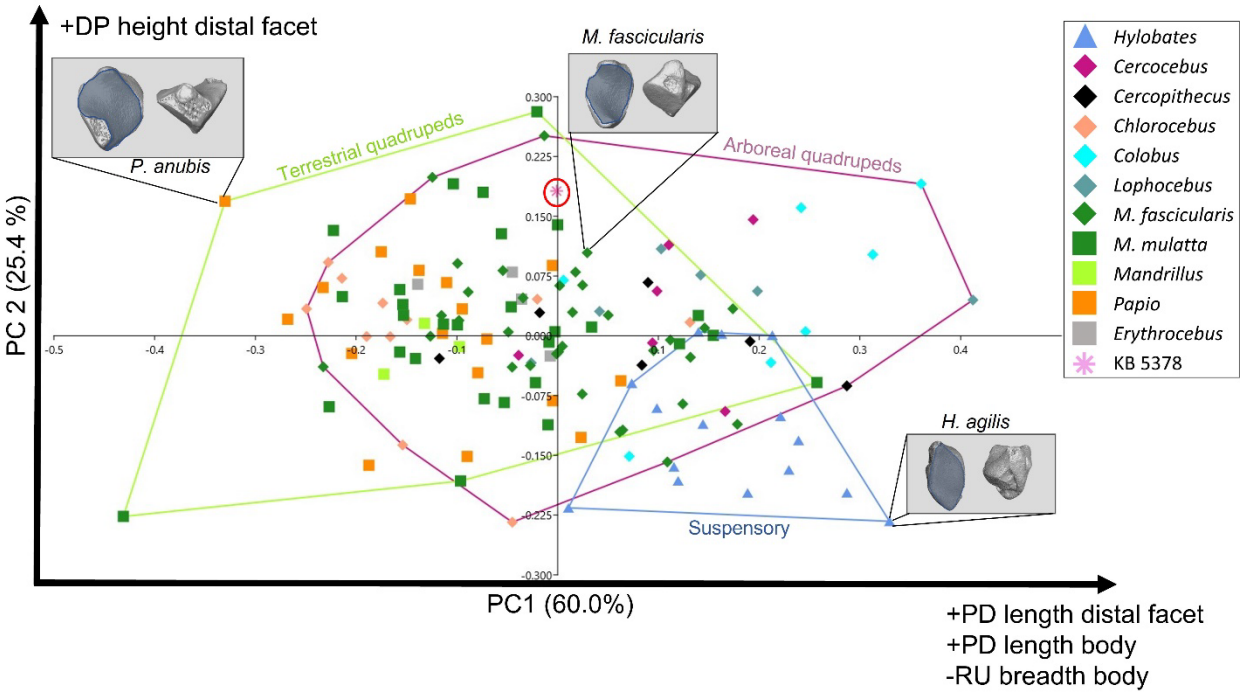

Supplementary Figure 1. Within-group PCA results of the os centrale. The percentage of variation described by each PC is provided in brackets on their respective axes. Locomotor groups are each surrounded by labelled convex hulls. Surface models of representative taxa are included to demonstrate the morphology reflected at various points of the plot. Relevant facets on each surface model are shaded for clarification of the change in morphology along each axis.

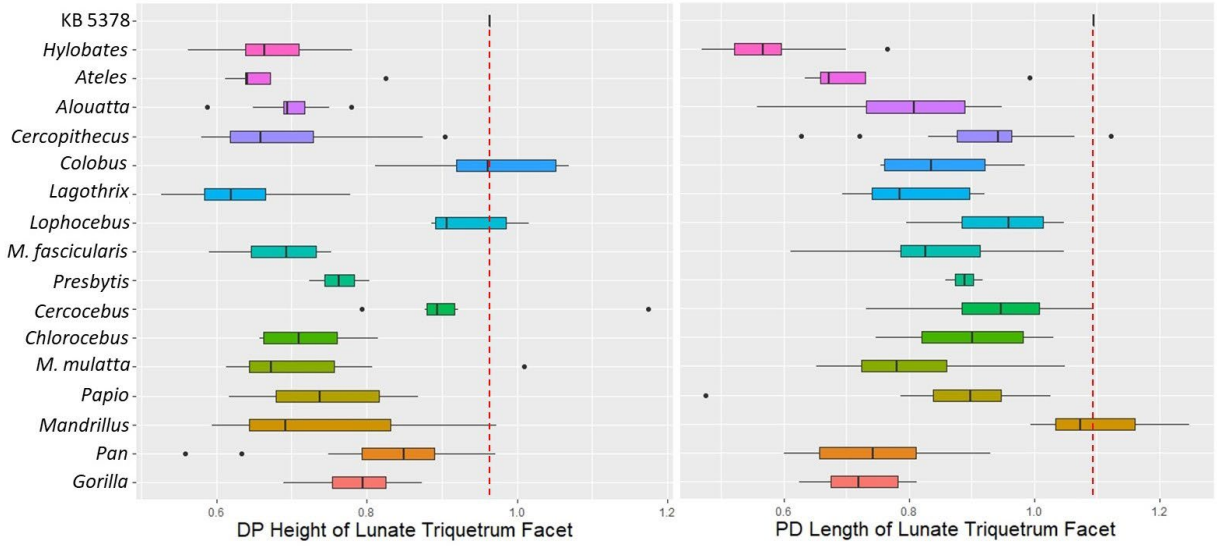

Supplementary Figure 2. Box-and-whisker plots of the lunate triquetrum facet shape variables. All values are scaled by geometric mean. The measurement value of KB 5378 is represented by a dashed red line.

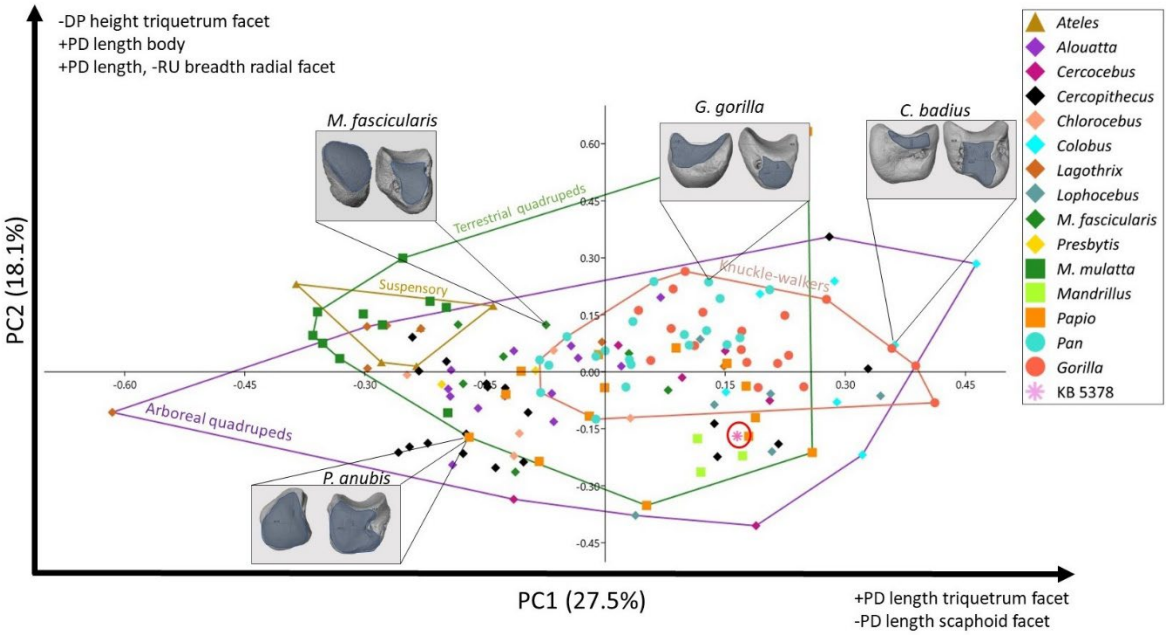

Supplementary Figure 3. Within-group PCA results of the lunate. The percentage of variation described by each PC is provided in brackets on their respective axes. Locomotor groups are each surrounded by labelled convex hulls. Surface models of representative taxa are included to demonstrate the morphology reflected at various points of the plot. Relevant facets on each surface model are shaded for clarification of the change in morphology along each axis.

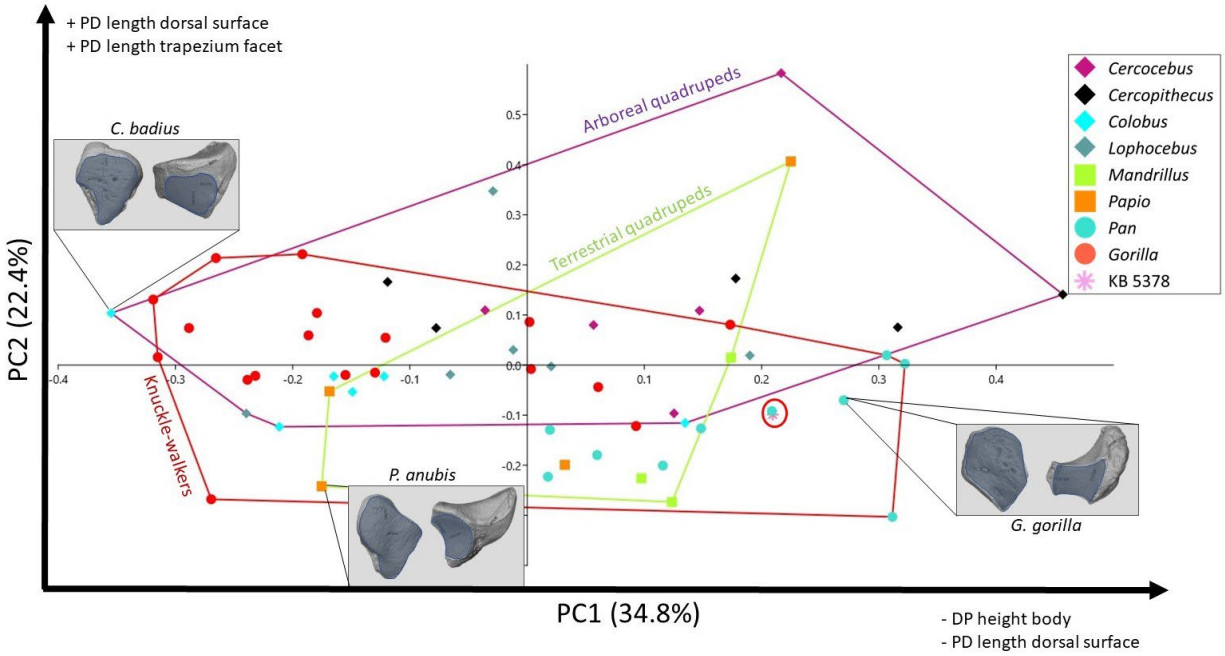

Supplementary Figure 4. Within-group PCA results of the trapezoid. The percentage of variation described by each PC is provided in brackets on their respective axes. Locomotor groups are each surrounded by labelled convex hulls. Surface models of representative taxa are included to demonstrate the morphology reflected at various points of the plot. Relevant facets on each surface model are shaded for clarification of the change in morphology along each axis.

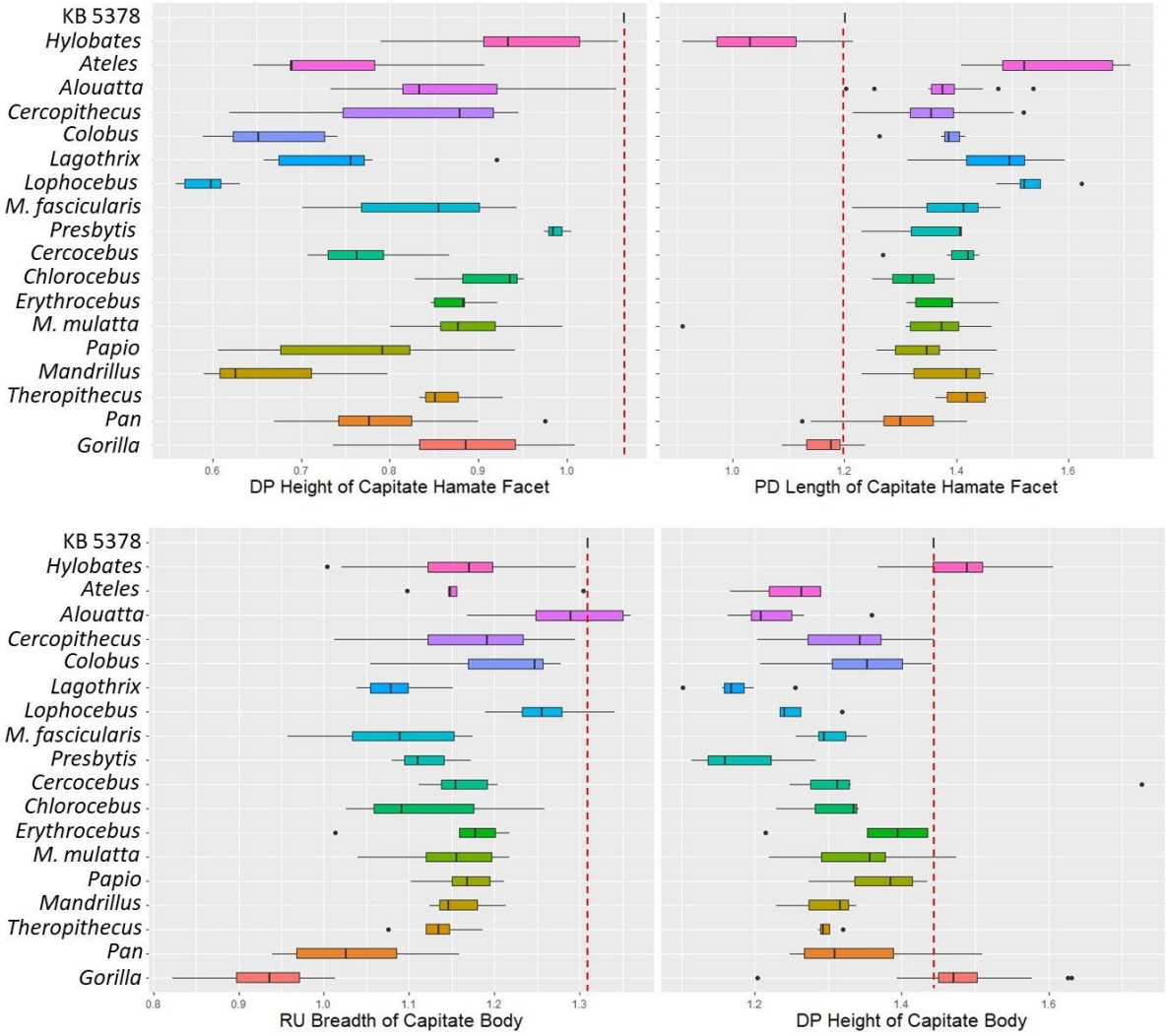

Supplementary Figure 5. Box-and-whisker plots of the capitate body and hamate facet shape variables. All values are scaled by geometric mean. The measurement value of KB 5378 is represented by a dashed red line.

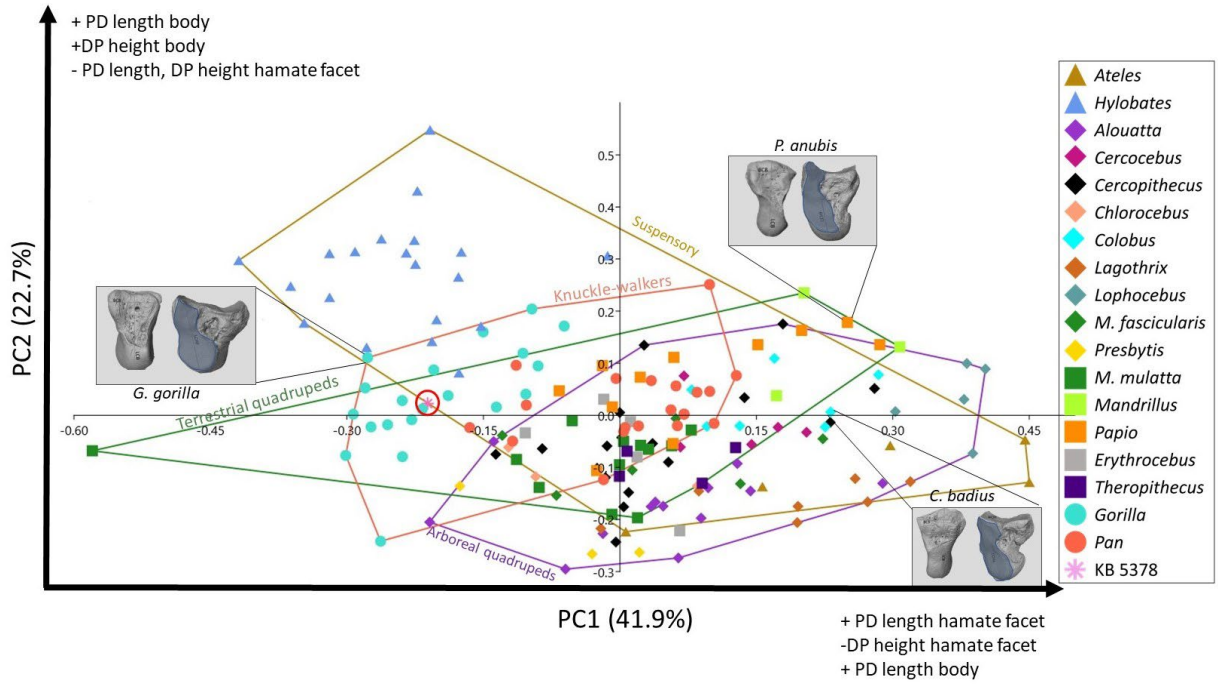

Supplementary Figure 6. Within-group PCA results of the capitate. The percentage of variation described by each PC is provided in brackets on their respective axes. Locomotor groups are each surrounded by labelled convex hulls. Surface models of representative taxa are included to demonstrate the morphology reflected at various points of the plot. Relevant facets on each surface model are shaded for clarification of the change in morphologies along each axis.

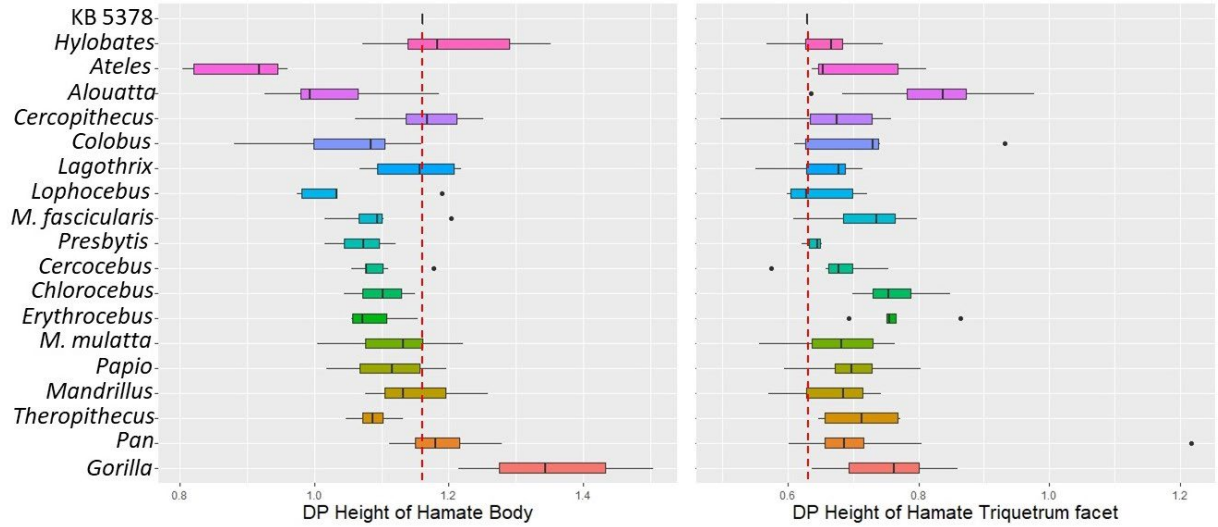

Supplementary Figure 7. Box-and-whisker plots of the dorsopalmar height of the hamate body including the hamulus, and dorsopalmar height of the triquetrum facet. All values are scaled by geometric mean. The measurement value of KB 5378 is represented by a dashed red line.

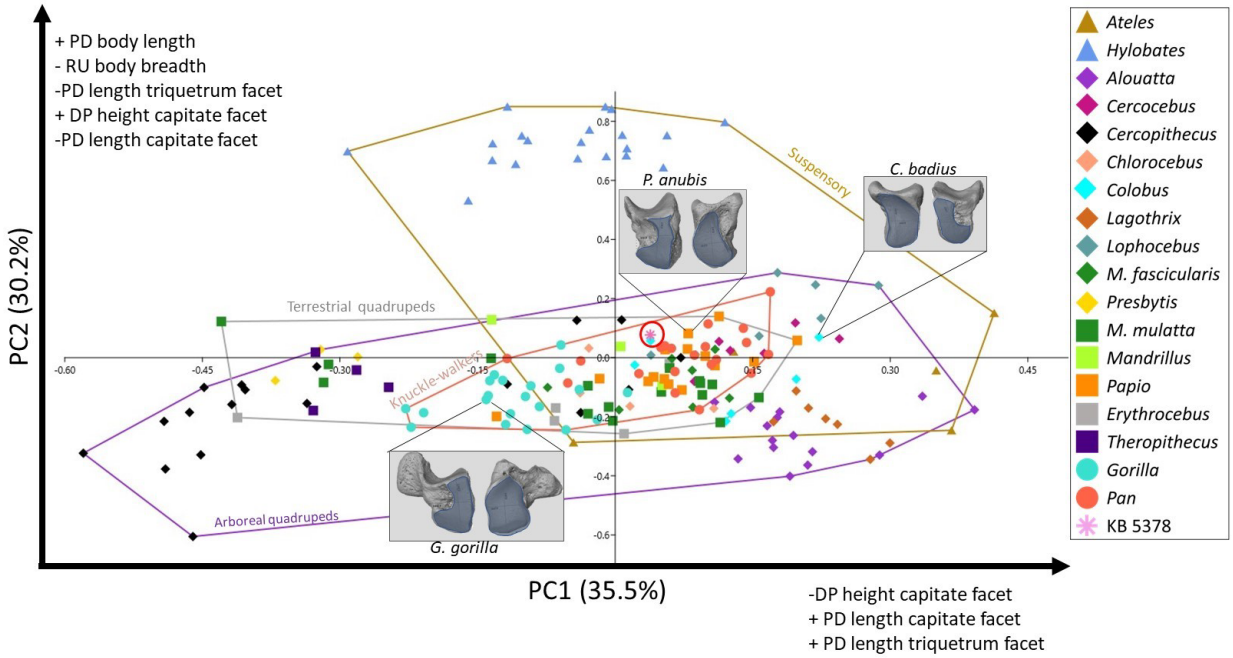

Supplementary Figure 8. Within-group PCA results of the hamate. The percentage of variation described by each PC is provided in brackets on their respective axes. Locomotor groups are each surrounded by labelled convex hulls. Surface models of representative taxa are included to demonstrate the morphology reflected at various points of the plot. Relevant facets on each surface model are shaded for clarification of the change in morphology along each axis.

SUPPLEMENTARY TABLE 1. DESCRIPTION OF CATEGORIZATION OF COMPARATIVE SAMPLE INTO LOCOMOTOR GROUPS (the arboreal quadrupedal category is organized, from top to bottom, on a scale of most arboreal, to least arboreal to further organize the diverse group of taxa therein).

Locomotor Group	Taxa	Description	Source
Suspensory	*Ateles*	26–38.6% of locomotion tail/arm suspension, while 22–25.4% arboreal quadrupedalism	(Cant 1986; Mittermeier 1978)
	Hylobates	51% of travel and 23% feeding used brachiation involving suspension by the forelimbs.	(Fleagle 1976; Hunt 1991)
Arboreal quadrupeds	*Alouatta*	96% of locomotion arboreal quadrupedal	(Cant 1986)
	Cercopithecus mitis, nictitans, ascanius	*C. mitis* and C. *ascanius* spend 54% and 42% of time using arboreal quadrupedalism in the upper and middle canopy. *C. ascanius* uses arboreal quadrupedalism 39% of its travel and feeding and prefers mid-canopy.	(Gebo and Chapman 1995; Gebo and Sargis 1994; Nakatsukasa 1994; Rose 1973)
	Colobus guereza	Arboreal quadrupedalism 41% of travel time, prefers upper canopy.	(Gebo and Chapman 1995; Morbeck 1977)
	Lagothrix lagotricha	41.8% of its travel time, and 42.8% of feeding time spent using arboreal quadrupedalism	(Defler 2000)
	Lophocebus albigena	Arboreal quadrupedalism 47% of travel time in mid canopy.	(Gebo and Chapman 1995)
	Macaca fascicularis	"An arboreal species that normally feeds and travels in the trees." (Fleagle 1998: 190)	(Cant 1988; Fleagle 1998; Rodman 1979)
	Presbytis	Arboreal quadrupeds that additionally utilize leaping and arm suspension.	(Fleagle 1978, Fleagle 1998; Patel 2010a)
	Cercocebus torquatus	"Spends considerable time on ground and lower stratum, arboreal for eating and sleeping (Nakatsukasa 1994 pg. 5, table 1"	(Nakatsukasa 1994; Patel 2010a)
	Chlorocebus aethiops	Travels and feeds on ground, keeping arboreal abilities for escape.	(Gebo and Sargis 1994; McGraw 2004; Patel 2010a)
Terrestrial quadruped	*Erythrocebus patas*	Spends 59.6% of time on ground, and 90.5% of feeding on ground.	(Gebo and Sargis 1994; Patel 2010b)
	Papio anubis, hamadryas, cynocephalus, doguera	Terrestrial but partly arboreal for sleeping and escape.	(Dunbar and Dunbar 1974; Patel 2010b; Rose 1973; Tuttle 1969)

	Macaca mulatta	Equally terrestrial and arboreal	(Fleagle 1998; Patel 2010b; Tuttle 1969)
	Mandrillus	Primarily terrestrial, with males being more terrestrial than females and young.	(Rowe 1996)
	Theropithecus gelada	Only 1.6% of individuals observed were in trees, known to be "the most terrestrial of non-human primates" (Fleagle 1998: 198)	(Dunbar and Dunbar 1974; Fleagle 1998)
Knuckle-walkers	*Pan troglodytes, paniscus*	"The knuckle-walking postures of chimpanzees and gorillas in unique among primates and allows these apes to utilize the opportunities of terrestrial locomotion…." (Tuttle 1967: 171)	(Hunt 1991; Tuttle 1967)
	Gorilla gorilla, beringei		(Hunt 1991; Tuttle 1967)

SUPPLEMENTARY TABLE 2. RAW DATA FOR ALL SHAPE VARIABLES FOR THE COMPARATIVE SAMPLE GIVEN IN MM (all meausurements were taken using digital calipers by either TLK or MR).

	OCH					OCL					OCB				
Genus	min	max	mean	std. dev	CI	min	max	mean	std. dev	CI	min	max	mean	std. dev	CI
Cercocebus	4.80	6.50	5.82	0.67	0.54	6.80	8.70	7.96	0.87	0.70	3.30	5.50	4.22	0.80	0.64
Cercopithecus	4.20	5.80	4.90	0.60	0.45	5.60	7.90	6.92	0.80	0.60	3.00	4.60	3.66	0.74	0.55
Colobus	5.00	6.50	5.75	0.56	0.42	7.00	9.00	7.97	0.70	0.52	2.60	5.10	3.62	0.98	0.72
Chlorocebus	3.40	5.40	4.39	0.58	0.34	4.80	7.20	5.86	0.60	0.35	2.90	4.60	3.97	0.44	0.26
Erythrocebus	4.70	7.50	4.96	1.52	1.49	6.00	8.90	7.03	1.80	1.76	3.50	6.30	3.89	1.34	1.31
Lophocebus	5.60	6.40	5.87	0.34	0.27	7.50	8.70	8.11	0.45	0.36	2.80	5.20	3.95	0.90	0.72
Macaca m.	3.80	7.40	5.73	1.13	0.41	5.30	9.40	7.49	1.07	0.39	2.40	7.20	4.77	1.22	0.44
Macaca f.	3.30	5.00	4.38	0.48	0.16	4.50	7.60	5.95	0.63	0.21	2.40	4.40	3.40	0.52	0.17
Mandrillus	6.80	9.40	8.15	1.31	1.48	10.20	13.10	11.88	1.48	1.68	7.30	9.00	8.18	0.86	0.97
Papio	4.50	12.00	8.24	1.54	0.69	6.00	13.40	10.53	1.74	0.78	3.40	9.20	7.26	1.49	0.67

	OCDFH					OCDFL				
Genus	min	max	mean	std. dev	CI	min	max	mean	std. dev	CI
Cercocebus	4.70	6.90	5.88	0.82	0.66	5.90	8.30	7.30	1.07	0.86
Cercopithecus	4.30	5.90	4.82	0.55	0.41	5.10	6.60	6.00	0.53	0.39
Colobus	4.50	6.60	5.54	0.72	0.53	6.10	7.60	7.13	0.50	0.37
Chlorocebus	3.60	5.10	4.46	0.48	0.28	4.30	5.40	4.74	0.40	0.24
Erythrocebus	4.30	7.50	5.62	1.18	1.15	4.80	8.00	6.16	1.26	1.24
Lophocebus	5.20	6.30	5.77	0.42	0.34	6.40	7.70	7.10	0.48	0.38
Macaca m.	3.20	7.30	5.56	0.97	0.35	3.80	8.10	6.17	0.94	0.34
Macaca f.	3.00	5.40	4.24	0.65	0.22	3.80	6.40	4.85	0.55	0.18
Mandrillus	9.00	10.10	9.46	0.58	0.65	9.50	9.80	9.68	0.13	0.14
Papio	3.40	11.80	8.28	1.80	0.81	4.50	11.90	8.96	1.47	0.66

	LLB					HLB					BLB					HLSF					LLSF				
Genus	min	max	mean	sd	ci	min	max	mean	sd	ci	min	max	mean	sd	ci	min	max	mean	sd	ci	min	max	mean	sd	ci
Alouatta	7.10	8.40	7.74	0.42	0.23	6.15	15.72	7.28	2.45	1.33	4.04	7.56	4.80	0.85	0.46	5.33	11.45	6.38	1.54	0.84	2.85	6.42	3.75	0.88	0.48
Ateles	8.50	10.90	9.86	1.03	0.90	6.15	7.87	6.72	0.46	0.40	4.04	5.03	4.62	0.31	0.27	5.33	7.02	6.04	0.52	0.45	2.85	5.11	3.66	0.60	0.53
Cercocebus	8.10	10.40	9.56	1.02	0.82	8.08	10.50	9.39	0.95	0.76	5.41	7.01	6.40	0.68	0.55	6.80	9.27	8.23	0.91	0.73	2.95	5.00	4.10	0.81	0.65
Cercopithecus	7.10	9.50	8.38	0.70	0.31	6.56	9.68	7.61	0.92	0.42	4.11	8.65	5.35	1.02	0.46	5.90	8.19	7.00	0.68	0.31	1.81	5.80	4.03	1.03	0.46
Chlorocebus	6.50	6.80	6.64	0.13	0.11	5.54	6.67	6.13	0.47	0.42	3.75	4.15	3.95	0.16	0.14	4.22	5.66	5.02	0.57	0.50	3.20	4.06	3.57	0.38	0.33
Colobus	8.90	10.50	9.79	0.50	0.37	8.73	10.29	9.34	0.65	0.48	4.96	5.96	5.49	0.30	0.22	4.99	8.99	7.48	1.53	1.13	2.24	3.60	3.01	0.45	0.33
Gorilla	16.00	26.00	21.07	2.77	1.22	17.89	28.87	22.88	3.52	1.54	13.90	20.11	16.94	2.42	1.06	12.51	20.94	16.70	2.55	1.12	7.38	12.84	9.99	1.41	0.62
Hylobates	8.60	10.60	9.37	0.59	0.26	8.14	9.54	8.87	0.42	0.18	4.99	7.79	6.39	0.82	0.36	6.24	8.80	7.64	0.67	0.29	5.61	9.34	7.55	0.92	0.40
Lagothrix	7.40	9.50	8.49	0.73	0.54	6.73	8.30	7.38	0.59	0.44	4.49	6.57	5.25	0.82	0.61	5.56	6.26	5.86	0.29	0.21	2.85	6.17	4.41	1.18	0.87
Lophocebus	9.30	10.80	9.93	0.62	0.50	6.65	10.50	8.35	1.55	1.24	4.11	6.59	5.01	0.92	0.73	5.90	9.07	7.29	1.12	0.89	1.81	4.40	2.96	0.92	0.74
M. fascicularis	7.00	8.50	7.50	0.50	0.37	6.15	7.55	6.51	0.49	0.36	3.84	4.97	4.39	0.47	0.35	5.53	6.43	6.16	0.32	0.23	2.70	4.28	3.51	0.62	0.46
M. mulatta	8.80	11.50	9.96	0.85	0.53	8.28	10.87	9.47	0.76	0.47	5.25	7.56	5.96	0.71	0.44	7.27	9.87	8.54	0.76	0.47	5.55	8.16	6.83	0.95	0.59
Mandrillus	14.30	14.80	14.45	0.30	0.34	12.22	14.31	13.41	1.08	1.22	8.76	9.46	9.23	0.40	0.46	8.45	11.84	10.25	1.70	1.93	4.54	5.84	5.29	0.67	0.76
Pan	13.80	20.80	16.02	1.76	0.77	8.73	28.87	16.31	7.73	3.39	4.96	20.11	11.11	6.16	2.70	4.99	20.94	12.36	5.29	2.32	2.24	11.98	6.36	3.19	1.40
Papio	12.40	16.90	14.76	1.66	0.84	10.92	16.26	13.50	1.78	0.90	6.75	9.61	7.89	0.83	0.42	9.72	14.03	11.96	1.21	0.61	3.92	8.10	6.05	1.07	0.54
Prebytis	7.70	8.60	8.11	0.64	0.88	7.55	7.91	7.73	0.25	0.35	5.44	5.51	5.48	0.05	0.07	7.19	7.42	7.31	0.16	0.23	4.41	5.06	4.74	0.46	0.64

	HLDF					BLDF					HLRF					BLRF				
Genus	min	max	mean	sd	ci	min	max	mean	sd	ci	min	max	mean	sd	ci	min	max	mean	sd	ci
Alouatta	5.56	10.40	6.26	1.23	0.67	3.09	6.62	3.70	0.89	0.48	4.49	13.35	6.25	2.12	1.15	4.47	9.25	5.71	1.11	0.60
Ateles	5.56	6.42	5.96	0.30	0.26	3.09	4.09	3.48	0.30	0.26	4.49	7.31	5.82	0.72	0.63	4.47	6.13	5.41	0.44	0.39
Cercocebus	6.82	8.47	7.64	0.71	0.56	3.66	5.41	4.79	0.63	0.51	5.92	9.55	7.42	1.46	1.17	5.23	8.64	6.74	1.17	0.94
Cercopithecus	5.36	7.69	6.58	0.63	0.28	2.86	4.79	4.12	0.53	0.24	5.36	8.76	6.84	1.10	0.49	4.88	7.17	6.11	0.64	0.29
Chlorocebus	4.96	5.67	5.33	0.27	0.23	3.02	3.84	3.43	0.32	0.28	5.07	6.40	5.85	0.59	0.52	4.68	5.57	5.03	0.35	0.31
Colobus	7.39	8.31	7.90	0.33	0.25	4.37	5.33	4.96	0.33	0.24	7.75	9.13	8.24	0.45	0.33	5.30	8.26	6.11	1.08	0.80
Gorilla	14.64	25.60	19.16	3.01	1.32	9.30	15.65	12.24	1.83	0.80	16.65	28.17	21.14	3.21	1.41	12.45	19.50	16.40	2.03	0.89
Hylobates	6.07	7.72	7.02	0.46	0.20	4.39	6.78	5.48	0.54	0.24	5.25	7.94	6.96	0.74	0.32	4.69	7.42	5.64	0.82	0.36
Lagothrix	6.12	6.91	6.44	0.31	0.23	2.80	4.55	3.69	0.66	0.49	4.28	6.87	5.95	0.80	0.59	4.25	6.03	5.06	0.64	0.48
Lophocebus	6.15	8.47	7.12	0.89	0.71	2.86	4.93	4.16	0.72	0.58	5.36	8.76	6.97	1.41	1.13	4.88	6.77	5.56	0.65	0.52
M. fascicularis	5.15	5.97	5.44	0.32	0.24	3.24	4.28	3.63	0.33	0.24	5.52	6.50	6.15	0.35	0.26	4.40	5.87	5.11	0.57	0.42
M. mulatta	6.52	9.03	7.63	0.81	0.50	4.39	5.35	4.82	0.35	0.22	7.78	10.99	9.02	0.87	0.54	4.21	7.77	6.28	1.12	0.69
Mandrillus	10.03	10.35	10.17	0.16	0.18	6.97	7.85	7.34	0.46	0.52	11.98	13.54	12.90	0.82	0.93	9.38	11.72	10.20	1.32	1.49
Pan	7.22	25.60	13.48	6.67	2.93	4.23	15.65	8.73	4.36	1.91	7.75	28.17	15.08	7.31	3.20	5.30	19.50	10.77	5.63	2.47
Papio	6.51	14.16	10.62	2.10	1.06	6.09	9.67	7.49	1.15	0.58	10.38	16.36	12.71	1.94	0.98	7.55	13.92	11.04	1.83	0.93
Prebytis	6.35	7.36	6.86	0.71	0.99	4.24	4.50	4.37	0.18	0.25	6.61	7.44	7.03	0.59	0.81	4.80	5.97	5.39	0.83	1.15

	HLTF					LLTF				
Genus	min	max	mean	sd	ci	min	max	mean	sd	ci
Alouatta	3.05	9.46	3.87	1.62	0.88	2.80	11.61	4.50	2.13	1.16
Ateles	3.05	3.77	3.45	0.22	0.20	2.80	5.60	4.07	0.73	0.64
Cercocebus	5.25	8.62	6.27	1.25	1.00	5.24	7.49	6.31	1.05	0.84
Cercopithecus	3.13	5.21	3.94	0.58	0.26	3.74	6.30	5.22	0.68	0.31
Chlorocebus	2.81	3.91	3.35	0.42	0.37	3.41	4.75	4.14	0.52	0.45
Colobus	5.07	7.00	6.18	0.66	0.49	4.75	6.17	5.41	0.64	0.47
Gorilla	8.64	16.33	12.46	1.89	0.83	9.68	13.66	11.38	1.10	0.48
Hylobates	3.33	5.01	4.27	0.48	0.21	2.78	4.59	3.66	0.53	0.23
Lagothrix	2.59	4.39	3.31	0.61	0.45	3.66	4.65	4.21	0.35	0.26
Lophocebus	3.68	6.38	4.99	0.94	0.75	3.74	6.71	5.18	0.99	0.79
M. fascicularis	2.82	4.28	3.35	0.45	0.34	3.00	5.96	4.14	0.95	0.70
M. mulatta	4.03	6.28	4.94	0.73	0.45	4.12	7.01	5.62	0.95	0.59
Mandrillus	5.21	10.13	7.41	2.50	2.83	9.42	12.42	10.73	1.53	1.74
Pan	5.07	16.33	9.25	3.69	1.62	4.75	13.66	8.86	3.24	1.42
Papio	5.69	9.35	7.25	1.06	0.54	4.50	10.40	8.47	1.50	0.76
Prebytis	4.35	4.69	4.52	0.24	0.33	5.16	5.36	5.26	0.14	0.20

	HTDB					LTDPS					LTDDS					BTDDS				
Genus	min	max	mean	sd	ci	min	max	mean	sd	ci	min	max	mean	sd	ci	min	max	mean	sd	ci
Cercocebus	6.56	8.44	7.78	0.71	0.63	1.27	3.49	2.64	0.82	0.72	8.41	10.48	9.56	0.84	0.74	5.83	7.84	7.19	0.82	0.72
Cercopithecus	6.15	8.15	6.91	0.82	0.72	0.65	2.35	1.76	0.66	0.58	5.61	7.90	6.73	0.93	0.82	4.14	5.55	4.78	0.53	0.46
Colobus	6.33	8.54	7.10	0.83	0.62	2.16	4.27	3.06	0.71	0.52	6.62	8.39	7.53	0.65	0.48	5.91	6.97	6.50	0.41	0.30
Gorilla	18.94	30.35	24.29	4.14	2.57	7.73	13.28	9.31	1.75	1.09	17.13	26.76	21.68	3.27	2.03	14.05	24.28	17.69	3.20	1.98
Lophocebus	6.66	9.39	7.87	1.04	0.84	1.68	3.37	2.48	0.63	0.51	5.96	8.77	7.70	1.10	0.88	5.01	6.99	6.16	0.90	0.72
Mandrillus	10.30	13.09	11.48	1.44	1.63	4.51	6.79	5.82	1.18	1.33	10.61	14.09	12.13	1.78	2.02	8.76	11.42	10.09	1.33	1.51
Pan	12.30	19.93	15.67	2.20	1.01	6.10	10.20	7.30	0.98	0.45	12.90	20.70	16.61	1.83	0.84	9.50	14.18	12.68	1.18	0.54
Papio	8.97	12.18	11.09	1.44	1.41	3.12	8.91	6.16	2.51	2.46	10.80	12.75	11.68	0.80	0.79	8.64	10.92	9.65	1.08	1.06

	HTDTMF					LTDTMF					HTDMc2					BTDMc2				
Genus	min	max	mean	sd	ci	min	max	mean	sd	ci	min	max	mean	sd	ci	min	max	mean	sd	ci
Cercocebus	5.74	6.72	6.16	0.38	0.33	4.42	6.28	5.41	0.67	0.58	8.10	9.58	8.98	0.67	0.59	5.97	7.17	6.70	0.49	0.43
Cercopithecus	4.30	6.39	5.06	0.80	0.70	3.16	5.41	4.21	0.82	0.72	5.68	7.81	6.72	0.92	0.81	3.79	4.71	4.29	0.40	0.35
Colobus	5.18	7.24	5.90	0.69	0.51	4.06	6.57	5.45	0.81	0.60	6.53	8.01	7.26	0.47	0.35	5.08	6.77	5.86	0.62	0.46
Gorilla	10.21	20.47	14.69	3.19	1.98	8.65	15.81	11.44	2.31	1.43	17.44	26.76	21.71	3.33	2.07	11.80	22.00	15.93	3.18	1.97
Lophocebus	5.37	7.08	6.02	0.56	0.45	3.88	7.03	5.63	1.02	0.82	7.19	9.07	8.06	0.67	0.54	5.64	6.62	5.90	0.38	0.31
Mandrillus	7.45	9.12	8.07	0.91	1.03	4.31	6.83	5.41	1.29	1.46	10.74	12.26	11.61	0.78	0.89	8.13	9.05	8.49	0.49	0.55
Pan	9.00	14.82	11.74	1.94	0.89	5.75	13.80	11.60	2.07	0.96	13.10	17.58	15.08	1.36	0.63	8.70	12.60	10.99	1.16	0.54
Papio	5.70	9.00	7.35	1.43	1.40	5.95	8.99	6.99	1.40	1.37	9.84	12.39	11.32	1.11	1.09	5.61	7.84	7.15	1.05	1.03

	LTMB					HTMB					LTDF					HTDF				
Genus	min	max	mean	sd	ci	min	max	mean	sd	ci	min	max	mean	sd	ci	min	max	mean	sd	ci
Cercocebus	7.73	10.09	9.34	0.96	0.77	4.35	5.84	5.15	0.64	0.51	7.18	8.98	8.04	0.66	0.53	3.35	5.29	4.07	0.74	0.59
Cercopithecus	4.20	8.89	7.45	1.92	1.68	3.56	5.21	4.19	0.63	0.55	6.13	7.87	7.18	0.64	0.57	2.47	3.50	3.12	0.43	0.38
Colobus	7.81	9.55	8.80	0.63	0.47	5.27	5.72	5.49	0.16	0.12	7.07	8.04	7.47	0.34	0.26	3.27	3.78	3.60	0.18	0.14
Gorilla	25.86	32.04	28.92	2.51	1.64	15.79	25.26	20.61	3.33	2.17	6.36	13.21	10.28	2.34	1.53	9.51	14.07	11.77	1.53	1.00
Lophocebus	8.46	9.68	9.16	0.52	0.42	4.16	5.53	5.19	0.52	0.42	7.11	9.01	8.01	0.67	0.54	3.36	4.79	4.05	0.49	0.39
Mandrillus	12.10	14.82	13.86	1.52	1.72	6.94	8.39	7.85	0.80	0.90	11.74	12.60	12.23	0.44	0.50	5.37	6.39	5.98	0.54	0.61
Pan	17.44	29.11	22.56	2.52	1.11	12.00	22.34	15.38	2.51	1.10	7.15	14.40	10.24	2.37	1.04	6.90	10.16	8.57	0.87	0.38
Papio	12.03	15.06	13.47	1.16	1.01	6.70	8.58	7.72	0.72	0.63	10.31	12.39	11.39	0.93	0.81	4.99	6.32	5.89	0.52	0.46

	BTPF					LTPF					LMc1					BMc1				
Genus	min	max	mean	sd	ci	min	max	mean	sd	ci	min	max	mean	sd	ci	min	max	mean	sd	ci
Cercocebus	5.84	8.05	7.15	0.84	0.67	3.34	4.91	4.34	0.59	0.47	5.37	7.65	6.57	0.82	0.66	4.46	5.81	5.20	0.52	0.42
Cercopithecus	4.59	5.50	5.03	0.41	0.36	3.20	4.00	3.69	0.40	0.35	4.60	6.14	5.34	0.61	0.53	3.54	4.80	4.29	0.48	0.42
Colobus	4.69	7.02	6.33	0.78	0.57	2.86	3.95	3.41	0.34	0.25	4.60	5.83	5.17	0.49	0.36	4.89	5.64	5.25	0.29	0.21
Gorilla	7.79	11.95	9.82	1.49	0.97	8.87	14.51	11.62	1.98	1.29	12.71	19.86	15.84	2.89	1.89	9.64	15.37	12.46	2.11	1.38
Lophocebus	5.48	6.59	6.06	0.38	0.31	3.62	4.84	4.32	0.47	0.38	6.15	7.25	6.70	0.42	0.34	3.92	5.63	4.82	0.71	0.57
Mandrillus	9.00	9.53	9.21	0.28	0.32	5.38	6.56	6.11	0.64	0.72	8.77	9.77	9.32	0.51	0.58	7.49	8.14	7.83	0.33	0.37
Pan	5.20	9.17	6.99	1.08	0.47	6.60	10.75	8.57	1.09	0.48	9.80	16.57	12.45	1.73	0.76	8.76	12.94	10.53	1.21	0.53
Papio	6.40	10.59	8.98	1.63	1.43	5.76	6.21	5.92	0.21	0.18	7.60	11.44	8.77	1.59	1.39	6.77	8.82	8.04	0.87	0.76

	LTDSF				
Genus	min	max	mean	sd	ci
Cercocebus	7.32	10.66	9.07	1.22	0.98
Cercopithecus	6.87	8.50	7.86	0.67	0.59
Colobus	7.99	9.41	8.80	0.54	0.40
Gorilla	11.79	21.33	17.14	2.98	1.95
Lophocebus	8.40	9.65	9.05	0.50	0.40
Mandrillus	12.32	14.78	13.85	1.34	1.51
Pan	10.70	22.65	14.74	3.33	1.46
Papio	11.82	15.01	13.19	1.19	1.04

	LCB					HCB					BCB					HCHF				
Genus	min	max	mean	sd	ci	min	max	mean	sd	ci	min	max	mean	sd	ci	min	max	mean	sd	ci
Alouatta	7.42	9.94	8.29	0.64	0.35	5.56	7.78	6.66	0.62	0.34	6.03	8.09	6.98	0.52	0.28	3.43	5.96	4.71	0.64	0.35
Ateles	8.58	12.17	10.27	1.58	1.39	6.95	8.17	7.61	0.51	0.45	6.51	7.43	7.14	0.38	0.33	3.64	5.17	4.53	0.58	0.50
Cercocebus	10.41	12.30	11.53	0.70	0.56	7.76	10.37	9.29	0.95	0.76	7.23	8.36	7.91	0.46	0.37	4.86	5.89	5.25	0.38	0.30
Cercopithecus	8.36	11.50	9.80	0.88	0.42	6.75	8.96	7.99	0.68	0.32	5.63	8.75	7.11	1.05	0.50	3.58	6.72	5.07	0.99	0.47
Chlorocebus	7.70	8.53	8.06	0.42	0.48	6.01	7.30	6.76	0.67	0.76	5.35	6.15	5.81	0.41	0.47	4.05	5.18	4.70	0.59	0.66
Colobus	10.39	13.07	11.54	1.01	0.75	8.92	10.29	9.57	0.56	0.41	7.15	9.63	8.59	0.87	0.64	3.87	5.56	4.76	0.52	0.38
Erythrocebus	7.62	12.68	10.32	1.92	1.69	5.91	11.05	8.82	1.89	1.66	4.93	9.07	7.44	1.55	1.36	4.30	6.55	5.61	0.87	0.76
Gorilla	21.94	32.77	26.78	3.59	1.57	21.66	31.94	26.37	3.51	1.54	13.82	21.52	16.73	2.13	0.93	11.75	22.09	15.77	2.37	1.04
Hylobates	9.60	12.43	10.98	0.79	0.35	7.41	10.14	8.77	0.62	0.27	4.93	7.95	6.81	0.73	0.32	4.51	6.94	5.57	0.61	0.27
Lagothrix	8.04	9.52	8.63	0.57	0.43	6.04	7.01	6.45	0.30	0.22	5.64	6.51	5.95	0.34	0.25	3.32	5.50	4.13	0.72	0.53
Lophocebus	10.58	12.94	11.70	1.01	0.81	7.68	9.10	8.36	0.53	0.42	7.80	9.05	8.29	0.44	0.36	3.54	4.12	3.91	0.24	0.19
M. fascicularis	8.04	8.50	8.21	0.19	0.15	5.96	7.07	6.70	0.44	0.35	4.54	6.39	5.59	0.72	0.58	3.33	4.94	4.30	0.59	0.47
M. mulatta	9.80	12.24	11.05	0.72	0.41	7.82	11.17	9.42	1.12	0.64	6.87	9.34	8.05	0.76	0.43	5.69	8.16	6.42	0.62	0.35
Mandrillus	16.77	19.83	18.22	1.54	1.74	12.06	13.23	12.74	0.61	0.69	11.12	11.81	11.42	0.35	0.40	5.73	7.88	6.60	1.13	1.28
Pan	20.68	26.49	23.55	1.99	0.87	16.46	24.17	19.43	2.33	1.02	12.36	17.27	14.94	1.40	0.62	8.41	14.84	11.33	1.64	0.72
Papio	14.91	20.89	17.71	1.78	1.05	11.63	15.95	14.20	1.43	0.85	10.47	13.29	12.06	1.00	0.59	5.59	9.77	7.91	1.34	0.79
Presbytis	9.75	10.82	10.23	0.54	0.62	7.52	8.19	7.75	0.38	0.43	7.00	7.95	7.34	0.53	0.60	6.28	6.61	6.47	0.17	0.19
Theropithecus	12.83	14.60	13.92	0.84	0.83	10.53	11.48	11.04	0.39	0.39	9.05	10.20	9.64	0.61	0.59	6.87	8.28	7.38	0.62	0.61

	LCHF					BCPF					HCPF					BCN				
Genus	min	max	mean	sd	ci	min	max	mean	sd	ci	min	max	mean	sd	ci	min	max	mean	sd	ci
Alouatta	6.54	8.66	7.46	0.57	0.31	3.26	4.67	3.61	0.38	0.21	3.58	5.01	4.34	0.47	0.25	2.79	4.10	3.60	0.31	0.17
Ateles	8.03	11.07	9.58	1.40	1.23	3.28	5.64	4.52	0.84	0.73	4.34	4.92	4.57	0.27	0.23	3.75	4.37	4.03	0.26	0.22
Cercocebus	8.58	10.33	9.51	0.72	0.58	4.67	6.21	5.30	0.55	0.44	5.16	6.44	5.80	0.52	0.41	3.43	4.97	4.09	0.59	0.47
Cercopithecus	6.88	9.87	8.22	0.86	0.41	3.51	5.14	4.25	0.52	0.25	4.12	6.25	5.01	0.56	0.26	3.01	4.82	3.67	0.43	0.21
Chlorocebus	6.80	6.89	6.84	0.05	0.05	3.38	4.22	3.82	0.42	0.48	4.01	4.67	4.44	0.37	0.42	3.02	3.05	3.04	0.02	0.02
Colobus	8.29	10.85	9.82	0.86	0.64	4.79	6.36	5.56	0.50	0.37	4.63	6.31	5.61	0.64	0.47	4.20	5.21	4.88	0.33	0.24
Erythrocebus	7.18	10.22	8.79	1.17	1.03	3.27	5.15	4.14	0.69	0.61	4.11	6.43	5.53	0.88	0.77	3.40	4.39	3.73	0.38	0.34
Gorilla	17.14	26.77	20.86	2.47	1.08	10.37	18.05	14.17	2.36	1.03	13.37	21.24	16.84	2.40	1.05	9.48	13.28	11.21	1.30	0.57
Hylobates	5.10	7.21	6.15	0.68	0.30	2.97	4.28	3.75	0.35	0.15	4.25	6.25	5.21	0.53	0.23	3.02	4.19	3.42	0.35	0.15
Lagothrix	7.33	9.24	8.07	0.60	0.45	3.77	4.87	4.33	0.37	0.28	4.17	5.33	4.79	0.40	0.29	3.30	4.08	3.75	0.33	0.24
Lophocebus	9.26	10.97	9.99	0.66	0.53	4.46	6.20	5.33	0.67	0.54	5.51	6.76	6.05	0.47	0.37	3.51	4.32	3.80	0.30	0.24
M. fascicularis	6.42	7.85	7.10	0.47	0.37	3.40	4.08	3.68	0.22	0.18	3.82	5.21	4.52	0.50	0.40	2.72	3.63	3.20	0.36	0.29
M. mulatta	5.46	11.03	9.37	1.37	0.77	4.13	5.72	4.96	0.49	0.28	4.58	6.79	5.87	0.60	0.34	3.25	4.91	4.05	0.45	0.25
Mandrillus	12.93	14.49	13.47	0.88	1.00	6.79	9.00	7.88	1.11	1.25	6.44	9.87	8.04	1.73	1.95	5.55	6.90	6.10	0.71	0.80
Pan	15.43	23.56	18.90	2.55	1.12	9.75	13.44	11.34	1.06	0.46	10.09	16.30	13.58	1.46	0.64	6.43	11.97	8.88	1.24	0.55
Papio	12.33	16.96	13.85	1.38	0.82	6.58	8.95	7.56	0.74	0.44	7.68	10.60	8.85	0.94	0.55	5.31	6.96	6.01	0.53	0.31
Presbytis	7.85	9.54	8.85	0.88	1.00	4.10	4.64	4.44	0.29	0.33	5.08	5.49	5.30	0.21	0.23	3.93	4.63	4.36	0.37	0.42
Theropithecus	10.88	12.47	12.05	0.78	0.76	5.47	6.10	5.94	0.31	0.31	6.82	7.43	7.07	0.26	0.25	4.68	5.34	5.00	0.29	0.28

	LHB					LHB-H					HHB					HHB-H				
Genus	min	max	mean	sd	ci	min	max	mean	sd	ci	min	max	mean	sd	ci	min	max	mean	sd	ci
Alouatta	8.30	11.06	9.34	0.76	0.38	7.48	11.06	8.87	0.90	0.46	5.75	9.25	7.21	0.88	0.45	5.04	7.46	5.90	0.62	0.32
Ateles	10.56	15.08	12.67	2.04	1.79	8.98	13.64	11.61	1.80	1.57	6.09	8.65	7.51	0.96	0.84	6.03	7.23	6.54	0.43	0.38
Cercocebus	10.81	13.50	12.01	1.01	0.81	10.81	13.50	12.01	1.01	0.81	7.80	9.88	8.99	0.72	0.58	6.46	7.34	6.73	0.38	0.31
Cercopithecus	7.66	11.11	9.60	1.00	0.46	7.43	11.11	9.43	1.01	0.47	6.75	9.23	8.12	0.73	0.34	4.20	6.84	5.81	0.73	0.34
Chlorocebus	7.90	9.98	8.57	0.98	0.96	7.79	9.55	8.43	0.80	0.79	5.95	7.94	6.81	1.01	0.99	4.74	6.61	5.44	0.83	0.81
Colobus	10.15	13.02	11.63	0.99	0.73	10.15	12.96	11.40	0.99	0.73	7.33	10.21	8.44	0.98	0.72	5.47	7.62	6.32	0.88	0.65
Erythrocebus	8.21	11.43	9.78	1.21	1.06	8.55	12.19	10.15	1.50	1.31	6.09	10.05	8.08	1.59	1.40	4.48	7.20	6.19	1.08	0.95
Gorilla	22.46	36.42	29.16	4.49	1.97	17.48	28.37	21.91	3.17	1.39	19.22	34.67	26.59	4.83	2.12	12.15	21.53	16.60	2.64	1.16
Hylobates	14.98	20.06	17.27	1.17	0.51	12.38	15.79	13.73	0.75	0.33	8.53	11.15	9.84	0.83	0.37	5.24	6.42	5.97	0.33	0.14
Lagothrix	8.03	9.83	8.90	0.59	0.44	8.03	9.83	8.90	0.59	0.44	6.79	9.20	7.90	0.82	0.61	4.97	6.63	5.70	0.59	0.44
Lophocebus	12.22	13.18	12.75	0.41	0.33	11.01	13.03	11.70	0.73	0.58	7.05	9.16	8.14	0.86	0.69	5.21	6.59	6.04	0.56	0.45
M. fascicularis	7.98	9.51	8.71	0.51	0.38	7.98	9.17	8.57	0.37	0.28	6.22	7.43	6.72	0.42	0.31	4.25	6.42	5.15	0.77	0.57
M. mulatta	9.88	13.69	11.53	0.91	0.44	9.88	13.56	11.42	0.84	0.41	8.01	11.30	9.21	0.93	0.45	5.61	8.08	6.81	0.77	0.38
Mandrillus	16.44	17.28	16.95	0.45	0.51	16.44	17.28	16.95	0.45	0.51	12.94	13.60	13.22	0.34	0.38	8.65	11.03	10.00	1.22	1.38
Pan	23.75	34.27	27.45	2.81	1.23	16.90	26.79	20.50	3.13	1.37	16.77	23.90	19.86	2.27	1.00	10.96	17.01	13.61	1.51	0.66
Papio	13.79	20.35	17.10	1.96	0.99	13.19	20.35	16.70	2.13	1.08	10.78	16.56	13.15	1.80	0.91	7.29	11.82	9.73	1.27	0.64
Presbytis	10.17	11.29	10.59	0.61	0.69	10.17	10.32	10.27	0.09	0.10	7.19	7.94	7.65	0.40	0.45	5.91	6.22	6.01	0.18	0.20
Theropithecus	13.14	15.34	14.08	0.92	0.90	13.14	15.34	14.08	0.92	0.90	9.83	11.73	10.81	0.86	0.84	8.06	9.24	8.57	0.49	0.48

	HHCF					LHCF					BHB				
Genus	min	max	mean	sd	ci	min	max	mean	sd	ci	min	max	mean	sd	ci
Alouatta	3.01	5.22	4.21	0.59	0.30	6.17	8.25	6.93	0.54	0.27	6.76	9.42	7.93	0.67	0.34
Ateles	4.68	7.45	5.61	1.16	1.01	5.82	11.24	9.31	2.21	1.94	7.77	10.27	9.12	0.89	0.78
Cercocebus	4.23	6.25	5.23	0.86	0.69	7.49	9.27	8.37	0.75	0.60	5.99	9.06	7.74	1.13	0.91
Cercopithecus	4.16	8.60	6.69	1.50	0.69	4.46	8.01	5.72	0.84	0.39	6.16	9.11	7.47	0.95	0.44
Chlorocebus	3.76	4.72	4.26	0.44	0.43	5.07	7.21	5.98	0.94	0.92	4.66	7.45	5.93	1.18	1.15
Colobus	4.49	6.46	5.39	0.64	0.47	6.86	8.62	7.73	0.66	0.49	7.14	10.14	8.47	0.93	0.69
Erythrocebus	4.23	7.61	5.87	1.26	1.10	4.82	8.10	6.79	1.35	1.18	5.36	8.92	7.47	1.44	1.26
Gorilla	11.78	17.46	13.92	1.68	0.74	14.72	25.23	19.08	3.14	1.38	14.94	25.89	19.70	3.21	1.41
Hylobates	4.56	5.98	5.23	0.42	0.18	4.53	7.87	5.87	0.73	0.32	5.60	7.56	6.73	0.52	0.23
Lagothrix	3.63	4.61	4.07	0.31	0.23	6.93	8.79	7.59	0.65	0.48	7.00	8.91	7.73	0.68	0.50
Lophocebus	3.54	5.37	4.67	0.69	0.56	7.31	8.77	7.93	0.58	0.46	6.62	8.34	7.42	0.70	0.56
M. fascicularis	3.58	4.70	4.18	0.45	0.33	5.26	6.74	6.21	0.53	0.39	5.71	6.91	6.20	0.47	0.35
M. mulatta	4.66	8.02	6.10	1.06	0.52	5.17	9.86	7.85	1.22	0.60	7.06	10.39	8.60	0.93	0.46
Mandrillus	7.19	7.80	7.57	0.33	0.38	8.41	11.60	10.06	1.60	1.81	10.52	13.42	12.14	1.48	1.68
Pan	8.06	14.08	10.70	1.63	0.71	15.60	23.08	18.88	2.18	0.96	13.54	21.83	16.53	1.80	0.79
Papio	5.93	9.45	7.69	0.93	0.47	8.95	14.29	11.57	1.51	0.76	10.13	14.55	11.81	1.36	0.69
Presbytis	6.71	7.71	7.23	0.50	0.57	4.83	5.47	5.20	0.33	0.38	6.57	7.39	7.11	0.47	0.53
Theropithecus	8.59	10.08	9.46	0.66	0.65	7.34	8.61	7.99	0.52	0.51	8.84	10.26	9.43	0.66	0.65

	HHTF					LHTF				
Genus	min	max	mean	sd	ci	min	max	mean	sd	ci
Alouatta	4.64	6.68	5.77	0.53	0.27	8.44	10.16	9.24	0.59	0.30
Ateles	4.80	6.77	5.92	0.73	0.64	8.05	13.22	11.31	1.97	1.73
Cercocebus	4.16	6.78	5.58	0.96	0.77	8.87	11.72	10.62	1.12	0.90
Cercopithecus	3.61	5.88	4.70	0.67	0.31	6.07	8.14	7.07	0.59	0.27
Chlorocebus	3.72	5.44	4.73	0.72	0.71	5.51	9.05	7.09	1.55	1.52
Colobus	4.68	7.42	5.76	1.00	0.74	9.66	11.55	10.34	0.73	0.54
Erythrocebus	4.00	7.52	5.70	1.31	1.15	6.69	10.16	8.03	1.46	1.28
Gorilla	11.74	19.10	14.71	2.01	0.88	15.64	27.71	19.84	3.40	1.49
Hylobates	4.42	6.16	5.39	0.39	0.17	8.72	12.41	10.42	1.16	0.51
Lagothrix	3.78	5.00	4.48	0.42	0.31	8.14	10.06	8.96	0.61	0.45
Lophocebus	4.41	5.69	5.15	0.56	0.45	9.65	11.84	10.39	0.87	0.70
M. fascicularis	3.54	4.89	4.44	0.52	0.39	6.66	7.79	7.08	0.40	0.30
M. mulatta	4.11	7.53	5.62	0.92	0.45	7.65	11.35	9.34	1.09	0.53
Mandrillus	6.52	9.07	7.66	1.30	1.47	12.33	13.90	13.08	0.79	0.89
Pan	9.00	19.27	11.91	2.42	1.06	10.67	22.37	17.70	2.82	1.24
Papio	6.67	10.17	8.21	0.95	0.48	10.61	16.24	13.91	1.71	0.87
Presbytis	4.33	4.83	4.58	0.25	0.28	7.42	8.57	8.05	0.58	0.66
Theropithecus	5.89	7.94	7.08	0.92	0.91	9.52	10.79	10.18	0.56	0.55

	LMc1					LMc2					LMc3				
Genus	min	max	mean	sd	ci	min	max	mean	sd	ci	min	max	mean	sd	ci
Gorilla	39.08	55.53	48.59	5.61	3.66	74.85	107.32	91.41	11.72	7.66	76.33	109.17	91.46	12.18	7.95
Lophocebus	20.20	24.01	21.99	1.63	1.60	39.12	41.80	40.84	1.18	1.16	39.39	41.43	40.52	0.85	0.84
Mandrillus	35.99	38.80	37.64	1.47	1.66	58.47	60.88	59.92	1.28	1.44	55.08	58.95	57.38	2.04	2.31
Pan	36.30	42.66	39.87	2.16	1.03	78.00	92.09	86.66	3.68	1.75	81.32	93.46	87.53	3.83	1.82
Papio	36.09	42.09	39.09	4.24	5.88	59.88	68.26	63.25	4.42	6.13	56.59	65.79	60.47	4.76	6.60

	LMc4					LMc5				
Genus	min	max	mean	sd	ci	min	max	mean	sd	ci
Gorilla	71.53	101.47	84.62	10.67	6.97	65.40	97.84	81.23	11.40	7.45
Lophocebus	38.27	41.41	40.11	1.41	1.38	35.43	37.97	37.07	1.13	1.11
Mandrillus	54.86	58.20	56.95	1.82	2.06	54.57	58.64	56.81	2.07	2.34
Pan	69.10	85.80	79.07	4.13	1.97	61.70	78.14	70.61	3.59	1.71
Papio	57.21	65.06	60.23	4.22	5.85	58.98	66.33	61.45	4.23	5.86

SUPPLEMENTARY TABLE 3. CARPAL VARIABLES INCLUDED IN GEOMETRIC MEAN (see Table 4 for abbreviations).

Bone	*Variables included in geometric mean*
Os centrale	OCH, OCL, OCB, OCDFH, OCDFL
Lunate	LLB, HLB, BLB, HLSF, LLSF, HLDF, BLDF, HLRF, BLRF, HLTF, LLTF
Trapezium	LTMB, HTMB, LTDF, HTDF, BTPF, LTPF, LMC1, BMC1, LTDSF
Trapezoid	HTDB, LTDPS, LTDDS, BTDDS, HTDTMF, LTDTMF, HTDMC2, BTDMC2
Capitate	LCB, HCB, BCB, LCHF, BCPF, HCPF
Hamate	LHB, LHB-H, HHB, HHB-H, BHB, HHCF, LHCF, HHTF, LHTF
Metacarpals	LMC1, LMC2, LMC3, LMC4, LMC5

SUPPLEMENTARY TABLE 4. LOADINGS OF EACH PRINCIPAL COMPONENT INCLUDED PER BONE.

Lunate	PC 1	PC 2	PC 3	PC 4	PC 5	PC 6	PC 7	PC 8	PC 9	PC 10	PC 11
LLB_g	0.038702	0.09366	0.31145	0.14835	0.10268	0.39066	-0.15653	0.67317	-0.43491	0.001695	0.20186
HLB_g	0.23154	0.30874	0.045416	0.02434	0.01193	0.1989	-0.03535	0.075478	0.49545	0.73685	0.11554
BLB_g	-0.08564	-0.0288	0.24392	0.016468	0.075303	0.18068	-0.46957	-0.64885	-0.36366	0.2199	0.26767
HLSF_g	-0.00838	0.25201	-0.22689	0.30172	0.74846	-0.37599	0.097113	-0.00889	-0.0888	0.012825	0.27349
LLSF_g	-0.80757	0.12602	-0.19142	-0.03485	-0.26717	-0.03112	0.049521	0.1178	0.082433	0.093175	0.43582
HLDF_g	0.10914	0.2953	0.07223	0.25207	-0.03968	0.52463	0.41055	-0.29402	0.19412	-0.43498	0.27098
BLDF_g	0.11543	-0.05341	0.16133	-0.17096	0.083111	-0.13842	-0.56178	0.1313	0.51701	-0.42493	0.34899
HLRF_g	0.22933	0.42235	0.18308	-0.667	-0.11361	-0.27128	0.25465	-0.02186	-0.25565	-0.01924	0.27031
BLRF_g	0.046781	-0.42295	0.58372	0.30077	-0.13178	-0.36156	0.35333	-0.00727	0.079637	0.13327	0.30108
HLTF_g	0.43769	-0.01311	-0.49399	0.32281	-0.49009	-0.16947	-0.14885	0.034109	-0.20435	0.01256	0.3548
LLTF_g	0.11716	-0.60679	-0.32219	-0.39058	0.27044	0.32467	0.21419	0.02835	0.002388	0.10856	0.35312

Hamate	PC 1	PC 2	PC 3	PC 4	PC 5	PC 6	PC 7	PC 8	PC 9
LHB_g	-0.02118	0.72972	-0.11541	-0.09315	0.12779	0.39434	-0.02911	-0.48396	0.19535
LHB-H_g	-0.00941	0.49184	-0.18082	-0.05224	-0.06315	-0.06853	0.005418	0.8139	0.2268
HHB_g	-0.20836	0.1628	0.65679	0.41983	-0.43093	-0.05883	0.23061	-0.04569	0.27934
HHB-H_g	-0.06214	-0.11223	0.14831	0.041402	0.046733	-0.02974	-0.88923	-0.00379	0.40746
BHB_g	0.041106	-0.32991	0.026312	0.26883	0.28108	0.76753	0.16173	0.23655	0.25745
HHCF_g	-0.66333	-0.15017	-0.40917	0.10493	0.18916	-0.27109	0.21857	-0.13053	0.43003
LHCF_g	0.51389	-0.13155	-0.4721	0.18784	-0.53085	-0.0324	0.061161	-0.1591	0.38541
HHTF_g	0.042478	-0.1801	0.2607	-0.8143	-0.1061	0.052469	0.21046	-0.00727	0.41996
LHTF_g	0.49458	0.073262	0.20412	0.17025	0.61963	-0.41116	0.18235	-0.05374	0.3004

Trapezium	PC 1	PC 2	PC 3	PC 4	PC 5	PC 6	PC 7	PC 8	PC 9
LTMB_g	0.18868	0.87962	0.067042	0.21914	0.27868	-0.10018	0.023318	0.11072	0.19404
HTMB_g	0.44069	-0.29759	0.68158	0.37732	-0.08356	-0.20311	-0.04625	0.093573	0.22623
LTDF_g	-0.60585	0.10064	0.12137	0.37285	-0.33604	0.23535	-0.46106	0.07279	0.28789
HTDF_g	0.17058	-0.01475	-0.25732	-0.0746	-0.09771	-0.28938	-0.23305	-0.70951	0.4979
BTPF_g	0.17252	-0.06955	0.17263	-0.50901	0.37816	0.48705	-0.40287	0.1498	0.33397
LTPF_g	0.082306	-0.1476	-0.44561	-0.0547	-0.12314	-0.37537	-0.04052	0.664	0.41385
LMC1F_g	0.065019	-0.25773	-0.33974	0.55796	0.39465	0.43395	0.30068	-0.06766	0.2521
BMC1F_g	0.067329	0.15377	0.11674	-0.24312	-0.54169	0.35708	0.58506	-0.00841	0.3685
LTDSF_g	-0.57336	-0.10328	0.30429	-0.18033	0.43075	-0.34006	0.36575	-0.04792	0.31342

Trapezoid	PC 1	PC 2	PC 3	PC 4	PC 5	PC 6	PC 7	PC 8
HTDB_g	0.5113	-0.14307	0.41371	-0.48244	0.31247	-0.28221	-0.25229	0.27066
LTDPS_g	-0.2211	-0.33057	-0.38631	-0.38575	-0.33561	0.1207	-0.01492	0.64527
LTDDS_g	0.38611	0.70981	-0.19714	0.050525	-0.43058	-0.07997	-0.277	0.19272
BTDDS_g	0.14803	-0.06158	-0.28594	0.42195	0.22341	-0.62278	0.39956	0.34216
HTDTMF_g	-0.14132	-0.12183	0.70267	0.39369	-0.46093	-0.05832	0.016268	0.31675
LTDTMF_g	-0.54934	0.54575	0.18265	-0.10509	0.46439	0.038042	0.009935	0.37253
HTDMC2_g	0.38824	0.1414	0.125	-0.0856	0.03381	0.52201	0.71083	0.16551
BTDMC2_g	0.21498	-0.17306	-0.12746	0.51428	0.35377	0.48393	-0.44057	0.29944

Capitate	PC 1	PC 2	PC 3	PC 4	PC 5	PC 6	PC 7
LCB_g	0.22293	0.57498	0.018846	0.6401	0.43978	-0.11216	0.060245
HCB_g	-0.20644	0.53551	-0.24567	-0.66265	0.36776	0.051772	0.18228
BCB_g	0.12276	0.068175	0.91509	-0.1901	0.075444	0.11696	0.2956
HCHF_g	-0.64008	-0.39373	0.005831	0.21995	0.42125	-0.1506	0.43212
LCHF_g	0.65664	-0.44238	-0.22246	-0.14051	0.46702	0.16075	0.24485
BCPF_g	0.20291	0.11925	-0.16585	-0.00426	-0.45979	-0.46438	0.70002
HCPF_g	-0.10275	0.11416	-0.15769	0.21655	-0.24226	0.84077	0.37292

Os Centrals	PC 1	PC 2	PC 3	PC 4	PC 5
OCH_g	-0.01475	0.4248	0.26193	-0.73315	0.46174
OCL_g	0.42299	-0.29738	0.73125	0.29188	0.33574
OCB_g	-0.63178	-0.50512	-0.11933	0.039162	0.5744
OCDFH_g	-0.03989	0.64339	-0.15984	0.59858	0.4479
OCDFL_g	0.64817	-0.24902	-0.59739	-0.13215	0.37885